

Sudan University of Science and Technology  
College of graduated studies



Development of a Method for Age  
Estimation Based on Face Wrinkles and  
Local Features

تطوير طريقة لتقدير العمر بناء على تجاعيد الوجه و الملامح  
المحلية

A Thesis Submitted in Fulfillment of the Requirements for  
PhD Degree in Computer Science

By  
Omaima FathElrahman Osman Hassan

Supervised by  
Dr. Moi Hoon Yap

September 2020

## **ACKNOWLEDGMENT**

Praise is to *Allah*, the Almighty for having guided me at every stage of my life.

In preparation of this thesis, there are many people have contributed towards my understanding and thoughts. I would like to acknowledge, and also, I wish to express my deep gratitude to my supervisor, Dr. Moi Hoon Yap for guidance, valuable time, technical and friendly dealing through out my study. Without their continued support, guidance and interest, thesis would not have been the same as presented here.

I have received direct or indirect help and support from many personalities that motivated and enabled me to conduct this research. Thanks are due to my colleagues Walied Merghani, and Remah Mutasim, my mother Salma Ahmed, my father E.FathErahman Osman for his help in collecting the data, my husband Mohammed Abdrahim Mobark and prof Elsadig Ezzaldeen for the many hours of proofreading papers and my family.

Special thanks to Sudan University of Science and Technology for providing me such a graceful opportunity to become a part of its family.

Finally, I thank my family and friends for their constant encouragement.

# Abstract

Research related to age estimation using face images has become increasingly important due to its potential use in various applications such as advertising and access control. Although there are several methods proposed in the state of the art of age estimation, it is still a challenging task due to the several factors and variations that affect the face age estimation process.

The primary aim of this thesis is to develop a robust age estimation method based on wrinkle and other local features. First, a robust wrinkle detection method was proposed, which localizes wrinkle regions using a simple and powerful matched filter. Then an adaptive thresholding technique was introduced for the first time to segment wrinkle regions. Experimental results revealed that the adaptive thresholding technique significantly increases the accuracy of the proposed algorithm when evaluated on FERET, Social Habits and our proposed in-house Sudanese dataset.

Second, a feature representation method called Wrinkle Local-based Descriptor (WLD) was proposed to represent face aging features based on Scattering Transform and wrinkle pattern. Three benchmark datasets namely FG-NET, FERET and PAL were used to evaluate the proposed method, in addition to our collected Sudanese dataset. Results showed that WLD has a great potential in age estimation, when evaluated on high and mid resolution images. Where the combination of Scattering Transform (ST) and wrinkle pattern yielded a superior result on FERET and PAL with MAE 2.09 and 2.15 years respectively, and 4.72 years for the Sudanese dataset. Finally, the effect of smoking on wrinkles was investigated using computer vision algorithms. The result showed that the density of wrinkles for smokers in two regions around the mouth was significantly higher than the non-smokers, at a p-value of 0.05.

## المستخلص

إزدادت أهمية البحوث المتعلقة بتقدير العمر من صورة الوجه نظراً لإستخدامها في العديد من التطبيقات مثل الإعلانات و التحكم في الوصول. بالرغم من أن هناك العديد من الطرق التي تم إقتراحها لحل مشكلة تقدير العمر لكنها لاتزال تشكل تحدياً بسبب وجود العديد من العوامل والإختلافات التي تؤثر على عملية تقدير العمر.

الهدف الأساسي من هذا البحث هو تطوير طريقة فعالة لتقدير العمر بناءً على التجاعيد و الخصائص المحلية الأخرى. أولاً, تم إقتراح طريقه فعالة لإكتشاف التجاعيد والتي تقوم بتحديد مناطق التجاعيد في الوجه بإستخدام أحد المرشحات البسيطة والفعالة و المسمى بفلتر المطابقة. بعد ذلك تم إستخدام تقنيات تقطيع الصورة المحليه لأول مرة لإستقطاع مناطق التجاعيد بدلاً عن التقنيات العامه التي كانت تستخدم في الدراسات السابقة. أظهرت نتائج التجارب أن تقنيات تقطيع الصورة المحليه زادت من دقة الخوارزمية بصورة ملحوظة عند تقييمها على مجموعة البيانات FERET, Social Habits و مجموعة البيانات السودانية التي تم جمعها.

ثانياً, تم تطوير طريقة تمثيل سمات الوجه لتقدير العمر بناءً " على تجاعيد الوجه والخصائص المحلية سميت ب Wrinkle Local-based Descriptor (WLD). لتقييم أداء طريقة تقدير العمر المقترحة تم إستخدام ثلاث من مجموعات البيانات العامه هي: FERET FG-NET, PAL , بالإضافة لمجموعة البيانات السودانية التي تم جمعها. أظهرت النتائج أن الطريقة المقترحة (WLD) لها قدرة كبيرة على تقدير العمر عند إستخدام صور ذات دقة عالية و متوسطة. إن إستخدام هذا الهجين من الخصائص أثمر نتائج متفوقة حيث أن متوسط الخطأ المطلق لمجموعة البيانات FERET هو 2.09 عام و لمجموعة البيانات PAL هو 2.15 عام, و 4.72 لمجموعة البيانات السودانية.

أخيراً, تم دراسة تأثير التدخين على التجاعيد بإستخدام خوارزميات الرؤية بالحاسوب, أظهرت النتائج أن كثافة التجاعيد للمدخنين أعلى بصورة واضحة في المناطق حول الفم عند القيمة الإحتمالية 0.05.

# Contents

<b>1</b>	<b>Introduction</b>	<b>1</b>
1.1	Background . . . . .	1
1.2	Problem Statement . . . . .	2
1.3	Research Aim and Objectives . . . . .	3
1.4	Research Methodology . . . . .	3
1.5	Expected Contributions . . . . .	3
1.6	Thesis Organisation . . . . .	4
<b>2</b>	<b>Literature Review</b>	<b>6</b>
2.1	Introduction . . . . .	6
2.2	Real-World Applications . . . . .	7
2.2.1	Access Control and Monitoring . . . . .	7
2.2.2	Electronic Customer Relationship Management (ECRM) . . . . .	8
2.2.3	Entertainment . . . . .	8
2.3	Face Aging Process . . . . .	8
2.3.1	Childhood Aging . . . . .	9
2.3.2	Adulthood Aging . . . . .	10
2.3.2.1	Wrinkle . . . . .	11
2.3.3	Facial Aging Factor . . . . .	12
2.3.3.1	Intrinsic Aging Factors . . . . .	13
2.3.3.2	Extrinsic Aging Factors . . . . .	14
2.4	Face Aging Database . . . . .	15
2.5	Wrinkle Detection Techniques . . . . .	17
2.6	Face Age Estimation Techniques . . . . .	21
2.6.1	Features Extraction . . . . .	21
2.6.1.1	Local-Based Algorithms . . . . .	22
2.6.1.2	Global-Based Algorithms . . . . .	25
2.6.1.3	Hybrid-Based Algorithms . . . . .	28

2.6.2	Age Learning Techniques . . . . .	32
2.6.2.1	Classification . . . . .	32
2.6.2.2	Regression . . . . .	34
2.6.2.3	Hierarchical . . . . .	35
2.6.2.4	Ordinal ranking . . . . .	36
2.6.2.5	Deep Learning . . . . .	37
2.7	Smoking and Facial Wrinkles . . . . .	43
2.8	Research Direction . . . . .	45
2.9	Summary . . . . .	46
<b>3</b>	<b>Methodology</b>	<b>47</b>
3.1	Introduction . . . . .	47
3.2	Datasets Collection and Acquisition . . . . .	47
3.2.1	Sudanese Dataset . . . . .	47
3.2.2	FERET . . . . .	49
3.2.3	FG-NET . . . . .	50
3.2.4	MORPH . . . . .	52
3.2.5	PAL . . . . .	52
3.2.6	Social Habit Dataset . . . . .	53
3.3	Face Detection and Alignment . . . . .	55
3.4	Features Representation using Wrinkle local-based Descriptor(WLD)	56
3.4.1	Wrinkle Detection Method . . . . .	56
3.4.1.1	Matched Filter . . . . .	57
3.4.1.2	Thresholding Technique . . . . .	59
3.4.2	Scattering Transform (ST) . . . . .	62
3.5	Age Prediction . . . . .	63
3.6	Validation . . . . .	64
3.6.1	Jaccard Similarity Index (JSI) . . . . .	64
3.6.2	BF score . . . . .	64
3.6.3	Mean Absolute Error . . . . .	65
3.7	The Modified Hybrid Hessian Filter . . . . .	66
3.7.1	Wrinkles Detection and Quantification . . . . .	66
3.8	Conclusion . . . . .	67

<b>4</b>	<b>Results and Discussion</b>	<b>68</b>
4.1	Introduction . . . . .	68
4.2	Experimental Results for Wrinkle Detection . . . . .	68
4.3	Experimental Results for Age estimation . . . . .	72
4.4	Experimental Results for Smoking and Wrinkles . . . . .	74
4.5	Summary . . . . .	78
<b>5</b>	<b>Conclusion and Future Works</b>	<b>79</b>
5.1	Conclusion . . . . .	79
5.2	Future Works . . . . .	80
<b>A</b>	<b>Dataset Questioner</b>	<b>82</b>
	<b>Bibliography</b>	<b>89</b>

# List of Tables

2.1	Facial appearance changes for different age groups. . . . .	11
2.2	Summary of face aging databases. . . . .	16
2.3	A summary of feature extraction methods. . . . .	31
2.4	Comparison between age learning techniques. . . . .	33
2.5	Comparison between different face age estimation algorithms organised by machine learning techniques and database (Part I). To clarify, the machine learning technique for classification and regression are referred to conventional machine learning algorithms. . . . .	40
2.6	Comparison between different face age estimation algorithms organised by machine learning techniques and database (Part II). The machine learning technique for hierarchical and ordinal ranking are referred to conventional machine learning algorithms. . . . .	41
2.7	Comparison between different face age estimation algorithms organised by machine learning techniques and database (Part III). The machine learning technique for hierarchical and ordinal ranking are referred to conventional machine learning algorithms. . . . .	42
3.1	The distribution of the images in FERET. . . . .	49
3.2	The distribution of the images in FG-NET. . . . .	52
3.3	Age range distribution of the images in MORPH album2. . . . .	52
3.4	Age range distribution of the images in PAL. . . . .	53
4.1	Parameter values for experiments in the three datasets. . . . .	72
4.2	Comparison of BF score results for proposed method and other state-of-the-art methods using manual annotation as a ground truth. . . . .	73
4.3	Comparison of MAE results between proposed method and state-of-the-arts methods on different datasets. . . . .	75
4.4	The average wrinkles density for smokers and non-smokers. . . . .	75



4.5	The average wrinkles density for smokers and non-smokers at each face region. . . . .	76
-----	---	----

# List of Figures

2.1	Face aging process in a male subject. Redrawn from FG-NET (Panis et al. 2015). . . . .	9
2.2	Face shape changes. The images for the same subject at different aging stages. Redrawn from FG-NET (Panis et al. 2015). . . . .	10
2.3	Fine-scale vs large-scale wrinkles. (a) Forehead wrinkle, redrawn from our in-house dataset; (b) Fine-scale wrinkles on the back of the hand	12
2.4	Permanent vs transient wrinkles. (a) Permanent wrinkle; (b) Transient wrinkle. Images were redrawn from FERET (Phillips et al. 1996) . .	13
2.5	Blood vessel in retinal image versus wrinkle image. Retinal image was obtained from DRIVE dataset (Mapayi et al. 2015), and wrinkle image from (Alarifi et al. 2017). . . . .	19
2.6	Illustration of the age estimation publications based on five age learning techniques over the past 10 years. There was an increase of classification and regression methods until 2012. With the growth of deep learning, it is expected that the number of publications using deep learning has a rapid growth from 2014. . . . .	39
2.7	The effect of smoking on face skin (Osman et al. 2017): (a) illustrates the skin from a non-smoker at age 80 and (b) illustrates the skin from a smoker at age 78 . . . . .	44
3.1	Research methodology. . . . .	48
3.2	Samples from our collected dataset. The label of each image describes age and smoking status (Smoker or Non-smoker) . . . . .	49
3.3	FERET samples. First row shows a different male subjects at different age, and second row shows a different female subjects at different age. The label of each image describes the age. . . . .	50

3.4	FG-NET samples. First row shows a male subject of same person at different age, second row also the same but the subject is a female and last row presents different subjects with poor image quality. The label of each image describes the age. . . . .	51
3.5	MORPH album2 samples. First row shows a male subject of same person at different age/illumination/position, second row also the same but the subject is a female. The label of each image describes the age. . . . .	53
3.6	PAL samples. First row shows a different male subjects at different age and race, second row for female. The label of each image describes age and race (African-American / Caucasian / Other). . . . .	54
3.7	Sample from social habits dataset that collected by Alarifi et. al. (Alarifi et al. 2017). The label of each image describes age and smoking status (Smoker or Non-smoker) . . . . .	54
3.8	Face detection: (a) Original image obtained from Social Habits dataset (Alarifi et al. 2017); (b) Facial landmark detection using Face++; and (c) Warped image. . . . .	55
3.9	Proposed methodology. . . . .	56
3.10	Scattering Transform Architecture. . . . .	63
3.11	Face mask with ten predefined wrinkle regions by (Ng et al. 2015a). . . . .	67
4.1	Dataset Samples. First row shows samples from Social habits dataset, where sccond raw for Sudanese dataset, and last row shows FERET samples. . . . .	69
4.2	Detection of wrinkle as region vs detection as line: (a) cropped forehead image, redrawn from Sudanese dataset; (b) wrinkle detection as a line using HLT (Ng et al. 2015b); and (c) detection of wrinkle region using our proposed method. . . . .	69
4.3	A global thresholding of matched filter response. Original image is redrawn from Social Habits dataset. T is a threshold value . . . . .	70
4.4	The effect of image enhancement step: (a) original images; (b) without CLAHE; (c) without filters; and (d) with filters . . . . .	71
4.5	(a) Original image redrawn from FERET; (b) HLT (Ng et al. 2015b); (c) Method in (Batoool & Chellappa 2015); and (d) Proposed method . . . . .	72
4.6	Wrinkle template. (a) Original images; (b) wrinkle template for wrinkles regions;and (c) Overlay the template on face image. . . . .	74
4.7	A graph illustrates the average wrinkles density versus the age groups. . . . .	77

4.8	A graph illustrates the average wrinkles density at each region. . . . .	77
4.9	Visual comparison of the wrinkles extracted from two participants. Left image: Wrinkles extracted from non-smoker at age 80. Right im- age: Wrinkles extracted from smoker at age 78 shows more prominent wrinkles in terms of depth and density. . . . .	78

# List of Abbreviations

AAM	Active Appearance Model
AGES	Aging Pattern Subspace
AI &R	Artificial Intelligence and Robotics
ASM	Angular Second Moment
BF score	Boundary F1 score
BIF	Bio-inspired Features
CACD	Cross-Age Celebrity Dataset
CBIF	Component Bio-Inspired Feature
CLAHE	Contrast limited adaptive histogram equalization
CNN	Convolutional Neural Networks
CSOHR	Cost-Sensitive Ordinal Hyperplanes Ranking
DAPP)	Directional Age-Primitive Pattern
ECRM	Electronic Customer Relationship Management
FAM	Facial Appearance Model
FERET	Face Recognition Technology Dataset
FG-NET	Face and Gesture Recognition Research Network Dataset
GLAAM	Global and Local feAture based Age estiMation
GLCM	Grey-level co-occurrence matrix
HAP	Hybrid Aging Patterns
HCI	Human Computer Interaction
HHF	Hybrid Hessian Filter
HLT	Hessian Line Tracking

HOIP	Human and Object Interaction Processing
IAD	Internet aging database
JSI	Jaccard Similarity Index
KLBP	Kernel-based Local Binary Patterns
KNN-SVR	K Nearest Neighbors Support Vector Regression
KPLS	kernel partial least squares
LARR	Locally Adjusted Robust Regression
LBP	Local Binary Patterns
LOWEX	Local Wrinkle-based Extractor
LPP	Locality Preserving Projections
LSDA	Locality Sensitive Discriminant Analysis
MAE	Mean Absolute Error
MAP	Multi-scale Aging Patterns
MAR	Multi-level Age Regression
MFA	Marginal Fisher Analysis
MLR	multiple linear regression
MORPH	Craniofacial Longitudinal Morphological Face Dataset
MPP	Marked Point Process
MWP	Multi-scale Wrinkle Patterns
NPP	Neighborhood Preserving Projections
OLPP	Orthogonal Locality Preserving Projections
OLS	ordinary least-square
OR-CNN	Ordinal Ranking - Convolutional Neural Networks
PAL	Park Aging Mind Laboratory Dataset
PCA	Principal Component Analysis

PLS	Partial least-squares
QF	Quadratic Function
sAM	supervised Appearance Model
SMO	Sequential Minimal Optimization
ST	Scattering Transform
STD	Standard Deviation
SVM	Support Vector Machine
SVR	Support Vector Regression
TTF	Topological Texture Features
UVR	Ultraviolet Radiation
YGA	Yahama Gender and Age

## List of Publications

- PUB1                      Osman, O.F., Elbashir, R.M.I., Abbass, I.E., Kendrick, C., Goyal, M., Yap, M.H.: Automated assessment of facial wrinkling: A case study on the effect of smoking. In: 2017 IEEE International Conference on Systems, Man, and Cybernetics (SMC). pp. 1081–1086 (Oct 2017). <https://doi.org/10.1109/SMC.2017.8122755>.
- PUB2                      O. F. Osman and M. H. Yap (2018), "Computational Intelligence in Automatic Face Age Estimation: A Survey," IEEE Transactions on Emerging Topics in Computational Intelligence, Vol. 2, issue 5.
- PUB3                      Omaima FathElrahman Osman (2020), "An effective age estimation method using scattering transform," International Journal of New Technology and Research, Vol,5, issue 6.





# Chapter 1

## Introduction

### 1.1 Background

Human face contains large amount of information related to personal characteristics, including identification, emotion, age, gender and race. This information has been used extensively in the face-based human-computer interaction (HCI) systems capable of interpreting the facial information found in human-to-human-communication (Choi et al. 2011).

Recently, with the increasing demand of automatic recognition and surveillance systems, research on human faces such as face recognition, face detection, facial expression recognition and gender classification, have attracted significant attention in both computer vision and pattern recognition (Chao et al. 2013).

Compared to these face related research, face age estimation is one of the popular research topics. It is an important technique that used in many real-world applications. Facial age estimation can be defined as: Label a face image automatically with the exact age (year) or the age group (year range) of the individual face (Geng et al. 2010). By extracting important features from faces of known ages, the age can be estimated for an individual face by solving the inverse problem using the same feature extraction technique (Ng et al. 2014b).

Age is one of the basic information that could use to enhance communication between people, because individuals have different preferences at different ages. Age estimation can be used in: access control and monitoring, complementary to soft biometric, electronic customer relationship management and entertainment. For example, in access control, some companies use the age estimation system and developed a vending machine with the property of preventing anyone under the legal age from buying cigarettes (*Japanese smokers to face age test* n.d.). In general, automatic age

estimation is useful in applications where we do not need to specifically identify the user, but want to know his or her age when accessing restricted content.

Although there are several techniques that are used in a literature to solve age estimation problem, it is yet largely unsolved and remained a challenging issue, because it is affected mainly by human aging process, including different changes in human face. In addition to these normal changes, there are many external factors such as environmental influence, solar radiation, lifestyle, disease, drug use, and psychological stress that can have effect on face aging process and make it uncontrollable and personalized process. The majority of the works on age estimation applied dimensionality reduction after extracting features. However, some valuable parts of the data (such as wrinkles) that represent discriminatory features might have been lost during dimensionality reduction process (Ng et al. 2014*b*). In addition, wrinkle-based representation researches is limited and the wrinkle detection methods that used have a poor detection. Also, most of existing computerized wrinkle detection algorithms extract wrinkle as one line pixel instead of wrinkle region, and evaluated using datasets that are either western, Chinese or Japanese, no other skin type (such as Sudanese) is used in the literature.

Age estimation systems are generally designed to use two steps: an aging feature extraction and a feature classification. Feature extraction is very important in age estimation, since the extracted features greatly affect the classification performance. For this reason, a great deal of effort has been directed towards the extraction of discriminative aging features.

## 1.2 Problem Statement

In addition to the limited number of researches in using wrinkles for face age estimation, the majority of the works on age estimation applied dimensionality reduction after extracting features, which lost some valuable information such as wrinkle.

The accuracy of age estimation process can be affected by several factors, smoking is one of the most influential factors in age estimation process (Fu et al. 2010). It can increase the risk of premature wrinkle development and the other side-effects on health (Just et al. 2007, Cope 2013, Strack & Wyrick 2012). However, there is no research that studies the effect of smoking on computerized age estimation algorithms using input face images for smokers. Due to the limited number of research in using wrinkles for face age estimation (Ng et al. 2015*a*), it is difficult to establish the association of smoking and other social habits with facial aging.

### 1.3 Research Aim and Objectives

This research aims to propose a new features representation method and investigate the discriminative power of wrinkle and other local features to estimate the age accurately. In order to achieve the primary aim, the following objectives have been established:

1. Collect data from smokers and non-smokers to establish a new Sudanese dataset and make it publicly available.
2. Develop a new method for wrinkles detection, that detect wrinkle as a region rather than one pixel line.
3. Develop new feature descriptors for face age estimation, based on wrinkle and other local features.
4. Evaluate the performance of the proposed algorithm with benchmark algorithms using the benchmark datasets and our collected dataset.

### 1.4 Research Methodology

Many steps were done to overcome the problem discussed in section 1.2. Firstly, the dataset was collected and acquired, in this step a Sudanese dataset was collected, and publicly available datasets was acquired. Secondly, pre-processing steps was done to prepare this data to used in next steps. Pre-processing steps include: face detection and alignment, image enhancement. Thirdly, a new feature descriptor was proposed which called Wrinkle Local-based Descriptor (WLD) to represent aging features. Where the combination of wrinkle and other local features were used to represent the age. Wrinkles was detected using the proposed wrinkle detection algorithm then wrinkle pattern was constructed using wrinkle location, intensity and density. Where Scattering Transform (ST) was introduced to represent local features. Then a combination of wrinkle and other local features were used as a new feature descriptor to represent the aging pattern. Finally, the age was predicted and evaluated using benchmark datasets and our collected dataset.

### 1.5 Expected Contributions

The fundamental contributions of this thesis are:

1. A new wrinkle detection method was proposed. Based on a Gaussian kernel the wrinkle regions (not line pixel) was localized. To segment these localized regions an adaptive thresholding technique was introduced for a first time for wrinkle regions segmentation.
2. A new wrinkle-based features descriptor was proposed for age estimation.
3. A new features descriptor, based on scattering transform and wrinkle pattern was proposed to estimate the age.
4. The performance of age estimation method was evaluated using our collected Sudanese dataset, this may insight future direction to Sudanese researchers to collect more data and develop our face analysis applications that can be useful for Sudanese companies and for a public.

In addition to scientific contribution, this research has a social contribution. Investigated the effect of smoking on the facial wrinkling, which have a direct effect on age estimation, this make people aware of the side-effects of smoking on their appearance. Although facial wrinkles are not a deadly condition, but some of social research suggests that people may perceive the development of facial wrinkles as a threat serious enough to consider quitting smoking (Strack & Wyrick 2012, Grogan et al. 2011, Campanile et al. 1998).

## 1.6 Thesis Organisation

This thesis is organized into six chapters as follow:

Chapter 1 provides an overview of this thesis, including Problem Statement, Aim and Objectives. It further summarizes the research methodology and highlights the contributions made by the thesis to the state of the art. Finally it outlines the thesis organization.

Chapter 2 presents a basic knowledge about the conventional ways of age estimation and wrinkle detection, aging process, the challenges in face age images and different age estimation methods. It is also compared and discussed advantages and disadvantages of each approach.

Chapter 3 provides an overview of the research methodology. It further highlights methods and techniques being applied for all steps in order to estimate the age.

Chapter 4 include the experimental results and discussion.

Finally, Chapter 5 concludes the thesis with a summary of contributions made by this thesis, limitations of the present context of research and an insight into future directions of research.

# Chapter 2

## Literature Review

### 2.1 Introduction

In human communication, face is the first source that provide different information about a person such as age, gender, expression and ethnicity, to facilitating human-to-human communication. The researchers in computer vision field developed face analysis applications from input face images such as face recognition (Meyers & Wolf 2008), facial expression recognition (Sarode & Bhatia 2010) and gender classification (Wang, Ricanek, Chen & Chang 2010) to improve human-computer interaction. Face age estimation is one of these application which is grown considerably recent and used in many real-world applications.

Face age estimation means "label a face image automatically with the exact age (eg. 20 year) or the age group (eg. young, adult) of the individual face" (Fu et al. 2010). The goal of automatic age estimation is to estimate age that is as close to actual or appearance age as possible. Where these types of ages can be defined (Geng et al. 2010) as :

1. Actual or real age which is the number of years that a person has lived.
2. Appearance age is the age information revealed by the visual appearance.
3. Perceived age is the individual age recognized by human subjects.
4. Estimated age is the individual age recognized by computer.

Age estimation is a complex process because it is affected mainly by human aging process, which can be described as uncontrolled and personalized process (Albert et al. 2007).

Age estimation is an important technique that used by many real-world applications

such as security control and monitoring, soft biometrics, Electronic Customer Relationship Management (ECRM), and forensic art, the details of these applications were found in next section. (Fu et al. 2010).

## 2.2 Real-World Applications

In the real world, human faces have always been considered as the first source of information during human communication. Various information can be gathered from person's face, such as age, gender, expression, ethnicity and identity, this can influence communication between people. According to evolution in HCI field, the researchers focus on human face analysis to develop natural user interfaces based on facial characteristics in order to offer natural Human-Computer interaction. As a result, researchers developed a lot of research depend on facial characteristics such as face recognition (Meyers & Wolf 2008, Han et al. 2012), facial expression recognition (Sarode & Bhatia 2010), age estimation (Osman & Yap 2018), race classification and gender classification (Wang, Ricanek, Chen & Chang 2010). Therefore, person identification from face images is required in many real-world applications (El Dib 2011).

Age estimation is useful in many real-world applications such as Access Control and Monitoring, Soft Biometric, Electronic Customer Relationship Management and Entertainment. This section describes the potential applications of age estimation.

### 2.2.1 Access Control and Monitoring

A robust access control and monitoring system are becoming more and more crucial in daily life, an accurate age estimation system can prevent children from entering to unauthorized places or websites, when a monitoring camera is used with the system (Fu et al. 2010), and prevent child and adult seniors from using danger games in a theme park (El Dib 2011). To control access in a cigarette vending machine, some Japanese company developed vending machine that check a user age by counting wrinkles and skin sags to prevent anyone under the legal age (20 years old) from buying a cigarette (*Japanese smokers to face age test* n.d.). Age estimation system also can be used in health care systems for customized services such as robotic nurse and intelligent intensive care unit (Fu et al. 2010). Age estimation as a soft biometrics can be used to improve the recognition accuracies in basic biometric system (face, fingerprints) (Dantcheva et al. 2016).



## 2.2.2 Electronic Customer Relationship Management (ECRM)

The effective marketing strategy which called ECRM, can benefits from age estimation systems by targeting specific customers in same age group for specific advertisements (KLOEPPEL 2010). It can provide important information for marketing study such as: the number of young and adult customers have visited a mall and what is a preferences of each age group (Guo 2012). However, it is difficult to realise these information while retaining privacy, but using automatic age estimation system can help to perform this task easily without violating the human privacy, where the face image of customer can be captured then classify the age and delete the images immediately (Fu et al. 2010).

## 2.2.3 Entertainment

Recently, age estimation system is introduced as application in some smartphone for **Entertainment** purposes such as iPhone Age Detector, when there are many photos and videos are captured, using age information can organize the images to make it easy to access and find the related images when needed (Automatic album management) (Guo 2012). This also can be used for age-based image and video retrieval systems (information retrieval), where users could have the ability to restore their images by determining a wanted age-group in e-photo albums.

Age estimation also can be used with age synthesis in **Forensic Art** to find lost people, when the photos of missing children or any other family members are outdated, the system can predict the age and use age synthesis to produce updated face image (Scherbaum et al. 2007). In HCI systems, computer interface can use a face image, classify the age and setup a workspace automatically according to the user's age group (Fu et al. 2010).

These applications highlight the contribution of age estimation in the real world and showed the importance of this topic and why it still needs more research to improve the accuracy of age estimation algorithms.

## 2.3 Face Aging Process

Facial aging is a dynamic process involving the aging of bony structures and soft-tissue. Facial aging result from: gravity, soft tissue maturation, skeletal remodeling, muscular facial activity, solar and stomognathic system changes. Some aspects of aging are fairly uncontrollable, and these are largely based on hereditary factors.



Figure 2.1: Face aging process in a male subject. Redrawn from FG-NET (Panis et al. 2015).

Other factors are somewhat controllable and are largely the result of exposure to the elements and harmful habits (Sveikata et al. 2011). Aging can be described as slow, relentless and irreversible process. Although aging it occurs at different rates from individual to individual as well as in each person at any given time, there are still some general changes and resemblances can be described. The most changes that appear during formative years is shape change, where the great changes that appear in adult is texture changes (Stone n.d.). Figure 2.1 shows face aging for male subject. Generally, there are two growth stages which make obvious changes in the human face: childhood and adulthood, the following sections described these stages.

### 2.3.1 Childhood Aging

In this stage the great changes that appear is a shape change ( cranium growth). In cranium growth through the 2-18 year, the skull is growth, bloc stoops back and make space on the skull surface. Nose, eyes, ear, and mouth are expanding and cover these spaces, cheeks extend to chin, skin color may change. cranium growth changes might continue to change until thirty (Fu et al. 2010). Albert et al. (Albert et al. 2007) reported that the horizontal changes in cranium is increase from 1.1 mm to 1.60 mm, and vertical changes increase by 1.60 mm. The facial skin relatively does not change too much compared with the cranium growth. But facial hairs, such as a mustache, may become dense and even bushy (Fu et al. 2010).

During formative years, geometry information known as anthropometric model was used for age classification and synthesis. Face anthropometry is the science of measuring sizes and proportions on human faces, it played a crucial role in developing facial aging models (Ramanathan et al. 2009). Farkas (Farkas 1994) provides a comprehensive overview of face anthropometry and its significant applications. He defines face anthropometry in terms of measurements taken from 57 carefully selected

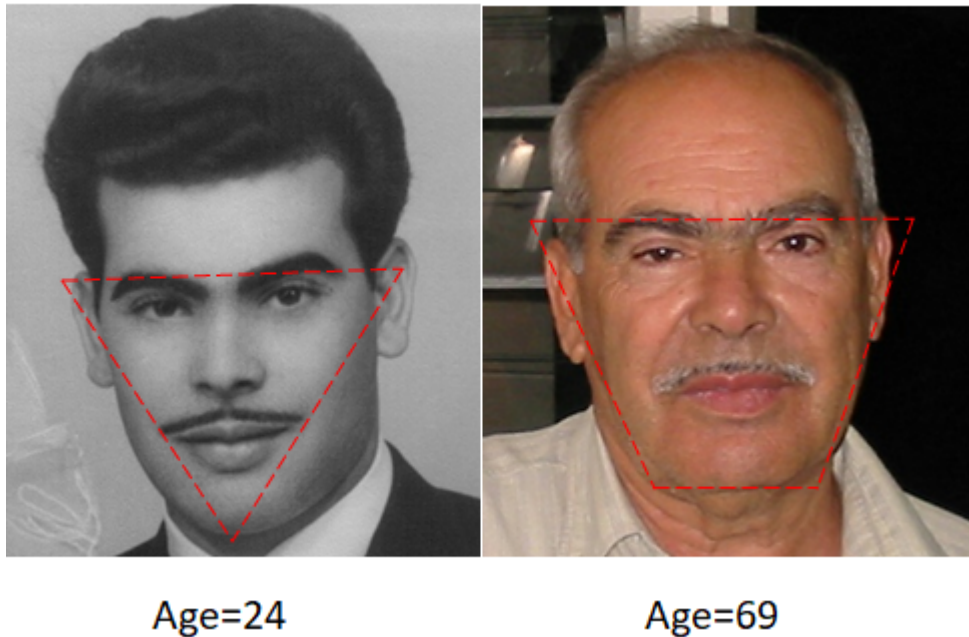


Figure 2.2: Face shape changes. The images for the same subject at different aging stages. Redrawn from FG-NET (Panis et al. 2015).

landmarks on human faces spread across 6 regions in the craniofacial complex (head, face, orbits, nose, lips and mouth, ear).

### 2.3.2 Adulthood Aging

In this stage the shape continues to change but less than in the previous stage. The skin loses its elasticity and skin tone, which eventually leads to fine and coarse wrinkles in Cheeks, eyelids, nose and chin. Dynamic wrinkles and folds due to muscle motion also become more distinct. The surface of skin might become rough and dry. Gravity causes stretching and looseness (laxity) in the supporting ligaments (flexible bands of tissues) of the face. As a result, the forehead and eyebrows droop, and folds of skin develop on the eyelid. Fat in the cheeks also droops, which results in deepening of the smile lines and the formation of jowls. The neck begins to sag and develops neck bands (KLOEPPEL 2010, Albert et al. 2007). Although the craniofacial growth is not dramatic during this stage, the facial geometry change is still evident up to 80 years (Stone n.d.), as shown in Figure 2.2.

During the 50s age group lower eyelid bags appear, glabellar (between the eyebrows) and forehead wrinkles appear. The outer brows begin to droop. Cheek fat begins to descend downward towards the jawline. Redundant neck skin begins to appear. Facial fat atrophy or wasting becomes evident with concavity of the sur-

Table 2.1: Facial appearance changes for different age groups.

Age range	Probable facial appearance changes
20-30	Slight craniofacial skeletal growth. Upper eyelid drooping begins. Eyes appear smaller. Nasolabial lines begin to form. Lateral orbital lines begin to form. Upper lip retrusion begins in females.
30-40	Circumoral striae begin to form. Lines begin to form from lateral edges of nose to lateral edges of mouth. Upper lip thickness decreasing.
40-50	Craniofacial skeletal remodeling progresses. Facial lines and folds continue to increase in depth. Nose and chin positioning affected as dental arch lengths decrease. Most profound morphological changes of the head, face, and neck are evident.
50-60	Facial lines and folds continue to increase in depth. Protuberance of nose and ears due to greater craniofacial convexity.
> 60	Decrease in craniofacial size. Protuberance of nose and ears continues. Concave appearance in cheek hollows due to alveolar bone remodeling. Diminished jaws.

face contour in the temple area and cheeks appearing. In some individuals the eyes become sunken as a result of fat atrophy rather than forming eyelid bags. Neck wrinkles, jowls (broken jawline), and marionette lines appear, the nasal tip droops. The lips thin so there is less dry vermillion (pink area where lipstick is applied) showing and perioral wrinkles appear. Platysmal banding appears in the neck. In age group more than 70 year old the facial skin thins, fat atrophies in the cheek and temples and skin pigment cells increase in number and size in a blotchy pattern giving rise to brown spots of the back of hand and face (senile lentigo). Face aging during this age period may cause the loss of flexible control of facial muscles and consequently the facial movements and behaviors may also change unintentionally (Stone n.d.). Table 2.1 shows facial appearance changes for different age groups, where the appearance changes starts from 20s with fine facial lines (Albert et al. 2007).

### 2.3.2.1 Wrinkle

In general, wrinkle can distinguish in to two types: fine-scale wrinkles are small wrinkles that cover the entire skin surface and large-scale wrinkles are distinct wrinkles unique to a particular body part (e.g., forehead wrinkles). Fine-scale wrinkles have a similar structure over the entire body except palms and soles in the sense that

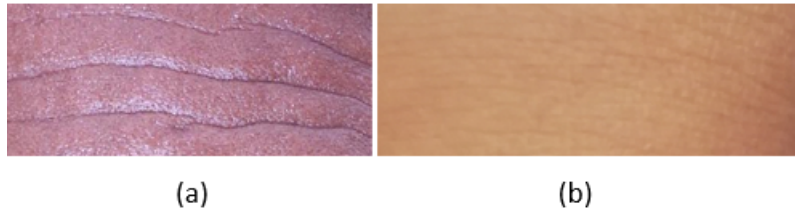


Figure 2.3: Fine-scale vs large-scale wrinkles. (a) Forehead wrinkle, redrawn from our in-house dataset; (b) Fine-scale wrinkles on the back of the hand

their furrows intersect each other over the surface. They are due to the atrophy of the collagen bundles both in the reticular dermis and the hypo-dermal connective tissue strands. Large-scale wrinkles are formed due to shrinking of the skin surface caused by body part movement. Skin material itself is incompressible, and therefore, when the skin surface shrinks, the excess skin buckles and forms wrinkles. These become gradually more prominent with repeated wrinkling and age. As shown in Figure 2.3, it is clear that in a large-scale wrinkle (Figure 2.3 (a)) each has a sharp furrow at its center line and round bulges on its both sides (Bando et al. 2002).

Xie et al. (Xie et al. 2016) divided face wrinkles into two categories, permanent and transient wrinkles. Permanent wrinkles are usually located on the faces of the aged person, whereas transient wrinkles appear in a relatively wide region when the expression is generated, such as in the cheek region. Figure 2.4 shows permanent and transient wrinkles.

Face is part of the body most visible to others, and its wrinkles are a hallmark of aging. Wrinkles have been widely investigated earlier for face age classification to classify adults group (Kwon & Lobo 1994, Kwon & da Vitoria Lobo 1999, Ramanathan & Chellappa 2006). Recently, some researchers investigated the effect of wrinkles for age estimation (Aznar-Casanova et al. 2010, Ng et al. 2014b, 2015a), they found that the number of wrinkles and the depth of furrows had a great effect on facial age estimation.

### 2.3.3 Facial Aging Factor

Aging is a process in which both intrinsic and extrinsic determinants lead progressively to a loss of structural integrity and physiological function. Intrinsic aging of the skin occurs inevitably as a natural consequence of physiological changes over time at variable yet inalterable genetically determined rates. Extrinsic factors are, to varying degrees, controllable and include environmental factors, such as exposure to sunlight,

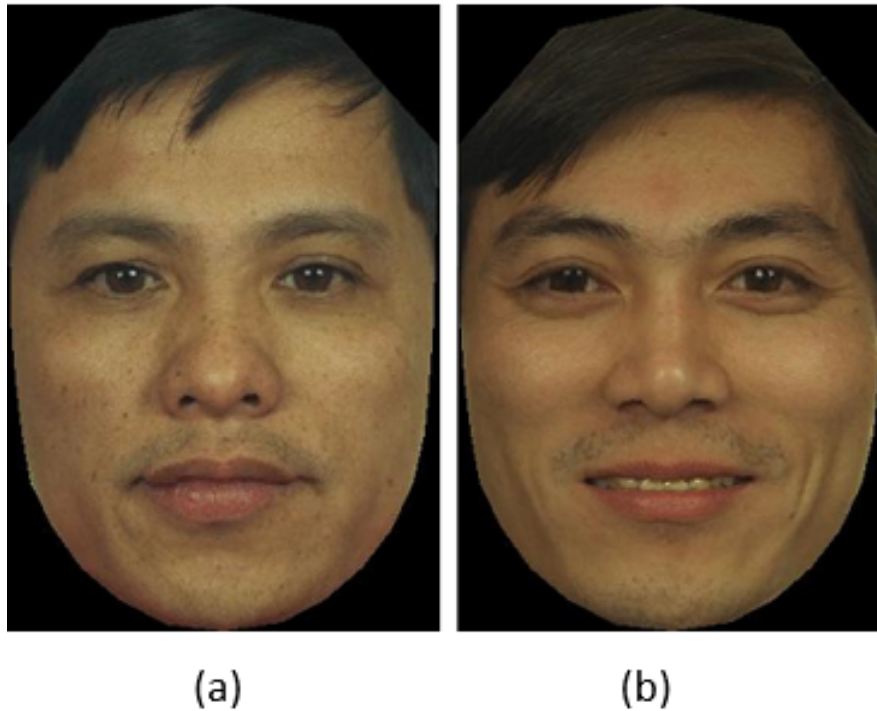


Figure 2.4: Permanent vs transient wrinkles. (a) Permanent wrinkle; (b) Transient wrinkle. Images were redrawn from FERET (Phillips et al. 1996)

pollution, disease, diet, cosmetic surgery, smoking and stress (Farage et al. 2008). The synergistic effects of intrinsic and extrinsic aging factors over the human lifespan produce deterioration of the cutaneous barrier (Friedman 2005). The influence of these factors makes the task of accurately capturing aging patterns more difficult, thus the aging process is described as uncontrollable and personalized process, which complicated the automatic age estimation (Fu et al. 2010). Following are the discussion of the two major factors of aging: intrinsic and extrinsic.

### 2.3.3.1 Intrinsic Aging Factors

Intrinsic aging of the skin occurs inevitably as a natural consequence of physiological changes over time at variable yet inalterable genetically determined rates (Farage et al. 2008). Some natural factors that causes this changes are: gravity, soft tissue maturation, skeletal remodeling, muscular facial activity, hyper-dynamic facial expressions, and stomatognathic system changes. Gravity and the longitudinal pull of muscles cause drooping or sagging of the skin and deeper structures of the cheeks, eyelids, nose, chin, legs etc. from areas of deeper attachment, the result is wrinkles and jowls in the face (KLOEPPPEL 2010). The greatest effect of ethnicity on aging

is primarily related to differences in pigmentation, which may contribute to more resistance to aging. Wrinkling in Asians has been documented to occur later and with less severity than in Caucasians (*Novel Aspects of Intrinsic and Extrinsic Aging of Human Skin: Beneficial Effects of Soy Extract* [n.d.]). Other changes related to advancing age include loss of tissue elasticity and facial volume and alterations in skin texture (Stone n.d.).

Wang et al. (Wang et al. 2013) studied influences of gender and race in age estimation. They conducted several experiments with and without gender and/or race classification. They found that the performance of age estimation was significantly increase with the pre-classification for gender and race.

### **2.3.3.2 Extrinsic Aging Factors**

Extrinsic factors are, to varying degrees, controllable and include environmental factors, such as lifestyle influence, exposure to sunlight, pollution, disease, diet, cosmetic surgery, smoking and stress (Albert et al. 2007, CLATICI et al. 2017). Skin is affected by ambient conditions such as temperature and humidity. Smoking was demonstrated to be an independent risk factor for premature wrinkling even when age, sun exposure and pigmentation were controlled. The decreased moisture in the stratum corneum of the face contributes to facial wrinkling due to direct toxicity of the smoke. Pursing the lips during smoking with contraction of the facial muscles and squinting due to eye irritation from the smoke might cause the formation of wrinkles around the mouth and eyes (crows feet) (Morita 2007). Yin et al. (Yin et al. 2001) found that the wrinkle depth is significantly more prominent in smokers with a smoking history of at least 35 pack per year than nonsmokers. The effects of Ultraviolet Radiation (UVR), usually through exposure to sunlight on the skin are profound, and are estimated to account for up to 90% of visible skin aging (Farage et al. 2008).

The effect of cosmetics on age estimation was studied by Chen et al. (Chen, Dantcheva & Ross 2014). Their experiments were conducted using a dataset that was collected for a study on the effect of makeup and cosmetics on automatic face recognition. They summarized that cosmetics can reduce the performance of automatic age estimation. To reduce the influence of cosmetics on face recognition tasks, Chen et al. (Chen et al. 2013) proposed a method to detect facial makeup automatically. After detected the makeup, a preprocessing step was applied to mitigate the impact of makeup. In contrast to the makeup that often used by people to look younger, smoking makes people look older. Both clinical and computerized studies

shows that smoking has a significant impact on age estimation, where the number and depth of wrinkles is increased with smoking that caused people look older.

## 2.4 Face Aging Database

There are different types of datasets that used in previous work on face age estimation such as CACD (Chen, Chen & Hsu 2014), FERET (Phillips et al. 1996), FG-NET (Panis et al. 2015, Günay & Nabiyeve 2015), MORPH (Ricanek Jr & Tesafaye 2006, *MORPH Database* n.d.), PAL (Minear & Park 2004), YGA (Fu et al. 2007, Guo, Mu, Fu, Dyer & Huang 2009), WIT (Ueki et al. 2006), HOIP (Fukai et al. 2011, Fu et al. 2010), AI &R (Fu et al. 2010, Fu & Zheng 2006), IAD (Ni et al. 2009), Iranian (Bastanfard et al. 2007) and LHI (Suo et al. 2007).

However, most of these datasets are not publicly available. The available datasets that provide a large amount of face image with accurate age information are: FG-NET, FERET, MORPH, PAL, CACD, Iranian face dataset (only male images are available). The FG-NET is a baseline dataset that used to compare new age estimation algorithms with many existing algorithms, it contains images for infants and also contains a series of images for individuals during different age progression stages. However, the FG-NET images are collected by scanning photographs, thus there are very large variations in resolution, background, illumination, and noise from scanning, this might complicate the detecting of texture information such as wrinkles.

MORPH is the benchmark database that contains huge number of images, it is a collection of mugshot images, including information about ethnic, gender, date of birth, and date of acquisition. 42,589 images from a total of images in MORPH (55,134) is African, others are European, Asian and Hispanic. FERET images were collected in a controlled environment and the resolution of images is high if compared to FG-NET and MORPH, hence it is more suitable when texture information is needed. PAL database contains wide age range especially for adult, it contains images for subject till 93 years old, which is important for research on aging, also the resolution of images is high. However, MORPH, FERET and PAL do not contain face images in childhood. Some databases do not include different ethnicity such as YGA, AI&R, and LHI are datasets for Asian subjects, and WIT contains only Japanese people.

Capturing face images in different ages for the same subject it is a big challenge in data collection. In some databases such as YGA, MORPH and LHI capture one or a small number of images for each subject. However, the databases that have a



Table 2.2: Summary of face aging databases.

Name	Number of Images	Number of Subjects	Age Range	Age Type	Status	Ethnicity	Expression
CACD	163,446	2,000	16-62	real Age	Public	Yes	Yes
FERET	14,126	1199	10-70	real Age	Public	Yes	Yes
FG-NET	1,002	82	0-69	real Age	Public	Yes	Yes
MORPH2	55,134	13,000	16-77	real Age	Public	Yes	Yes
PAL	1,142	576	18-93	Age Range	Public	Yes	No
YGA	8000	1600	0-93	real Age	Private	Asian	Yes
WIT	26,222	5,500	3-85	Age Range	Private	Japanese	No
AI&R (V2.0)	34	17	22-61	Age Range	Private	Asian	yes
HOIP	306,600	300	15-64	Age Range	Private	Japanese	No
Iranian	3,600	616	1-90	real Age	Private	Middle-East	Yes
LHI	8,000	8,000	9-89	real Age	Private	Asian	no
IAD	219,892	-	1-80	real Age	Private	Yes	Yes

limited number of face images to each subject might not be good to use for the age progression algorithms (Guo 2012), FG-NET have 10 images per subject, and WIT captures 1 - 14 image samples from each individual. AI&R database include limited number of face images. Some of these databases were collected in a wider age range such as FG-NET and YGA.

CACD is the largest publicly available databases that used recently in age estimation, face recognition and retrieval across age research (Chen, Chen & Hsu 2014), it contains images for a large number of celebrities that collected from Internet across ten years. However, this dataset does not include face images with age of 10 or younger. Even though Internet is a good platform for data collection, it is very hard to label the ground-truth age in web collected databases or the ground-truth age might not be accurate. In addition, the data that collected from the Internet could be noisy.

Although there are a number of datasets for age estimation, but a large dataset with balanced distribution of individuals, ethnicity, gender, and age range it is still needed. Table 2.2 provides a summary and a comparison of different face aging databases. Details about some of these datasets will be presented in chapter 3.

## 2.5 Wrinkle Detection Techniques

Wrinkles can be defined as a small furrows appear on the facial skin as a natural result of aging or from expression (Ng et al. 2015*b*). With a rapid growth of face analysis research, an accurate detection of wrinkles has an important role in many face analysis applications, including age estimation and synthesis, recognition across aging (Fu et al. 2010), soft biometrics (Batool et al. 2013), cosmetic and facial retouching (Batool & Chellappa 2014), expression recognition, simulation, and animation (Xie et al. 2016).

Aznar et al.(Aznar-Casanova et al. 2010) investigated the effectiveness of wrinkle in **facial age estimation**, they found that the number and depth of wrinkles has a clear effect on age estimation. Osman and Yap (Osman & Yap 2018) discussed several works that focus on wrinkles as one of the features that can increase the accuracy of age estimation algorithms.

Batool and Chellappa. (Batool et al. 2013) assessed the possibility of wrinkle pattern(specifically in forehead) to be as one of the **soft biometrics**. They stated that different subjects might have a similar wrinkle curve in a same area, but it is difficult to have set of wrinkles (pattern) in such area. They conducted their experiment on both manually and automatically detected wrinkles. For automatic detection they used Marked Point Processes(MPP) (Batool & Chellappa 2012). However, due to the challenges in automatic wrinkle detection, the recognition rate of manually detected wrinkle yielded a better results than automatic detection.

Wrinkle detection can be used in **media and entertainment industry**. In this area, Batool and Chellappa (Batool & Chellappa 2014) applied wrinkle detection as one of steps for retouching of facial skin. They claimed that the wrinkle can removed efficiently after detecting it instead of being blended or blurred. They stated that wrinkle creates a valley and causes curvature in the surrounding skin resulting a specific intensity gradients in skin which look like discontinuities in surrounding skin textures. As a result, an efficient wrinkle inpainting process must remove wrinkle region (wrinkle line and the surrounding curved skin area).

In 1989 Grove et al.(Grove et al. 1989) introduced the use of skin silicone replicas to analyzed and evaluated the effect of topical agents on facial lines and wrinkles. They stated that Silicone rubber impression materials can be used to make a mold of the skin that faithfully captures the surface topography. After taking the skin surface replicas they applied digital image processing techniques to assess facial lines and wrinkles. They found that there is strong association exists between the evolution of

wrinkles in the crow's-feet region and the degree of past sun exposure after controlling for age and smoking history.

Recently, several wrinkles detection methods have been proposed and evaluated in literatures, most of these methods can be classified into two classes: edge-based detection method and curvilinear-based (curve or line). In 1999, Kwon and Lobo (Kwon & da Vitoria Lobo 1999) applied snakelets-based methods and extract wrinkle as small snake segment. They used wrinkle feature for age classification to differentiate young from adults. The wrinkles were extracted from several regions, such as on the forehead, after the eyes, and near the cheek bones. A wrinkle geography map drops multiple snakelets in polygonal regions, where wrinkles may typically be found. The presence of wrinkles in a region is based on the detection of curves in that region, if any curve was found then the region was classified as a wrinkle. They focus on forehead wrinkle, next to the eyes and near the cheek bones. Although, some noise appear as curve, it was detected as a wrinkle. They complicated the detection by applying multiple thresholds.

In (Hayashi et al. 2002), (Horng et al. 2001) and (Ng et al. 2014b) edge detection methods were applied to extract wrinkle. Hayashi et al. (Hayashi et al. 2002) applied density and accumulated histogram to enhance wrinkle region, then edge detection method, thinning process and Hough transform were applied for final wrinkle modeling. Horng et al. (Horng et al. 2001) used Sobel operator to localize wrinkles in forehead, two eye corners, and two cheeks.

Ng et al.(Ng et al. 2014b) investigated the efficiency of wrinkle in age estimation. They divided image into 12 different regions, then Canny operator was used to detect the wrinkles from these regions. The detected wrinkles presented as a pattern to classify age into two groups. They found that the number of wrinkles has a clear effect on age group classification. However, edge-based detection methods is inefficient because wrinkles cannot be treated as an edge. Wrinkle appear as a line segment -rather than a boundary- that have a specific intensity gradients than their neighborhood. Although edge operators can well point the intensity gradients, it cannot distinguish between intensity gradients caused by wrinkles, illumination variation and other factors (Batool & Chellappa 2012).

As a curvilinear-based methods, Batool and Chellappa (Batool & Chellappa 2012) modeled wrinkles as line segments using Marked Point Process (MPP). They stated three significant observations about wrinkles: (1) wrinkles cannot be detected well as texture feature using general texture feature extraction methods; (2) wrinkle cannot be detect using edge detection method which produce wrinkle boundaries rather

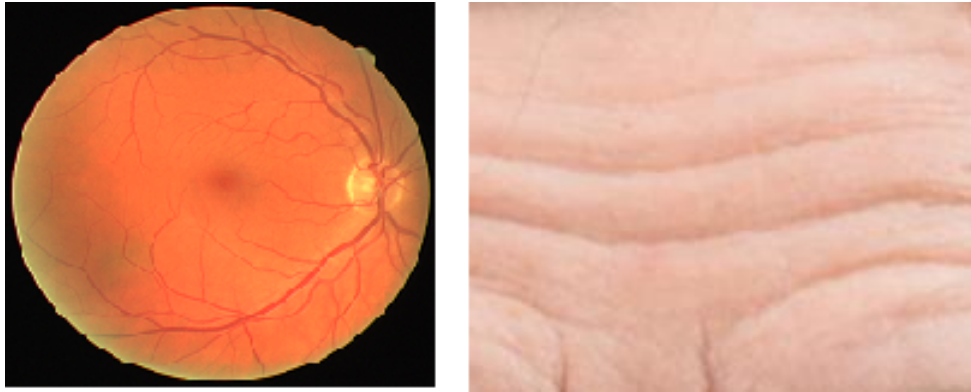


Figure 2.5: Blood vessel in retinal image versus wrinkle image. Retinal image was obtained from DRIVE dataset (Mapayi et al. 2015), and wrinkle image from (Alarifi et al. 2017).

than wrinkle; (3) wrinkles appear as continuous and discontinuous curvilinear in skin texture. However, in this work only coarse and continuous wrinkles were detected.

In 2014, Ng et al.(Ng et al. 2014a) stated that wrinkles and blood vessel in retinal image have a similar line patterns, this is shown clearly in Figure 2.5. Based on this observation they introduced a vessel based enhancement filter for wrinkle localizations, their proposed method called hybrid Hessian filter (HHF), it composed of the directional gradient and Hessian matrix. The authors stated that this method was introduced basically to overcome the poor localization of wrinkles, and is deal with illumination variation problem and pepper noise. Although HHF yielded a good result, the detection is closed to forehead and focus on coarse wrinkle.

Batool and Chellappa. (Batool & Chellappa 2015) applied Gabor filter bank with specific parameter values to enhance the wrinkle curvilinear, they follow this step by using image morphology instead of simple threshold technique to segment enhanced curvilinear shapes. They stated that Gabor filter bank highlighted the wrinkle curvilinear efficiently, but a simple thresholding technique (with threshold value of 0.5) produce a result where the wrinkles are not well localized as curves. Based on their assumption that wrinkle is continuous, they trace wrinkle curves from key wrinkle sites. based on the direction of the connected segment, it searched around each end point of the connected segment and the pixel was joined to a wrinkle segment if a neighboring point is found at the end of a segment, this process was repeated for 30 iterations. However, the process of finding the extension of wrinkle curves from key wrinkle sites increase the computation time. In addition, this method unverified using available datasets that used by state-of-the-arts methods.

In 2015 Ng et al. (Ng et al. 2015b) extended HHF and proposed Hessian Line Tracking (HLT) to overcome the weakness in HHF by detecting fine wrinkles. HLT applied a multi-scale segmentation technique to track wrinkle lines based on neighbourhood properties. The image was processed using HHF firstly, based on the produced Hessian matrix the ridge area was chosen to be the started point of line tracking(which called it Seeding process), 10 different scales were used in order to detect coarse and fine wrinkle. Although HLT achieved 84% for JSI, applying HLT with 10 scales for all seeds increase the computational cost. However, the work in (Batool & Chellappa 2012, Ng et al. 2014a, Batool & Chellappa 2015, Ng et al. 2015b) applied thinning process and displayed the detected wrinkle in one pixel.

In 2018 Yap et al. (Yap et al. 2018) developed an automated facial wrinkles annotator based on HHF to annotate coarse and fine wrinkles regions, and provide wrinkles depth information by generating a probabilistic wrinkle map. They stated that their automatic annotator can be used to generate the ground truth efficiently than manual annotation. In this work (Yap et al. 2018).

Cula et al. (Cula et al. 2013) detected a forehead wrinkle automatically using Gabor filter responses. They stated that wrinkle appear in images as line segments rather than continuous lines, and present linear surface irregularities similar to the fingerprints. Based on the observation they applied image enhancement techniques as in fingerprints to remove noise and to increase contrast. They also stated that wrinkle detection is more difficult than fingerprint detection because the appearance of wrinkles is more varied and significantly noisier, whereas fingerprint features appear as continuous lines with almost constant thickness and frequency. They developed a quantification method combined wrinkle depth information obtained from filter responses and wrinkle length. they claimed that combining wrinkle depth and length provides better assessment of degree of facial wrinkling. However, the correctness of wrinkle detection is not validated with the ground truth information.

Due to the manual generation of the ground truth for wrinkle which used to evaluated the effectiveness of the automatic algorithms, deep learning has not been used before to solve wrinkle detection problem. Manual annotation of wrinkle that used traditionally in the previous works Batool & Chellappa (2015)Batool et al. (2013)Batool & Chellappa (2014)Ng et al. (2014a)Ng et al. (2015b) to generate the ground truth is complex and time consuming process, it is difficult to apply it for a hug dataset that needed for deep learning.

Wrinkles detection is a challenging task. following are some factors that might complicate the detection of wrinkles (Batool & Chellappa 2015).

1. Very light wrinkles. The most common reason for low detection rates was wrinkles' being very light. The intensity gradients caused by the granular skin texture are comparable to those caused by wrinkles. Consequently, the algorithm picks non-wrinkle sites as wrinkles which increasing false alarm rate.
2. Skin discolorations. This problem was more pronounced in subjects of lighter skin color which is more prone to having moles and brown / dark spots.
3. Illumination and bright spots. Due to the publicly available images being under uncontrolled acquisition settings, most of the images had some illumination variation. The variation caused 'bright spots' in images where light is reflected from skin surface due to greasy skin.

## 2.6 Face Age Estimation Techniques

This section contains a survey on face age estimation techniques using computational intelligence algorithms. The state-of-the-art age estimation algorithms predict the exact age or to identify the age range such as teenager or child (Chao et al. 2013). Most of these algorithms are composed of two phases: features extraction and age learning (Chao et al. 2013, Fu et al. 2010, Ng et al. 2014b).

### 2.6.1 Features Extraction

The performance of age estimation system is affected mainly by features extracted from face images. Feature extraction means the face features related to facial appearance changes caused by aging extracted from human face to represent the age (Bekhouche et al. 2016).

Facial features can be classified as local, global, and hybrid. Local and global features have different roles in face perception. Both of them contains a discriminative data for face analysis. Local information is embedded in the detailed local variations of the facial appearance, while global information means the overall structural configuration of the facial contour (Su et al. 2009). As such, facial features are responsible for corresponding classification of age estimation algorithms local-based, global-based and hybrid.

### 2.6.1.1 Local-Based Algorithms

Local features include the geometry of facial components including age spots, depth, wrinkles, and freckles. Local features are usually used in age groups classification. i.e., infant, young and adults, due to the unique characteristics found on local features to differentiate between age groups. For example, the changes in distance ratios between eyes, nose, and mouth are shown clearly in babyhood, while wrinkles are more notable in adulthood. Thus, these features are more suitable to classify age into groups (Choi et al. 2011).

The first publication on face age estimation was by Kwon and Lobo (Kwon & Lobo 1994, Kwon & da Vitoria Lobo 1999). They outlined a computational theory for age classification in which they used a combination of distance ratios between facial parts and wrinkle analysis to classify people into children, young adults, and senior adults. They consult studies in cranio-facial research and suggest that the revised cardioidal strain transformation model is the best model to describe human head growth. To differentiate baby faces from the two older groups, a set of distance ratios was computed between the face parts (mouth, nose, forehead, chin, and eyes). Snakelets analysis are used to find wrinkles to differentiate young adults from senior adults. They used only 47 face images in their experiment (Kwon & da Vitoria Lobo 1999).

Since the methods used by Kwon and Lobo (Kwon & Lobo 1994, Kwon & da Vitoria Lobo 1999) for localization are computationally expensive and database that they used is small (Wang et al. 2009), Horng et al. (Horng et al. 2001) proposed age classification algorithm that classify the age into four groups: children, young, middle-aged adults, and senior adults. Firstly, they applied Sobel edge operator to define the positions of eyes, noses, and mouths. To extract the features from the face, two geometric features were used as distances ratios between eyes, noses, and mouths to distinguish babies from other groups. The degree of wrinkles from five areas (forehead, two cheeks, and two eye corners) was found using Sobel edge magnitudes to differentiate between young adults, middle-aged adults, and senior adults. Finally, two back-propagation neural networks were constructed to classify the age. The first one was employed to distinguish the baby face from other classes using geometric features. If it is not a baby, then the second network was used to differentiate between the others three adult groups based on wrinkle features. They achieved 81.58% identification rate using 115 gray-level images (Horng et al. 2001).

In 2006, Ramanathan and Chellappa (Ramanathan & Chellappa 2006) proposed a craniofacial growth model to estimate the age during formative years (0 - 18 years).

They described the growth of a face using growth parameters that defined over facial landmarks commonly used in anthropometric studies. They detected facial features from eyes, mouth and the outer contour of the face by fitting ellipses of various sizes and orientations.

However, the basic model used by (Kwon & Lobo 1994, Kwon & da Vitoria Lobo 1999, Horng et al. 2001, Ramanathan & Chellappa 2006), known as anthropometric model, consider the geometry information only rather than texture information to be appropriate for identifying young age group. It is not useful for the identification of the adults because most changes pertaining to them appear as texture, so that in (Kwon & Lobo 1994, Horng et al. 2001) the authors used wrinkles analysis in addition to anthropometric model to extract aging features. Anthropometric model is sensitive to head pose in that only front face can be used to measure facial geometries. The model also is inappropriate to predict the age in detail (Ng et al. 2014b, Fu et al. 2010).

In computer vision, the biologically inspired model (Riesenhuber & Poggio 1999) have shown superior results in some tasks such as face recognition (Meyers & Wolf 2008) and object category recognition (Serre et al. 2007). The model in (Riesenhuber & Poggio 1999) consists of simple (S) and complex (C) layers alternately. S units are created using Gabor filters at four orientations and 16 scales. There are 8 bands of units for each orientation created by grouping the adjacent two scales of S units together. Then C units were generated by taking the maximum values within a local spatial neighborhood and across the scales within a band. The MAX operator is used as pooling filter in C units (Riesenhuber & Poggio 1999).

In 2009 Guo et al. (Guo, Mu, Fu & Huang 2009) introduced biologically inspired model in age estimation task for the first time and called it Biologically Inspired Feature (BIF). They applied the model in (Riesenhuber & Poggio 1999) with some improvements in C units generated using non-linear operations including the MAX operation and an standard deviation (STD) operation to obtain a high-performance. Both of these processes were done independently for every orientation and scale band. For every face image, a feature vector was constructed by concatenating the outputs of C units. After extracting the biologically inspired features in C, Principal Component Analysis (PCA) was applied for dimensionality reduction while Support Vector Machine (SVM) was applied for age learning. Although the BIF showed a significant improvements in age estimation accuracy, it represent the face images in a high dimension feature vector (Guo 2012).



Ylioinas et al. (Ylioinas et al. 2013) proposed an age estimation model using Kernel Local Binary Pattern (KLBP) to represent facial features. Firstly, the face was aligned using similarity transformation and the face pose was corrected using an flipping operation to evaluate the pose correction method. For feature extraction the method compared between a histogram and a kernel density estimate for LBP. Finally, a Support Vector Regression (SVR) was applied for age estimation. Ylioinas et al. (Ylioinas et al. 2013) found that the kernel method was more powerful than the histogram using pose corrected images, which achieved 5.09 and 5.23 respectively for MAE. Using the original images, the MAE is 5.20 for kernel and 5.39 for histogram, which means that the pose correction enhanced the age estimation performance (Ylioinas et al. 2013).

In 2013 Gunay et al. (Günay & Nabiyev 2013) also extracted local features to estimate the age using Radon transform. After the pre-processing step which included cropping, scaling and resize images to  $88 \times 88$ , The Radon transform was applied for an image matrix  $f(x,y)$  to compute the projections in specified direction. The result from this projection is that a new image  $R(x,\alpha)$ , which is a sum of the intensities of the pixels in each direction, includes more geometric information than the original image. The concatenation of the Radon projections taken at  $\theta = k\pi/6$  where  $k = 0,1,2,3,4,5$  from local image was used to generate the feature vector. However, the Radon projections produce a high dimension feature vector, so that the PCA was applied to reduce the dimension. Finally, multiple linear regression (MLR) was applied for age learning. Local radon feature achieved a better result on FG-NET (6.18) than MORPH (6.65) and FERET (6.98) (Günay & Nabiyev 2013), which means that the radon feature work better on images with lower resolution (Ng, Yap, Cheng & Hsu 2017).

Recently, there are different works that focus on wrinkles in age estimation algorithms (Aznar-Casanova et al. 2010, Choi et al. 2010, Hadchum & Wongthanavas 2015, Ng et al. 2015a, 2014b, Khan et al. 2015). El-Dib and Onsi (El Dib & Onsi 2011) investigated the ability of wrinkled appearance in eyes, the face parts excluding the forehead and the whole face to estimate the age. They found that the wrinkled appearance in eyes has a significant features related to the age, when it was compared with the other parts. In 2015, Ng et al. (Ng et al. 2015a) investigated the influence of wrinkles on specific age estimation. They localized and presented the wrinkles in a significative way to estimate the age. They proposed a multi-scale aging patterns (MAP) method, which extract the features directly from local patches. MAP was generated by applying a multi-scale filter to different face parts and wrinkles, and thus transformed into meaningful aging patterns. Wrinkles appear in a different sizes.

To present this feature, MAP extends a method that used dynamic scale filter called Hybrid Hessian Filter (HHF), which is a wrinkle detection method proposed by Ng et al. (Ng et al. 2014a). Based on multi-level analysis of Hessian eigenvalues, the local behavior of the face image is emphasized and wrinkles were identified subsequently. Then a multi-scale aging patterns were constructed from extracted wrinkles. Finally, supervised learning algorithm was applied to learn and predict the age. This work demonstrated the ability of wrinkles to estimate the age on high resolution images, where the MAE is 4.87 on FERET (Ng et al. 2015a).

Chang and Chen (Chang & Chen 2015) introduced a framework for age estimation, which applied scattering transform to extract the features from face images and proposed a Cost-Sensitive Ordinal Hyperplanes Ranking (CSOHR) approach for age learning. Scattering Transform (ST) descriptor is a generalization of traditional BIF, where the first-layer of ST and BIF extract the features in a same way, except that the ST employed the Gaussian average in the pooling operators and BIF used standard deviation. ST provides a locally translation invariant representation, which linearizes small deformations, and provides co-occurrence coefficients which characterize textures. This feature is reduced in BIF by pooling operator. After extracting the features using ST, the ranking (or ordinal regression) method CSOHR that focus on pairwise ranking approach was used for age rank estimation. CSOHR with ST achieved 3.82 for MAE in MORPH album2 dataset and 4.70 in FG-NET with slower computation time than BIF for feature extraction and other Multiple Hyperplanes Ranker (MHR) for age learning. However, some features might be lost during dimensionality reduction process using PCA.

### 2.6.1.2 Global-Based Algorithms

Global features (also known as Holistic) are generally used to predict the age. It contain personal features such as gender, identity, ethnicity, and expression. Personal features are clearer in global features than aging features. Subspace learning techniques have been used extensively to extract global features. These include Locality Sensitive Discriminant Analysis (LSDA), Marginal Fisher Analysis (MFA) (Guo, Mu, Fu, Dyer & Huang 2009), PCA, Neighborhood Preserving Projections (NPP), Locality Preserving Projections (LPP), and Orthogonal LPP (OLPP) (Fu et al. 2007, Guo et al. 2008a). However, Active Appearance Model (AAM) (Cootes et al. 2001) is a most widely used method to extract global features for age estimation and to provide information about the shape and appearance of a face (Choi et al. 2011, Bukar et al. 2016).

AAM is a statistical appearance models proposed by Cootes (2001)(Cootes et al. 2001). It combines shape and texture variation. Building a face model require face images marked with points to determine the main features. The model apply Procrustes analysis to align the sets of points (represented as a vector) and build a statistical shape model. It then warps images by the mean shape, and normalized texture vector by applying a linear transformation. To build a texture model eigen-analysis was applied. Finally, a combined appearance model was generated by learning the correlations between shape and texture (Cootes et al. 2001).

In 2002 AAM was introduced by Lanitis et al. (Lanitis et al. 2002) for first time for face age estimation. They generated statistical model from a set of training examples represented by a set of variables. They calculated the mean ( $X_m$ ) and standard deviation from training set, then applied principal components analysis (PCA) on covariance matrix of the deviation. Their experiment focus on age variation from childhood to adulthood (up to 30 years old). The images were aligned and warped to the mean shape to train shape and intensity model. Then the projection was used to define the aging variations using this formula: (age = f(b)). Three formulation were investigated for aging function (f): linear, quadratic and cubic. Based on their experiment, quadratic function achieved the best result (Lanitis et al. 2002).

Geng et al. (Geng et al. 2007) adopted AAM in their work. They developed an age estimation model known as AGES (AGing pattErn Subspace), which used a series of personal face images to model the aging process. An aging pattern can be defined as a sequence of personal face images sorted in time order, by learning a representative subspace. A projection was used to construct the aging pattern for unseen face image, which define the variation in the data set. While the position in aging pattern defines the specific age, the authors claimed that by using this feature the personalized characteristics were utilized well. An aging pattern can be completed if all positions in aging pattern are filled, otherwise it is called an incomplete aging. There are two stages in AGES: learning stage and age estimation. The aging pattern is highly incomplete, so that an iterative PCA was applied in learning stage to construct a representative subspace. The missing parts in the aging pattern were firstly initialized; and then the first subspace was constructed by applying standard PCA to the initialized data set. By solving a linear system, the subspace is used to reconstruct the missing parts, then the PCA is applied to updated the aging pattern. These processes was repeated to minimize the reconstruction error. The age was estimated in two steps determine a suitable aging pattern from aging pattern subspace, and then find the specific age position within aging pattern (Geng

et al. 2007). However, the process of reconstruction of missing face images produces a highly redundant face image, and this can increase the prediction error. In addition, the personalized method for age estimation such as AGES and methods in (Zhang & Yeung 2010, Geng & Smith-Miles 2009, Lanitis et al. 2002) can improve the performance of age estimation. However, this method is limited because it is difficult to acquire sequences of facial images for a single person during aging process (Chang & Chen 2015).

Although AAM considers shape and texture features, it produces a high dimensional feature vector; and this may contain an outliers in the age labeling space that may not directly reflect the identical age labels (Chao et al. 2013). Some valuable parts of the data (such as wrinkles) that represent discriminatory features might have been lost during dimensionality reduction process (Ng et al. 2014b).

Fu et al. (Fu et al. 2007) adopted the Manifold Learning Model for first time to estimate the age. Generally, in age manifold, an aging pattern can be learned from many subjects at various ages. Thus, many personal faces are needed to represent ages as each person may have images at specific age or in an age range. Age manifold use manifold embedding technique like OLPP to learn an aging pattern in low dimension from numerous face images at each age. In this model, each subject may have images only at one age in the database. The authors claimed that this feature makes manifold model more flexible and easier to collect a big aging face database (Fu et al. 2010). By using this model to solve age estimation problem, the age manifold is learned to map the original data into a low-dimensional subspace after a pre-processing steps, in training phase. A regression function then was defined to fit the manifold data for further testing. In the testing phase, an input face image is transformed to the learning feature as in training phase. The age is predicted through the learned manifold mapping and regression model fitting. To learn a low-dimensional manifold in the embedded subspace of image space, a projection function which can be linear or nonlinear might use. This model compared between four different algorithms that use linear methods for projection to manifold space: LPP, OLPP, NPP, and PCA. They found that the OLPP achieved better performance than others. After finding the low dimensional manifold, an age estimation was defined as a multiple linear regression problem in the manifold space.

However, using manifold model required large size of training data to learn the embedded manifold (Fu et al. 2007, 2010). Another issue in this model is sensitivity to image mis-alignment caused by many factors, such as head rotation, different facial expression, and shape variations in facial growth and aging (Guo 2012).

Luu et al. (Luu et al. 2009) introduced an age estimation technique using AAM and Support Vector Machines (SVMs). For each input face image  $I$ , 86 landmarks were determined and feature vector  $x_i$  with size  $30 \times 1$  was extracted using AAM. SVM was used to train a binary classification module, which consists of two parts: classifier  $f(x)$  to differentiate between youths (0 - 20) and adults (21 to 69) and two aging functions:  $f_1(x)$  as growth and development function and  $f_2(x)$  as adult aging function. Finally, Support Vector Machine for regression (SVR) was used for age prediction. This algorithm outperforms the existing algorithms that used AAM by using the combination of binary classification and then age prediction.

In 2013 Chao et al. (Chao et al. 2013) adopted AAM for features extraction on their approach. After extracting feature using AAM, this approach added two steps: distance metric adjustment and dimensionality reduction to explore the relation between face features and age labels and mitigate the over-fitting problem in training the age prediction function. For this purpose, the Relevant Component Analysis (RCA) was applied for distance metric adjustment and LPP was used for dimensionality reduction. For age prediction an age-oriented local regression named K Nearest Neighbors Support Vector Regression (KNN-SVR) was proposed. Although this approach achieved a good result, it used considerably additional functions which might increase the computational complexity.

In 2016 Bukar et al. (Bukar et al. 2016) proposed supervised Appearance Model (sAM) for age and gender estimation that improves the AAM by using the partial least-squares (PLS) as the core of the model rather than PCA. They claimed that their proposed model (sAM) effectively represents the face features than AAM, whereas the PLS preserves worthy parts of the data that represent discriminatory features. PLS creates latent features via a linear combination of the predictor variables and response (class labels). Because sAM considers both shape and texture features, it was used as feature extractor in age estimation model, whereas ordinary least-square (OLS) and quadratic function (QF) regressions were used for age learning with QF showing better results than OLS. The sAM model represents the faces in a convenient way to solve both age and gender classification problems, but it does not outperform the methods that used AAM.

### 2.6.1.3 Hybrid-Based Algorithms

In various face related applications, the local and global features were combined as hybrid features to offer superior performance. Choi et al. (Choi et al. 2011) introduced hybrid features representation and hierarchical classifier to increase the age estimation

accuracy. For local features extraction, a set of region specific Gabor filters were used to extract wrinkle features. LBP was used for skin features, and AAM was used for global features extraction. SVM and SVR were used for age classification and age regression. However, the combination of extracted features using this three methods (Gabor, LBP and AAM) produced a high dimension feature vector which can increase the computation time.

Guo et al. (Guo et al. 2011) also used hybrid features for age estimation. They extracted global features using Active Shape Model (ASM) and both Radon projection and 2D-DCT for local features, where the facial image is converted into Radon space then 2D-DCT is used to obtain the features from this space. Finally, SVM and SVR was used for age estimation. Their results showed that Radon-DCT achieves better results on FG-NET, where the MAE is 4.18 years.

Gunay and Nabiyevev (Günay & Nabiyevev 2015, 2016) conducted several experiments to estimate the age using different local and global methods to produce hybrid-based age estimation algorithms. In 2015 they proposed an age estimation method called “Global and Local feAture based Age estiMation (GLAAM)” that used AAM to extract global features and 2D-DCT for local features. PCA was applied to reduce the dimensionality after concatenating the local and global features. Finally, the age was estimated with multiple linear regression (Günay & Nabiyevev 2015). They stated that: in order to estimate the age accurately, the design of age estimation system requires careful selection of the face feature and there are some issues that need to take into consideration:

1. Robust discriminative aging features extraction method is needed, to reduce the negative effect of individual variations.
2. Face feature must be extracted from raw face images directly to speed up processing.
3. To facilitate the implementation of the classifiers, extracted face feature must lie in a low dimensional space.
4. Minimization of the computational costs using suitable image size.

In 2016 Gunay and Nabiyevev (Günay & Nabiyevev 2016) repeated the experiment using different methods for local features. They applied Gabor filters to extract wrinkles and LBP for skin features, and applied PCA to reduce the dimensionality. Based on three types of features that were extracted (global, wrinkles and skin), Gunay

and Nabiyeu (Günay & Nabiyeu 2016) modeled three aging functions separately with multiple linear regression, then they got the final decision by performing a decision level fusion to combine the results. They applied Gabor filter and LBP for local features to produce better result than 2D-DCT, where the MAE is 5.39 years for first experiment (AAM and 2D-DCT) and 4.87 years for second one (AAM, Gabor and LBP).

As mentioned above, wrinkle-based features are more effective for face representation. Based on this observation, and the fact that the hybrid based features can offering superior performance for age estimation, Ng et al. (Ng, Yap, Cheng & Hsu 2017) proposed Hybrid Ageing Patterns (HAP) feature representation to increase the age estimation accuracy. HAP combines the proposed Multi-scale Wrinkle Patterns (MWP) and Facial Appearance Model (FAM). MWP is a wrinkle-based feature representation method based on the wrinkle statistics, and proposed a wrinkle detection method called Hessian Line Tracking (HLT) (Ng et al. 2015*b*) to extract wrinkle. The multi-scale wrinkles was extracted from ten regions: forehead, glabella, upper eyelids, crows feet (or eye corners), lower eyelids (or eye bag), cheeks, nasolabial grooves (or nasolabial folds), upper lips, marionette and lower lips. Then the wrinkle intensity and wrinkle density were calculated to represent the pattern. FAM is a generative parametric model that combined shape and texture features. PCA is used in FAM to reduce the dimension. After extracting the features using MWP and FAM the hybrid pattern was constructed. Finally, SVR was used to estimate age from the patterns. HAP outperform the existing method on FERET and MORPH, where the MAE is 3.02 and 3.68 respectively.

Although the hybrid features can improve the performance of age estimation algorithm, it may increase the complexity and computation time for age estimation algorithms.

At end of this section, different methods and algorithms can be applied to estimate the age were explained in this section. Local features contains unique features that differentiate between age groups, so that it is suitable to handle age-group classification problem. On the other hand, individual characteristics might be more notable in global features, so that it is more suitable to predict the exact age. AAM can be recognized as a main model that extract the global feature, due to its ability to extract both shape and texture features. In hybrid features, Guo et al. (Guo, Mu, Fu, Dyer & Huang 2009) found that the performance of age estimation can be increased when combining BIF and manifold learning techniques. In addition to hybrid feature, using manifold learning techniques can reduce the dimensionality in BIF,

Table 2.3: A summary of feature extraction methods.

Features Type	Year	Authors
Local	1994	Kwon and Lobo (Kwon & Lobo 1994)
	2001	Horng et al.(Horng et al. 2001)
	2006	Ramanathan and Chellappa (Ramanathan & Chellappa 2006)
	2008	Gunay et al. (Günay & Nabiyev 2008), Yan et al. (Yan et al. 2008)
	2009	Gao et al. (Gao & Ai 2009), Guo et al. (Guo, Mu, Fu & Huang 2009)
	2011	Choi et al. (Choi et al. 2010), El Dib and Onsi (El Dib & Onsi 2011)
	2012	Lin et al. (Lin et al. 2012)
	2013	Ylioinas et al. (Ylioinas et al. 2013), Gunay et al. (Günay & Nabiyev 2013)
	2014	Ng et al. (Ng et al. 2014b)
	2015	Ng et al. (Ng et al. 2015a). Dibeklioglu et al. (Dibeklioglu et al. 2015), Chang et al. (Chang & Chen 2015), Hadchum and Wongthanavas (Hadchum & Wongthanavas 2015), Khan et al (Khan et al. 2015)
2017	Hsu et al. (Jison Hsu et al. 2017)	
Global	2002	Lanitis et al. (Lanitis et al. 2002)
	2004	Lanitis et al. (Lanitis et al. 2004)
	2006	Ueki et al. (Ueki et al. 2006)
	2007	Geng et al. (Geng et al. 2007), Fu et al. (Fu et al. 2007)
	2008	Guo et al. (Guo et al. 2008a)
	2009	Geng et al. (Geng & Smith-Miles 2009), Geng and Kate (Geng & Smith-Miles 2009), Luu et al. (Luu et al. 2009)
	2010	Chang et al. (Chang et al. 2010), Zhang et al. (Zhang & Yeung 2010)
	2011	Chang et al. (Chang et al. 2011)
	2013	Chao et al. (Chao et al. 2013)
	2016	Bukar et al. (Bukar et al. 2016)
Hybrid	2008	Suo et al (Suo et al. 2008)
	2009	Guo et al. (Guo, Mu, Fu, Dyer & Huang 2009)
	2010	Luu et al. (Luu et al. 2010)
	2011	Choi et al. (Choi et al. 2011), Guo et al. (Guo et al. 2011)
	2013	Weng et al. (Weng et al. 2013), Tharwat et al. (Tharwat et al. 2013)
	2015	Gunay and Nabiyev (Günay & Nabiyev 2015), Huerta et al. (Huerta et al. 2015)
	2016	Gunay and Nabiyev (Günay & Nabiyev 2016), Bekhouche et al. (Bekhouche et al. 2016), Qiu (Qiu et al. 2016)
	2017	Ng et al. (Ng, Yap, Cheng & Hsu 2017, Ng, Cheng, Hsu & Yap 2017)



while BIF addresses the problem of sensitivity to image mis-alignment in manifold learning techniques as it has the capability to deal with different changes in scale, translation and rotation. Table 2.3 summarizes the published work in age estimation using different types of features.

More recently, researchers investigated the effectiveness of some appearance-based features and found that:

1. Wrinkles can increase the age estimation accuracy (Ng et al. 2015*a*, Ng, Yap, Cheng & Hsu 2017). There is little research that focuses on age estimation based on wrinkles. However, most of them classified the age into groups rather than predict exact age.
2. BIF, introduced by Guo et al. (Guo, Mu, Fu & Huang 2009), achieved good results in age estimation. In 2017, Hsu et al. (Jison Hsu et al. 2017) proposed the Component Bio-Inspired Feature (CBIF) that achieved MAE of 3.38 on FG-NET.

## 2.6.2 Age Learning Techniques

As mentioned above, the existing facial age estimation methods consist of two phases: features extraction and age learning techniques. Once the features are extracted from the face images, learning technique is needed in order to classify or predict the age. In general, age learning techniques can be classified into three groups: age groups classification, regression or single-level age estimation and hierarchical age estimation (Choi et al. 2011). Other techniques include ordinal ranking and deep learning. For clarification, It is noted that the machine learning techniques for classification, regression, hierarchical and ordinal ranking are referred to as conventional machine learning methods (non deep learning approaches). The strength and weakness of these five categories were summarized in Table 2.4; a detailed review of these five categories is given follow.

### 2.6.2.1 Classification

Classification is an approach used to classify the age into multiple age groups such as babies, young, middle-aged adults, or old adults (Kwon & Lobo 1994, Kwon & da Vitoria Lobo 1999, Horng et al. 2001, Ramanathan & Chellappa 2006, Wang et al. 2009, Ueki et al. 2006, Lanitis et al. 2004, Bouchrika et al. 2015). This section review the classification methods based on conventional machine learning algorithms such

Table 2.4: Comparison between age learning techniques.

Category	Strength	Weakness
Classification	More appropriate for age range classification.	Not appropriate to predict the age. Class labels are uncorrelated.
Regression	Ability to predict age using a single estimator.	Does not consider the differences of age feature values according to age groups. It is difficult for regressor to learned a non-stationary kernels.
Hierarchical	The performance is improved by considering the differences of age feature values according to age groups.	The errors in the age group estimation step are propagated to the specific age prediction step when using an age group estimator with a hard boundary not including overlapped class.
Ordinal ranking	Preserve the relative order of age labels and provides more stable information than exact age values.	Time consuming.
Deep Learning	Do not require predefined or hand crafted features	Require large-scale data for training process.

as SVM (Lian & Lu 2005), Linear Discriminant Analysis (LDA) (Gao & Ai 2009), Artificial Neural Networks (ANN) (Horng et al. 2001), nearest neighbor classifier (Lanitis et al. 2004) or distance measure (Günay & Nabiyevev 2008) for age group classification. The most notable work was by Guo et al. (Guo, Mu, Fu & Huang 2009) who achieved MAE of 4.77 using BIF features on FG-NET. It is noted that they used both classification and regression approaches to learn age.

Ng et al. (Ng et al. 2014b) developed ANN with three layers: input, hidden and output to classify the age into two groups and applied their proposed method to investigate the effectiveness of wrinkles in age classification, which called Local Wrinkle-based Extractor (LOWEX) that used Canny edge detection to detect the wrinkles from different face regions. Their proposed method with ANN achieved 80% on FG-NET. Im et al. (mi Im et al. 2016) extracted wrinkles feature using Gabor filter and applied SVM for age classification. Their experiment was tested on private data with average accuracy of 76.92%. In 2017, Iqbal et al. (Iqbal et al. 2017) proposed local descriptor called Directional Age-Primitive Pattern (DAPP) and applied SVM to classify the age into 7 groups. They achieved accuracy of 73.1% on data collected from flickr.com.

In classification, the class labels are uncorrelated and each label is independent from each others. However, there is strong interrelationships between labels, and the age labels is well-ordered in reality. For example, a person with 12 years old is more likely to be 11 or 13 years old. However, classification approaches do not reflect this property.

### 2.6.2.2 Regression

Regression approaches consider age label as a set of sequential numbers (e.g., 10, 11, 12,...). This sequence fits the ordinal nature of age label. This is a very popular age learning technique it includes many methods that can be used for regression such as SVR (Guo et al. 2008a), Quadratic Regression (Lanitis et al. 2004), Multiple Linear Regression (Günay & Nabiyevev 2015), and Multilayer Perceptron (MLP) (Jadid & Sheijani 2016). Since 2007, Geng et al. (Geng et al. 2007) has achieved MAE of 6.77 years on FG-NET using facial appearance features. Fu et al. (Fu et al. 2007) applied multiple linear regression for age estimation after finding the low dimensional aging manifold using manifold embedding technique like OLPP. Later on, Guo et al. (Guo et al. 2008a) used the manifold model to improve their work by using Locally Adjusted Robust Regression (LARR), which applied global and local steps respectively to learn the data. In the global learning, SVR was used for regression over all ages of the training data. Then a local adjustment within a limited range of ages centered at the regression result, where the linear SVM was used for local age adjustment. LARR produced MAE of 5.07 on FG-NET.

Guo et al. (Guo, Mu, Fu, Dyer & Huang 2009, Guo & Mu 2010) studied the effect of gender and race on age estimation. They applied different classifier and regressor to perform the gender, race and age estimation. However, these tasks were performed separately in different steps, where the gender or race classification was performed first, then the age was estimated within different class. To improve this work, in 2011, Guo et al. (Guo & Mu 2011) proposed a kernel partial least squares (KPLS) regression algorithm for age estimation. KPLS have a flexible output vector that allows to overcome a number of related classification problems such as race, gender and age. It contains multiple labels in a same output vector. In addition, KPLS performs dimensionality reduction and learns the aging function in a single step. In this framework, KPLS was used to classify race, gender and estimate the age in single step. This age estimation method achieved MAE of 4.18 on MORPH.

In 2013, Chao et al. (Chao et al. 2013) proposed an age estimation algorithm using KNN-SVR. The authors claimed that the local regression function is more likely to

overcome the problem of complicated facial aging. The MAE was 4.38 on FG-NET. Recently, Ng et al. (Ng, Yap, Cheng & Hsu 2017) applied SVR with their proposed feature descriptor Hybrid Aging Patterns to estimate the age. They achieved a MAE of 3.02 on FERET. In 2017, Ng et al. (Ng, Cheng, Hsu & Yap 2017) proposed a Multi-layer Age Regression (MAR) approach to estimate the age, consisting of two layers. Both layers produced a real number in output rather than class labels. FAM was used to extract the features in the first layer. FAM, BIF, KLBP and MWP were used to extract the features in second layer, then SVR was used for age prediction. Their experiment was validation on four dataset, i.e. FG-NET, MORPH, FERET and PAL. The best result was MAE of 3.00 on FERET. When compared this approach with LARR and Probabilistic Fusion Approach (PFA) (Guo et al. 2008*a,b*), PFA and LARR outperformed on FG-NET with the MAE of 4.97 and 5.07 respectively. PFA and LARR applied SVM rather than SVR in the second layer, and treat each age value in the age group as a class label.

The strength of regression is its ability to predict age using a single estimator. However, the personalized property in aging process produces non-stationary feature space, which is difficult for regressors to learn non-stationary kernels (Chang et al. 2011).

### 2.6.2.3 Hierarchical

Hierarchical age estimation combines the classification and regression methods to predict age. It provides more accurate result and simplifies the computational load, where the data was firstly classified into age groups, then the age was predicted from these pre-defined groups (Choi et al. 2011). Choi et al. (Choi et al. 2011) applied age group classification followed by age regression to predict the age using SVM and SVR respectively. The hybrid features were extracted using AAM, LBP and Gabor. By using this combination of hybrid and hierarchical approach to predict the age, the MAE was 4.6 on FG-NET. Han et al. (Han et al. 2013) also applied SVM and SVR, where SVM was used to classify the age into four groups after extracting features using BIF. Within each group, SVR was used to predict the age. In order to reduce the age classification error that produced from strict group boundaries, they used training samples for regression with distance up to 5 years between age groups. The MAE was 4.6 and 4.2 on FG-NET and MORPH respectively. Later, Han et al (Han et al. 2015) improved their work and proposed a generic framework for gender, race and age estimation. In this framework, in order to fix the problem of low-quality images, they applied a quality assessment method to preprocess the images before extracting

features. After preprocessing, the same steps and methods used in a previous work (Han et al. 2013) were applied for classification and regression. The MAE was reduced by approximately 1 year for both datasets, with MAE of 3.8 on FG-NET and MAE of 3.6 on MORPH.

Li et al. (Li et al. 2012) used Sparse Representation-based classification (SRC) algorithm to classify the age into two groups using the shape feature. The texture feature was concatenated with the shape feature and applied the Ordinal Hyperplane Ranker to estimate the age accurately. The MAE was 4.32 on FG-NET. Angulu et al. (Angulu et al. 2017) used ANN to classify the age into 6 groups then applied SVR to predict the age within these groups, after extracting the features using Multi-Frequency Biologically Inspired Features (MF-BIF). They achieved MAE of 4.02 on FG-NET. In 2017, Hsu et al. (Jison Hsu et al. 2017) performed the age classification and regression using traditional SVM and SVR after extracting the features using Component Bio-Inspired Feature (CBIF). To reduce the classification error produced from strict age boundaries, they proposed moving segmentation method to find the age boundaries that can improve the accuracy. After applying the moving segmentation window, they found that the best age boundaries on FG-NET was at 11, 28 and 38 year, and the age boundaries on MORPH were at 29, 44 and 60 year. Based on their experiments, they found that the number of age groups in classification step have notable effect on the overall performance. The MAE was 3.38 on FG-NET and 3.21 on MORPH using 4 groups in classification step.

#### 2.6.2.4 Ordinal ranking

Recently, there has been growing interest in age estimation to **ordinal ranking** (also called ordinal regression) due to the diversity in human aging processes at different age range. Hence, given two labels  $x_1$  and  $x_2$ , the “greater than” information ( $x_2 > x_1$  or  $x_1 > x_2$ ) is more reliable property for age estimation than the differences between the labels; and provides more stable information than exact age values. Ordinal ranking is built like when we ask a human “Who is the older between two people?”. It seems easy to answer this question than asking people to predict the person’s age. In ranking approach, the input face is compared with the known age faces from the database. This produces a series of comparisons. Age can then be estimated by integrating the results from these comparison. The age labels  $l_i$  is treated as a rank order  $l_i \in \{1, \dots, x\}$  where  $x$  is the labels number. Based on a given  $x$ , the dataset D

was separated into two subsets  $\{D_x^+$  and  $D_x^-\}$  as follows (Chang et al. 2010):

$$\begin{aligned} D_x^+ &= (d_i, +1) | l_i > x \\ D_x^- &= (d_i, -1) | l_i < x \end{aligned} \tag{2.1}$$

where  $D_x^+$  indicate to data that bigger than  $x$ , and  $D_x^-$  the data that smaller than  $x$ .

These two subsets were used to learn the binary classifier and answer the query “Is the face older than age  $x$ ?”; then making positive or negative decisions between the two sides (as a binary decision). By using these processes the age estimation task was reduced to a binary classification problem (any classification algorithm can be used as the binary classifier) at each query. Ordinal relationships between the age labels can then be recognized from a series of these query results.

Chang et al. (Chang et al. 2010) applied the ordinal ranker approach for age estimation in their work. They improved the work in (Yang et al. 2010), (Chang et al. 2010) and (Qin et al. 2007). In (Yang et al. 2010) RankBoost algorithm applied cannot reflect the multiple thresholds of different classes properly due to the use of single hyperplane ranker in the feature space. On the other hand, parallel hyperplanes in (Chang et al. 2010) is more suitable when the database contains small number of classes. The RED-SVM used in (Chang et al. 2010) constructs  $K - 1$  parallel hyperplanes that separate the hyperspace into  $K$  ranks by using  $k - 1$  thresholds. However, it is difficult to separate data using parallel hyperplanes when predicting the exact age as the  $k$  is always large. The Multiple Hyperplanes Ranker used in (Qin et al. 2007) overlooks some potentially valuable cues provided by a well ordered set of labels. To overcome the limitations in previous work that used ranking approach, Chang et al. (Chang et al. 2010) introduced an ordinal hyperplanes ranker (OHRank), which aggregates  $K - 1$  binary classifiers based on the order of labels, after extracting the features using AAM. OHRank achieved 4.48 MAE on FG-NET.

### 2.6.2.5 Deep Learning

More recently, convolutional networks and deep learning approach have been successfully applied to several tasks related to facial analysis, including face alignment (Zhang et al. 2016), face detection (Sun et al. 2013), face verification (Taigman et al. 2014), facial skin analysis (Alarifi et al. 2017), and demographic estimation (Yang et al. 2011) to estimate the age and gender and to address face recognition problem. Later, many researchers implemented deep learning for age estimation (Dong et al. 2016, Gurpinar et al. 2016, Huerta et al. 2015, Malli et al. 2016, Qiu et al. 2016, Rothe

et al. 2016, Wang et al. 2015, Zheng et al. 2016, Zhu et al. 2015), due to its superior performance over existing methods.

Generally, the basic methodology in deep learning approach is similar; it consists of alternating convolutional and pooling layers followed by fully-connected layers with the input to successive layers being the feature maps from previous layers. Weights in layers are changed simultaneously for representative features and classification with a specific loss function through back-propagation. The key of success in this approach is the accurate choice of parameters found in different layers (Huerta et al. 2015). However, deep learning requires a huge amount of data for training process.

CNN can be developed in three ways: training a network from scratch, fine tuning an existing model, or using off the shelf CNN features. Training CNN from scratch requires an enormous amount of data (Niu et al. 2016). Fine tuning involves transferring the weights of first  $n$  layers learned from a base network to a target network. The target network is then trained using a new dataset for a specific task, usually different from that of the base network (Rothe et al. 2016). The CNN can be used as a feature extractor instead of being a classifier, this approach is known as off-the-shelf feature (Wang et al. 2015).

Deep learning was introduced by Wang et al. (Wang et al. 2015) for a first time to solve age estimation problem. Their CNN architecture consists of three convolution layers, two pooling layers and full connection layer. Wang et al. (Wang et al. 2015) yield good results on FG-NET and Morph. However, this CNN was used to represent the features then traditional linear SVR was applied for age prediction.

In 2016, Rothe et al. (Rothe et al. 2016) proposed CNN called DEX based on VGG-16 architecture CNN (Simonyan & Zisserman 2014). VGG is much deeper CNN with small size for filters. DEX was pre-trained on the ImageNet (Russakovsky et al. 2015) for image classification and fine-tune on the images from IMDB-WIKI dataset introduced by Rothe et al. (Rothe et al. 2016). Their experiments on MORPH yield MAE of 3.25. Rothe et al. (Rothe et al. 2016) improves this result by fine-tuning the CNN on IMDB-WIKI before fine-tuning on the MORPH, this resulted MAE of 2.68 years. DEX achieved 4.63 on FG-NET without fine-tuning on IMDB-WIKI and 3.09 when fine-tuning on IMDB-WIKI before fine-tuning on FG-NET.

Niu et al. (Niu et al. 2016) proposed CNN called OR-CNN (Ordinal Ranking-CNN) to address age estimation problem consists of 3 convolutional, 3 normalization, and 2 pooling layers followed by a fully connected layer. They used binary ordinal age labels to train a series of basic CNNs, one for each age group. The binary results then are aggregated for the final age prediction. They claimed that the ranking method

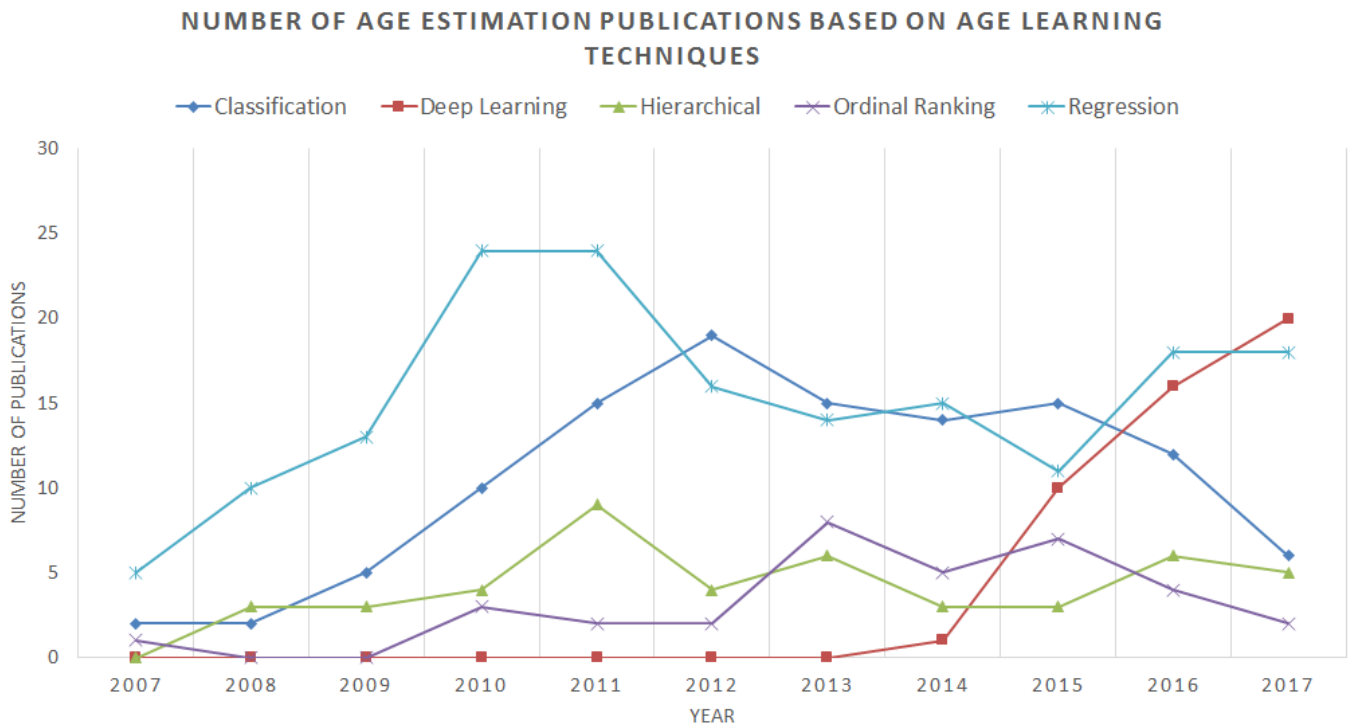


Figure 2.6: Illustration of the age estimation publications based on five age learning techniques over the past 10 years. There was an increase of classification and regression methods until 2012. With the growth of deep learning, it is expected that the number of publications using deep learning has a rapid growth from 2014.

is preferred for age estimation as it produces smaller prediction error than softmax classifier, because softmax does not consider the ordinal relation between ages. Their experiment on MORPH achieved 3.27 years for MAE and 3.34 years using Asian face age dataset.

In 2017, Chen et al. (Chen et al. 2017) also proposed a Ranking Convolutional Neural Network (Ranking-CNN) framework. Ranking-CNN consists of three convolutional and sub-sampling layers, and three fully connected layers. Ranking-CNN outperforms the existing methods for age estimation where the MAE is 2.69 years on MORPH. It is noted that the researchers preferred MORPH to FG-NET due to the dependency of deep learning on large-scale database.

Figure 2.6 compares the number of publications over the past decades based on our review. It illustrates the popularity of classification and regression techniques for age learning. However, from 2014, due to the rapid growth of deep learning, researchers started to explore and invest their time on deep learning technique.

In age learning, ordinal ranking and deep learning algorithms have recently demon-



Table 2.5: Comparison between different face age estimation algorithms organised by machine learning techniques and database (Part I). To clarify, the machine learning technique for classification and regression are referred to conventional machine learning algorithms.

Machine Learning Technique	Database	Algorithm	Feature Extraction Method	MAE	CS (0-10) (%)	Accuracy (%)	
Classification	FG-NET	Mohan et al. 2010 (Mohan et al. 2010)	Topological Texture Features (TTF)	-	-	<b>94.1</b>	
		Wang et al. 2010 (Wang, Xia, Le, Yang & Liao 2010)	ASM+BIF	-	-	90	
		Liu et al. 2012 (Liu et al. 2012)	AAM	-	-	79.2	
		Zheng et al. 2013 (Zheng et al. 2013)	LBP	-	-	74.60	
		NG et al. 2014 (Ng et al. 2014b)	LOWEX	-	-	80	
		MORPH	Zhou et al. 2011 (Zhou et al. 2011)	Radon transform	-	-	~87
		Mirzaei et al. 2011 (Mirzaei & Toygar 2011)	LBP	-	-	67.23	
	FERET	Gunay et al. 2008 (Günay & Nabiyev 2008)	LBP	-	-	80	
		web data	Gao et al. 2009 (Gao & Ai 2009)	Gabor Filter	-	-	91
			Gao et al.	LBP	-	-	84.6

Table 2.6: Comparison between different face age estimation algorithms organised by machine learning techniques and database (Part II). The machine learning technique for hierarchical and ordinal ranking are referred to conventional machine learning algorithms.

Machine Learning Technique	Database	Algorithm	Feature Extraction Method	MAE	CS (0-10) (%)	Accuracy (%)
Regression	FERET	Ng et al. 2015 (Ng et al. 2015a)	multi-scale aging patterns (MAP)	4.87	-	-
		Ng et al. 2017 (Ng, Yap, Cheng & Hsu 2017)	HAP	<b>3.02</b>	-	-
	MORPH	Lu and Tan. 2010 (Lu & Tan 2010)	cost-sensitive locality preserving projections (CSLPP)	4.24	-	-
		Huerta et al. 2015 (Huerta et al. 2015)	HOG + LBP + SURF	4.25	~ 90	-
		Ng et al. 2017 (Ng, Yap, Cheng & Hsu 2017)	HAP	3.68	-	-
		Luu et al. 2010 (Luu et al. 2010)	AAM + Local Ternary Patterns (LTP)	4.23	~ 91	-
Hierarchical	FG-NET	Choi et al. 2011 (Choi et al. 2011)	AAM + LBP + Gabor Filter	4.65	~ 91	-
		Li et al. 2012 (Li et al. 2012)	ASM+LBP	4.32	~	-
		Han et al. 2013 (Han et al. 2013)	BIF	4.6	-	-
		Hsu et al. 2017 (Jison Hsu et al.	CBIF	3.38	-	-
		41				

Table 2.7: Comparison between different face age estimation algorithms organised by machine learning techniques and database (Part III). The machine learning technique for hierarchical and ordinal ranking are referred to conventional machine learning algorithms.

Machine Learning Technique	Database	Algorithm	Feature Extraction Method	MAE	CS (0-10) (%)	Accuracy (%)
Ordinal Ranking	FG-NET	Yan et al. 2007 (Yan et al. 2007)	AGES	5.33	~ 85	-
		Chang et al. 2010 (Chang et al. 2010)	AAM	5.79	~ 85	-
		Chang et al. 2011 (Chang et al. 2011)	AAM	4.48	~ 90	-
		Liu et al. 2016 (Liu & Sun 2016)	AAM	4.14	-	-
	MORPH	Weng et al. 2013 (Weng et al. 2013)	PCA+LBP+BIF	4.20	~ 95	-
	Chang et al. 2015 (Chang & Chen 2015)	ST	<b>3.82</b>	-	-	
Deep Learning		Huerta et al. 2015 (Huerta et al. 2015)	Deep Learning	3.88	-	-
		Niu et al. 2016 (Niu et al. 2016)	Deep Learning	3.27	~ 95	-
		Liu et al. 2016 (Liu et al. 2016)	42 ASM	3.48	-	-
	MORPH	Niu et al. 2016 (Niu et al. 2016)	Deep Learning	3.34	~95	-

strated great success in handling age estimation problem. Ordinal ranking provides more stable information using a relative order of age labels. Due to the lack of face aging datasets, deep learning was used as features extractor (off the shelf CNN) (Gurpinar et al. 2016, Wang et al. 2015, Zheng et al. 2016) or fine-tuning the CNN with different datasets (Dong et al. 2016, Rothe et al. 2016, Malli et al. 2016, Rothe et al. 2018).

## 2.7 Smoking and Facial Wrinkles

Smoking is a major health problem and a leading cause of preventable death and responsible for more than 30% of cancer-related deaths (Campanile et al. 1998). In United States smoking is responsible for approximately 443,000 premature deaths yearly (KLOEPPEL 2010). On average, chronic smoking shortens life expectancy by at least 10 years (Doll et al. 2004). The skin, like every other organ system in a human body, is affected negatively by smoking (Gill et al. 2013), leaving it dry, wrinkled and discolored (Cope 2013).

Wrinkling is a normal phenomenon associated with age progression, it is a popular feature that troubled individuals (Aizen & Gilhar 2001). However, The effect of smoking on wrinkling might have potential impact on the overall performance of these applications.

In the earliest work since 1965, Ippen and Ippen (Ippen & Ippen 1965) defined cigarette skin as pale, grayish, wrinkled skin, especially on the cheeks, with thick skin between the wrinkles. They conducted their experiment on German women. They stated that the wrinkles and folds covered the smoker's face, especially on the cheeks. Daniell (DANIELL 1971) later reported a similar relation in both men and women. In 1985, Model (Model 1985) reported that individuals who had smoked a cigarette for ten years or more can be identified by their facial features alone, which called "smoker face". "Smoker face" contains more lines or wrinkles on the face. Multifactorial components of smoking affect on skin, toxic components of cigarette smoke are absorbed systemically and cause vascular and connective tissue damage in the skin, this makes premature aging, wrinkles, and poor skin tone are the main effects of smoking on the skin (Aizen & Gilhar 2001).

The decreased moisture in the stratum corneum of the face contributes to facial wrinkling due to direct toxicity of the smoke. Pursing the lips during smoking with contraction of the facial muscles and squinting due to eye irritation from the smoke might cause the formation of wrinkles around the mouth and eyes (crow's feet).



Figure 2.7: The effect of smoking on face skin (Osman et al. 2017): (a) illustrates the skin from a non-smoker at age 80 and (b) illustrates the skin from a smoker at age 78 .

Smoking was determined to be a strong predictor of skin aging (Morita 2007). Yin et al. (Yin et al. 2001) found that the wrinkle depth is significantly more prominent in smokers with a smoking history of at least 35 packs per year than non-smokers. Figure 2.7 illustrates the effect of smoking on skin, where a smoker's skin patch (Figure 2.7(b)) has deeper wrinkles compared to the skin patch of a non-smoker (Figure 2.7(a)).

Smoking increases the risk of premature wrinkle development (Cope 2013, Strack & Wyrick 2012). In (2013) Cope (Cope 2013) stated that the effects of smoking on skin in general appear as:

1. Premature aging.
2. Increased wrinkles.
3. Grey, dull color.
4. Poor circulation.
5. Suppressed immunity.
6. Collagen damage.

In (2001) Bulpitt et al. (Bulpitt et al. 2001) investigated the factors that can affect on people face appearance and make them looks older, they found that alcohol consumption, employment grade, serum high-density lipoprotein cholesterol, glucose, albumin, and calcium does not relate to looking older for man and women. On the

other hands, they recognized that smoking is one of the factors that make people looks older.

Raitio et al. (Raitio et al. 2004) conducted study to find out the effect of smoking on wrinkling and aging for male in Northern Finland. They estimate the age, habits, and facial wrinkling. They found that tobacco smoke is extrinsic risk factor for accelerated skin aging, and smokers appear older than their age in an average of 2.1 years for every 10 years of smoking. No considerable difference in estimation that done by clinical assessment and by computerized image analysis. In 2009 Guyuron et al. (Guyuron et al. 2009) reach results close to Raitio et al. (Raitio et al. 2004) result. Where they conducted a study to identify the environmental factors that contribute to facial aging in identical twins. They found that, the twin who longer smoked, is look older than non-smoked twin. The minimum duration of smoking to result in perceived age change was 5 years. Each 10 years of smoking culminated to a 2.5 year older appearance.

Detecting the effect of some extrinsic factors like smoking and educating the public can reduce the amount of skin damage and the need for rejuvenation. Although facial wrinkles are not a deadly condition, some research suggests that people may perceive the development of facial wrinkles as a threat serious enough to consider quitting smoking (Strack & Wyrick 2012, Grogan et al. 2011, Campanile et al. 1998).

However, the majority of studies that investigated the association between smoking and wrinkles assessed the wrinkles using subjective method (such as clinical scores for facial wrinkles). Clinical scores on wrinkles might be partially influenced by the judgment of individual investigator. Thus, it is necessary to use an objective method to evaluate the facial wrinkles.

## **2.8 Research Direction**

Based on the literature, age estimation is still challenging problem due to different reasons. First, age estimation is affected mainly by human aging process, where there are different changes appear in human face during this process. In addition to these normal changes, there are many external factors such as environmental factors, solar radiation, lifestyle, disease, face lift, smoking, drug use, and psychological stress that can effect on face aging process and make it uncontrollable and personalized process (Albert et al. 2007). Its difficult to define a pattern that described a specific age for all subjects. For example, these are weak arguments if we say two wrinkles at the eye corner is classified as age 20, three wrinkles as 30 years old and so on.

Such vague arguments will cause ambiguity if the person's age is between 20 and 30. Second, the existing variations in the input image such as: a different illumination, pose and facial expression also have a significant impact on age estimation system performance (Dibeklioglu et al. 2015). Finally, It is difficult to collect a large set of facial images for people throughout their life which are sufficient to present detailed aging progression (Fu et al. 2010). In 2014, Nagan and Grother. (Ngan & Grother 2014) performed a large scale empirical evaluation of facial age estimation algorithms. They used black-box testing methodology designed to model operational reality where software is shipped and used "as-is" without algorithmic training. Their evaluation emphasized the direct effect of these factors on estimating age.

Aznar et al. (Aznar-Casanova et al. 2010) studied the influence of wrinkles on facial age judgments. Their results indicated that the greater the number of wrinkles and the depth of furrows has a direct effect on age estimation. However, the majority of the research on age estimation used local representation methods that capture general local features instead of wrinkle. For example, in (Günay & Nabiyevev 2013) regional local Radon transform was applied to extract local features, however, using Principal Component Analysis (PCA) to reduce the dimension decreases aging representation such as wrinkles which is classified as a noise (Fu et al. 2010). There are several researches that applied local representation methods such as (Kwon & Lobo 1994, Guo, Mu, Fu & Huang 2009, Günay & Nabiyevev 2013, Ylioinas et al. 2013, Chang & Chen 2015) but not focusing on wrinkle-based features. As a result, follow is a few research questions that will be answered in the following contribution chapters:

1. How to extract wrinkles accurately from high and low resolution face images.
2. How to represent wrinkles as aging features in the context of face age estimation.
3. How to make use of these combined features to predict the age.

## 2.9 Summary

This chapter provides a full survey in age estimation, including the importance of estimating age, explain the stages of human face aging, comprehensive and critical review for related work, comprehensive study on databases, different types of facial features and features extraction methods. It it also present the relationship between wrinkle and aging, and mentioned to some wrinkle detection algorithms and why it is still challenging.

# Chapter 3

## Methodology

### 3.1 Introduction

This chapter describes each of the component techniques that used in methodology. This consist of collecting and acquiring datasets, pre-processing techniques including face detection and alignment, features representation using the combination of wrinkle and local features, age prediction and number of different scientific measurements that used to validate the proposed methods. Figure 3.1 describe the general methodology of this thesis, where the next sections describe the details of each component of this methodology.

### 3.2 Datasets Collection and Acquisition

To evaluate the proposed methods on Sudanese skin, a Sudanese dataset was collected. In addition to four benchmark datasets FERET (Phillips et al. 1996), FG-NET (Panis et al. 2015, Günay & Nabiyevev 2015), MORPH (Ricanek Jr & Tesafaye 2006, *MORPH Database* n.d.), and PAL (Minear & Park 2004), and social habits dataset. The next sections discuss these datasets.

#### 3.2.1 Sudanese Dataset

The majority of the proposed methods were evaluated using datasets that are either western, Chinese or Japanese, no other skin type (such as Sudanese) is used in the literature. In addition, the publicly available datasets dose not contain smoking status. Therefore, a Sudanese dataset was collected including subject smoking status.

Collected dataset consist of 138 Sudanese participants in age range between 16-80, with a mean age of 29.1 ( $\pm 12.6$ ) and 1,787 total of images. There are 64 non-smokers



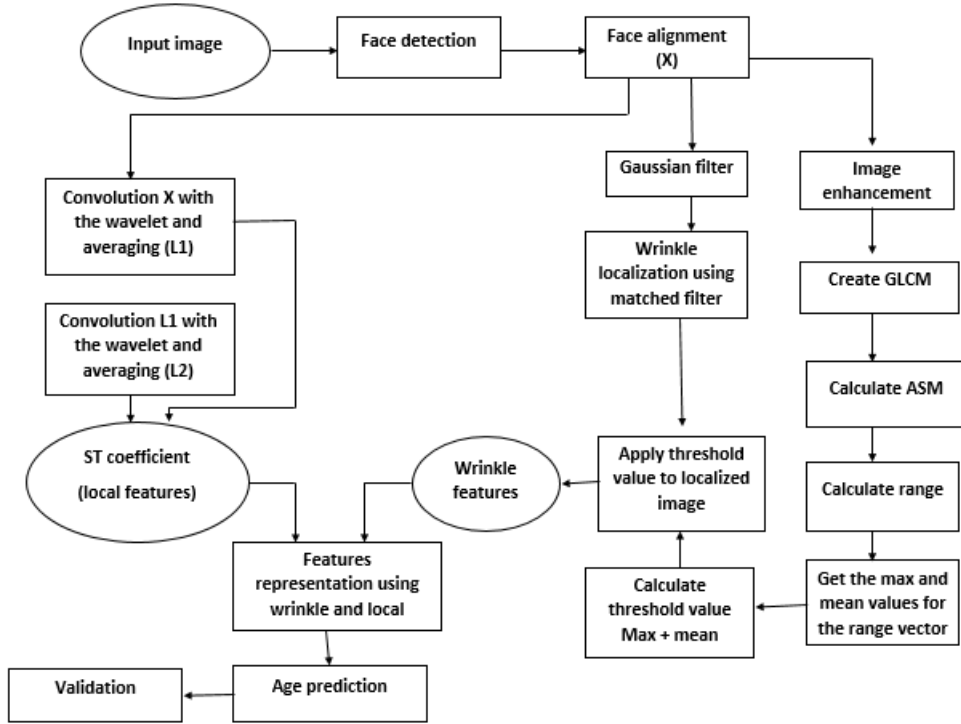


Figure 3.1: Research methodology.

(no history of smoking) and 74 smokers (where some has stopped smoking). The main reported gender was male with a total number of 132 participants, there were only 6 female. The data collection was not under a controlled environment, it collected in a different places. Each participant was asked to fill the questionnaire firstly (see Appendix A), then the image was taken from a top part of participant.

Four expressionless images of each participant were captured at different angles to allow for a full view of the face in addition to the frontal face. Next, universal facial expressions ( happiness, sadness, surprise, disgust, anger and fear) based on Ekman's (Ekman & Keltner 1997) were taken. The replication of these expressions allows for the dataset to include within it some variation in the way each participant's facial skin changes due to natural expressions. Being able to differentiate between actual wrinkles and ridges caused by expression lines would be extremely useful when analyzing facial conditions in the future, as would the ability to distinguish between changes caused by natural expressions and deformities caused by other reasons like aging and social habits.

The images were taken with a Cannon EOS 600D using the flash, all images were taken under natural lighting. As one of a preprocessing step, the images were cropped to show only the face part. Figure 3.2 shows samples of Sudanese dataset.



Figure 3.2: Samples from our collected dataset. The label of each image describes age and smoking status (Smoker or Non-smoker)

The dataset is an on-going project of data collection. Therefore, in the future, the dataset is likely to increase in size and quality.

Table 3.1: The distribution of the images in FERET.

Age Range	Number of Images
10-19	38
20-29	950
30-39	629
40-49	474
50-59	209
60-70	66

### 3.2.2 FERET

FERET dataset is a part of the Face Recognition Technology (FERET) program that develop to produce reliable face recognition systems. It contains of a total of 2366 images 994 subjects (403 female, 591 male) from 10 to 70 age range. It was collected in 15 sessions from August 1993 to July 1996, in George Mason University and US Army Research Laboratory facilities. For each individual a set of images were acquired under relatively unconstrained conditions. FERET dataset present multiple problems related to face recognition, where the set of images that acquired for each individual include frontal views, different facial expression, lighting, and different pose (Phillips et al. 1996, *FERET Database* n.d.). Table 3.1 shows the distribution of the

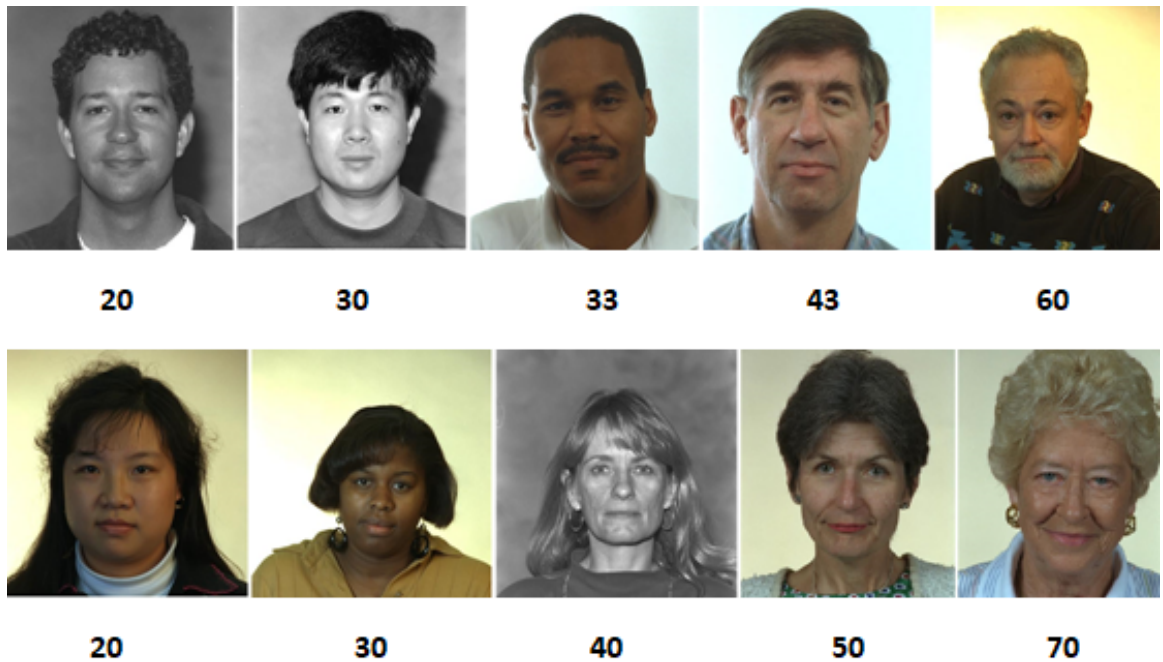


Figure 3.3: FERET samples. First row shows a different male subjects at different age, and second row shows a different female subjects at different age. The label of each image describes the age.

images in FERET. The images was taken in a semi-controlled environment, part of these images are in gray-scale as shown in Figure 3.3.

### 3.2.3 FG-NET

FG-NET database is part of Face and Gesture Recognition Network project and started in 2004, the dataset consist of 1002 face images (color or gray scale face image ) for 82 subjects with approximately 10 images per subject in different expression and pose. The age range in FG-NET is between 0 to 69, but more than 700 of them are under 20 years old (this distribution is clear in table 3.2), making the FG-NET highly imbalanced (Panis et al. 2015, Chao et al. 2013). FG-NET was collected from a real life albums, so the images involve all possible variations including illumination, pose, expression, spectacles, etc. Figure 3.4 show samples from FGNET. The first and second row are clear images but the last row is considered as unclear which do not have sufficient texture information such as wrinkles.

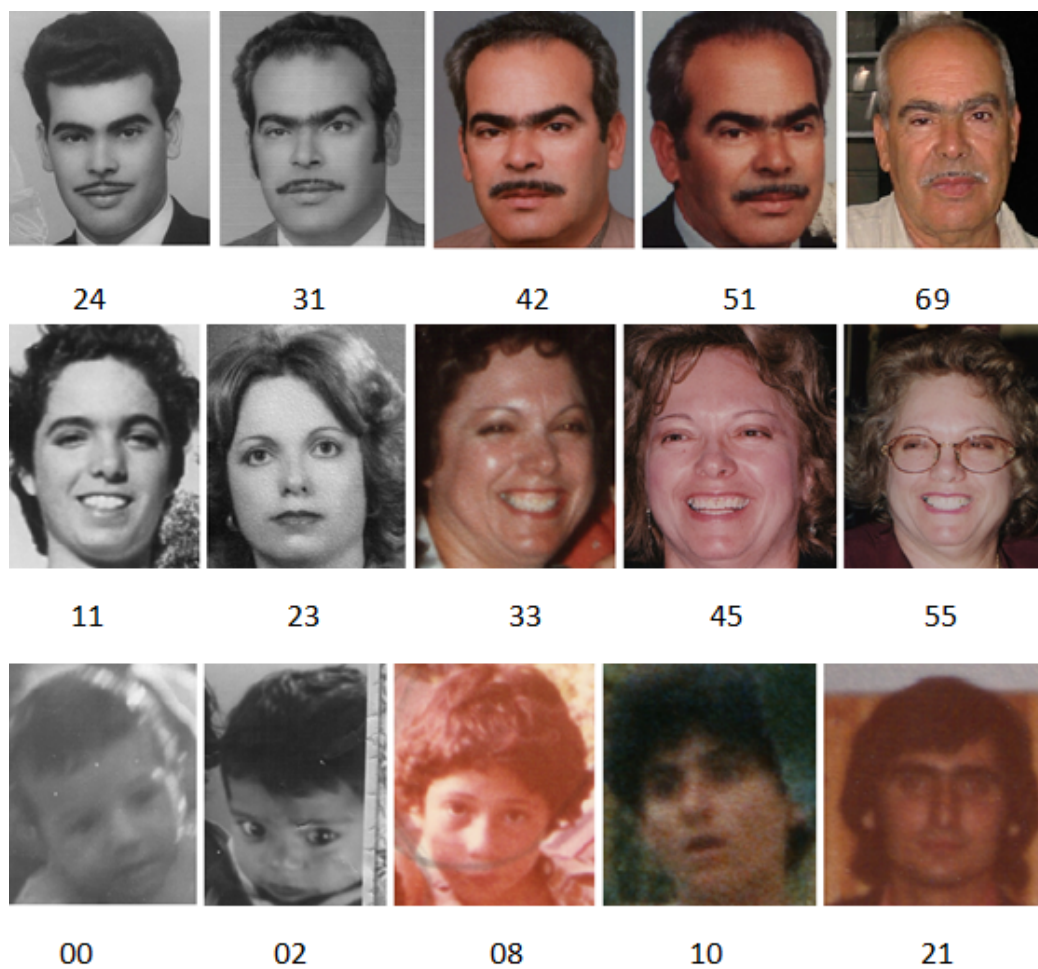


Figure 3.4: FG-NET samples. First row shows a male subject of same person at different age, second row also the same but the subject is a female and last row presents different subjects with poor image quality. The label of each image describes the age.

Table 3.2: The distribution of the images in FG-NET.

Age Range	Number of Images
0-9	371
10-19	339
20-29	144
30-39	70
40-49	46
50-59	15
60-69	8

### 3.2.4 MORPH

MORPH was funded by Face Aging Group at the University of North for face biometrics applications, Carolina a Wilmington. It was organized into two albums. The publicly available album of MORPH contains 55,000 unique images of more than 13,000 individuals, spanning from 2003 to late 2007. The Age range is between 16 to 77 with a median age of 33. The average number of images per individual is 4 and the average time between photos is 164 days, As seen in Figure 3.5. (Ricanek Jr & Tesafaye 2006). Table 3.3 shows the age range distribution of the MORPH dataset.

Table 3.3: Age range distribution of the images in MORPH album2.

Age Range	Number of images
16-19	7,469
20-29	16,325
30-39	15,357
40-49	12,050
50+	3,933

### 3.2.5 PAL

The Productive Aging Lab Face database (PAL) consist of 1,142 face images for 575 subject in age range from 18 to 93 year, with neutral expression except some smiling expression. PAL dataset was developed to be more representative of age groups



Figure 3.5: MORPH album2 samples. First row shows a male subject of same person at different age/illumination/position, second row also the same but the subject is a female. The label of each image describes the age.

across the lifespan, with a special emphasis on recruiting older adults, which allow researchers interested in using facial stimuli access to a wider age range of adult faces than other datasets (Minear & Park 2004). Table 3.4 shows the age distribution in PAL, and Figure 3.6 shows samples from PAL.

Table 3.4: Age range distribution of the images in PAL.

Age Range	Number of images
18-29	218
30-49	76
50-69	123
70+	158

### 3.2.6 Social Habit Dataset

The other social habits dataset that used in the experiments was collected by Alarifi et. al. (Alarifi et al. 2017) in Manchester. It consists of 164 participants with mean



Figure 3.6: PAL samples. First row shows a different male subjects at different age and race, second row for female. The label of each image describes age and race (African-American / Caucasian / Other).

age of 48.43 ( $\pm 21.44$ ) and age range between 18 to 92. There are 25 different self-reported ethnicities in this dataset including African, Arabic, Chinese and Malaysian. The ethnic group with most participants is White British with 119 images. There are 85 participants never smoked, 21 currently smoke tobacco in some form, 1 smokes electronic cigarettes only, 6 had partaken in smoking a few times in their lives and 51 used to smoke but stopped. The main reported gender was female with a total number of 107 participants, there were also 56 male participants and 1 trans-gender participant. This dataset was collected under a controlled environment with a high-quality images. Figure 3.7 shows samples from this dataset.



Figure 3.7: Sample from social habits dataset that collected by Alarifi et. al. (Alarifi et al. 2017). The label of each image describes age and smoking status (Smoker or Non-smoker)

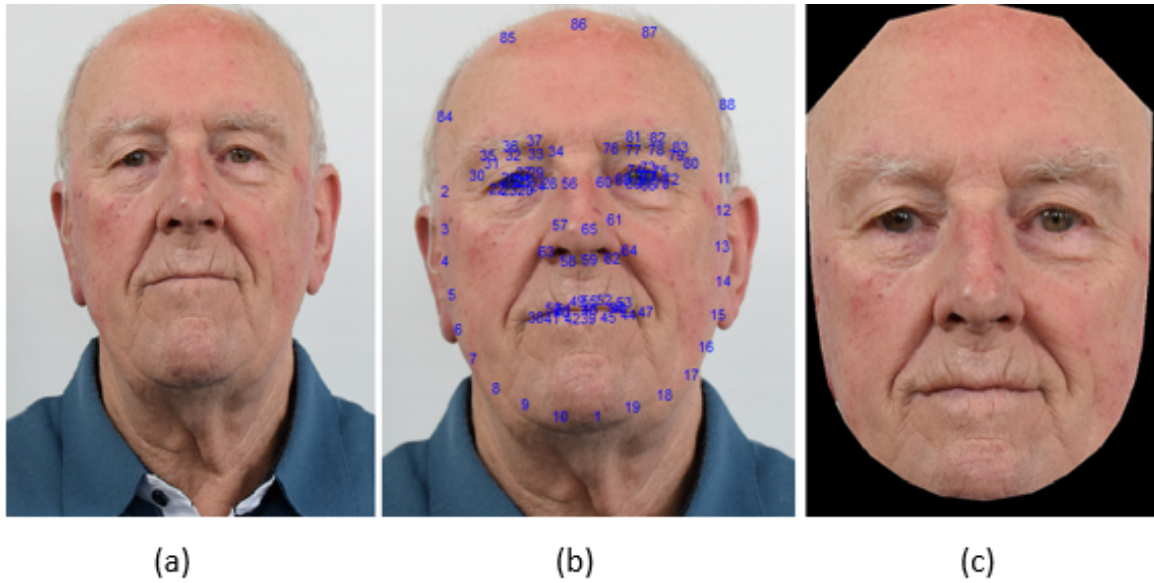


Figure 3.8: Face detection: (a) Original image obtained from Social Habits dataset (Alarifi et al. 2017); (b) Facial landmark detection using Face++; and (c) Warped image.

### 3.3 Face Detection and Alignment

In common cases, the face images that captured can include background regions and part of human body in addition to a human face. Background region and other human body does not contain any information about age, so it must be removed firstly. Therefore, as in many face research (Ng et al. 2014b, 2015a), the face was detected firstly as a pre-processing step. In this thesis on-line Face++ detector (Zhou et al. 2013) was used for face detection. Face++ is a facial landmark detection tool that utilized a deep learning approach to detect the face, it is also provide some face analysis applications such as gender, age, race and expression. A total of 88 landmarks were detected using Face++ (as shown in Figure 3.8(b)). Once the face was detected, a linear transformation is determined between each image and template (mean shape image) through the Procrustes analysis (Goodall 1991). In this work, the local transformation is defined as the projection of a shape  $S$  to a new shape 'S' using three landmark points: the center landmarks of eyes and mouth. Then, a warped image is generated by an affine geometric transformation (Ng et al. 2015a) as shown in Figure 3.8(c). These steps were applied to all datasets used in this thesis except FG-NET which obtained with 68 landmarks.



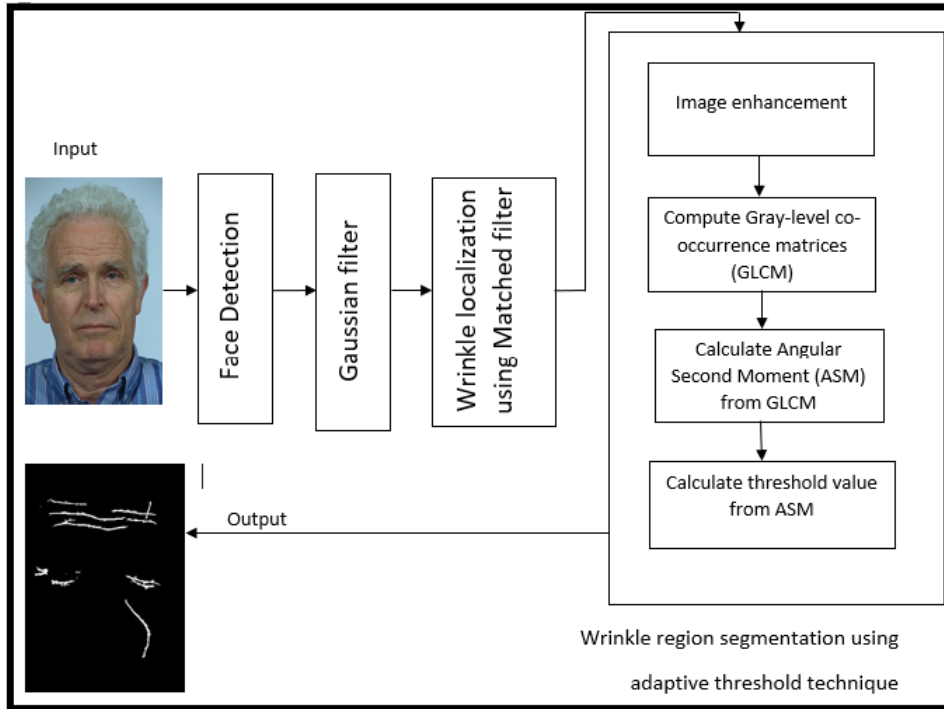


Figure 3.9: Proposed methodology.

### 3.4 Features Representation using Wrinkle local-based Descriptor(WLD)

The proposed method WLD was applied to extract aging features for age estimation. Where a combination of wrinkle and local features was used to create WLD. Wrinkles were detected using the proposed method for wrinkle detection, where local features were detected using scattering transform. The details about wrinkle detection method and scattering transform discussed in the next sections.

#### 3.4.1 Wrinkle Detection Method

This section described the details about the proposed wrinkle detection method. The face was detected firstly using face++ detector. Secondly, the matched filter was applied to localized wrinkle regions. Thirdly, adaptive thresholding technique was applied for wrinkle region segmentation. Figure 3.9 illustrate the proposed methodology for wrinkle detection and Algorithm 1 describe the proposed method.

The proposed algorithm is considered because it applied matched filter to locate wrinkle regions efficiently then adaptive thresholding technique based on Angular Second Moment (ASM) was used to segment wrinkle region from the background. ASM

**Algorithm 1:** Segmentation of wrinkle region

- 1 Input image.
- 2 Face detection and alignment.
- 3 Convert colored face image to the gray scale.
- 4 Apply Gaussian filter.
- 5 Apply median filter.
- 6 Localize the wrinkle region using 2D matched filter.
- 7 Segment wrinkle region using ASM-based threshold (details in Algorithm 2).

is one of the features that extracted from Gray-level co-occurrence matrix (GLCM) (Haralick et al. 1973), it has an ability to captures the textural information needed for the robust wrinkles segmentation.

#### 3.4.1.1 Matched Filter

A two dimensional matched filter was widely used for fingerprint detection (O’Gorman & Nickerson 1988) and blood vessel detection in a retinal images (Chaudhuri et al. 1989), but not for wrinkle detection. Gorman et al. (O’Gorman & Nickerson 1988) stated that a fingerprint images contains a narrow ridges separated by a narrow background valleys. This pattern may be corrupted by a various kinds of noise causing a breaks in the ridges, bridges between ridges, and overall gray-intensity variations. They also stated that, matched filter is optimal filter for a signal detection that can be designed to perform fingerprint image enhancement effectively.

Later on, Chaudhuri et al. (Chaudhuri et al. 1989) applied matched filter to detect the blood vessel in a retinal images. They stated that blood vessel have poor local contrast and the application edge detection algorithms yield results which are not satisfactory. Therefore, they introduced an operator for detecting blood vessels based on the optical and spatial properties of objects to be recognized. The grey-level profile of the cross section of a blood vessel is approximated by a Gaussian shaped curve. The concept of matched filter detection of signals is used to detect the piecewise linear segments of blood vessel in these images.

Let us consider the detection of arbitrary 1-D signal  $s(t)$  in an additive Gaussian white noise. If the signal is passed through a filter with a transfer function  $H(f)$ , the output signal  $s_0(t)$  is given by (Chaudhuri et al. 1989):

$$s_0(t) = \int H(f)\{S(f) + \eta(f)\} \exp(j2\pi ft)df \quad (3.1)$$

where  $S(f)$  is a Fourier transform of  $s(t)$ , and  $\eta(f)$  is the noise spectrum. Using Schwarz inequality it can be proven that the filter  $H(f)$  that can be maximizes the

output signal-to-noise ratio is given by  $H_{opt}(f) = S * (f)$ . Since the input signal  $s(t)$  is real valued,  $h_{opt}(t) = s(-t)$ . This optimal filter with impulse response  $h(t)$  is commonly known as a matched filter for the signal  $s(t)$ . In a typical communication system, if there are  $n$  different signals  $s_i(t), i = 1, 2, 3, \dots, n$ , the received signal is passed through a stack of  $n$  matched filter. If the response due to the  $j$ th filter is maximum, it is concluded that the signal  $s_j(t)$  was transmitted.

Under the present context, it may be noted that the intensity profile can be assumed to be symmetrical about the straight line passing through the center of vessel. Hence,  $s(-t) = s(t)$ . The optimal filter must have the same shape as the intensity profile itself. In the other word, the optimal filter is given by  $h_{opt}(d) = -\exp(-d^2/2\sigma^2)$ . The negative sign indicate that the vessels are darker than the background. Also note further that instead  $n$  different type of objects, having to be identified, the problem reduces to deciding whether or not a particular pixel belong to blood vessel. If the magnitude of the filter output at a given pixel location exceeds a certain threshold, the pixel is labeled as a part of vessel.

When the concept of the matched filter is extended to a two dimensional images, it must be appreciated that a vessel may be oriented at any angle  $\theta(0 < \theta < \pi)$ . The matched filter  $s(t)$  will have it is peak response only when it is aligned at an angle  $\theta \pm \pi/2$ . Thus the filter need to be rotated for all possible angles. The corresponding responses are to be compared and for each pixel only the maximum response is to be retained.

Consider the response of this filter for a pixel belonging to the background retina, Assuming the background to have constant intensity with zero mean additive Gaussian white noise, the expected value of the filter output should ideally be zero. The convolution kernel is, therefore, modified by subtracting the mean value of  $s(t)$  from the function itself. It has already been mentioned that the vessel may be considered as a piecewise linear segments. Instead of matching a single intensity profile of the cross section of vessel, a significant improvement can be achieved by matching a number of cross section (of identical profile) along its length simultaneously. Such a kernel may be mathematically expressed as (Chaudhuri et al. 1989)

$$K(x, y) = -\exp\left(\frac{-x^2}{2\sigma^2}\right) \text{ for } |y| \leq L/2 \quad (3.2)$$

where  $L$  is length of the segment for which the vessel is assumed to have a fixed orientation. For the vessel at different orientations, the kernel has to be rotated accordingly.

From the above explanation, it is clear that matched filter retains the computational simplicity of the enhancement / thresholding type of edge operators, and at the same time incorporates the advantages of using model-based edge detectors. It would be interesting to find out the performance of matched filter on wrinkle detection.

The implementation of a two-dimensional matched filter kernel that used in this work is designed as follows: Let  $\bar{P} = [xy]$  be a discrete point in the kernel, and  $\theta_i$  be the orientation of the  $i$ th kernel matched to a wrinkle region at an angle  $\theta_i$ . In order to compute the weighting coefficients for the kernel it is assumed to be centered about the origin  $[0\ 0]$ . The rotation matrix is given by (Chaudhuri et al. 1989):

$$\bar{r} = \begin{bmatrix} \cos \theta_i & -\sin \theta_i \\ \sin \theta_i & \cos \theta_i \end{bmatrix} \quad (3.3)$$

and the corresponding point at the rotated coordinate system is given by  $\bar{P}_i = [uv]$ . A set of 12 different kernel is applied and at each pixel only the maximum of their responses is retained.

A Gaussian curve has infinitely long double sided trail. A trail was truncated to  $u = \pm 3\sigma$ . A neighborhood  $N$  is defined such that  $N = (u, v) | u| \leq 3\sigma, |v| \leq L/2$ . The corresponding weights in the  $i$ th kernel are given by (Chaudhuri et al. 1989)

$$K_i(x, y) = -\exp\left(\frac{-u^2}{2\sigma^2}\right) \forall \bar{P}_i \in N \quad (3.4)$$

If  $A$  denotes the number of points in  $N$ , the mean value of the kernel is determined as (Chaudhuri et al. 1989):

$$m_i = \sum_{\bar{P}_i \in N} K_i(x, y) / A \quad (3.5)$$

Thus the convolutional mask that used is given by  $K'_i(x, y) = K_i(x, y) - m_i \forall \bar{P}_i \in N$ .

### 3.4.1.2 Thresholding Technique

Although signal processing techniques such as gabor filters, gaussian filters and wavelet transforms can be used to enhance the detection of wrinkles, it still involve false detections caused by other factors and variation that found on existing face images datasets. An optimal thresholding technique is needed to segment the enhanced wrinkles region efficiently (Batool & Chellappa 2015). Global thresholding where global or standard threshold value is taken as mean value is inefficient to segment the wrinkle region from skin, due to the illumination variations and other skin features

that cause intensity gradients Lookalike wrinkles. To overcome this issue adaptive thresholding was used in this work to segment wrinkle region efficiently.

To increase the accuracy, image enhancement techniques were applied as a pre-processing step before the calculation of threshold value. Next sections discussed these techniques and calculation of threshold value from GLCM features, and brief description found in Algorithm 2.

<p><b>Algorithm 2:</b> Adaptive thresholding techniques</p>
---

- |  |
|--|
| <ol style="list-style-type: none"> <li>1 Input image.</li> <li>2 Convert colored image to the gray scale.</li> <li>3 Apply CLAHE.</li> <li>4 Apply average filter.</li> <li>5 Apply gaussian filter.</li> <li>6 Compute GLCM.</li> <li>7 Compute ASM.</li> <li>8 Calculate the range for ASM array.</li> <li>9 Get the max and mean for the range values.</li> <li>10 Use the summation of max and mean value as a threshold value.</li> </ol> |
|--|

### Image Enhancement

An efficient image enhancement techniques is needed to deal with the low quality and low contrast images. In this paper, a combination of different enhancement filters include: contrast limited adaptive histogram equalization (CLAHE), average filter and Gaussian filter were applied to gray image before calculation of the threshold value.

CLAHE enhances the contrast of images by transforming the values in the intensity image. It operates on small data regions named tiles, rather than the entire image. Each tile's contrast is enhanced, so that the histogram of the output region approximately matches the specified histogram. The neighboring tiles are then combined using bilinear interpolation in order to eliminate artificially induced boundaries. The contrast, especially in homogeneous areas, can be limited in order to avoid amplifying the noise which might be present in the image (Zuiderveld 1994).

### Gray-Level Co-occurrence Matrix (GLCM)

GLCM it also called gray-tone spatial dependence matrix is powerful technique for texture image segmentation (Haralick et al. 1973, Mokji & Bakar 2007). It contains information about spacial pattern in texture image and number\ nature of boundaries present, therefore it is valuable for the computation of threshold value (Mokji & Bakar 2007). Haralick et al. (Haralick et al. 1973) computed a set of gray-level co-occurrence

matrices from a various angular relationships  $\phi$  and distance ( $d$ ) between neighboring pixel pairs on the image. The distance  $d$  is represents the distance from the pixel of interest and measured in pixel number while  $\phi$  is quantized in four directions (horizontal:  $0^\circ$ , diagonal:  $45^\circ$ , vertical:  $90^\circ$ , and anti-diagonal:  $135^\circ$ ).

Suppose a gray image  $I$  has  $M$  rows and  $N$  columns, the gray-level co-occurrence matrix  $C(i, j)$  for distance  $d$  and orientation  $\phi$  is defined as (Haralick et al. 1973):

$$C(i, j) = \frac{1}{R} \sum_{x=0}^{M-1} \sum_{y=0}^{N-1} (P\{I(x, y) = i, I(x \pm d\phi_1, y \pm d\phi_2) = j\}) \quad (3.6)$$

For each of the intensity pair (i,j), equation (2) counts the number of times that the pixel with value i occurred at relative distance  $d$  and direction  $\phi$  with the pixel of value j in the input image I. If this spacial relationship is found then  $P\{.\} = 1$ , otherwise  $P\{.\} = 0$ .  $1/R$  is a normalizing factor.

Haralick et al. (Haralick et al. 1973) defined a set of 14 features from the gray-level co-occurrence matrix. ASM or energy is one of these features, it measures the texture homogeneity. In this paper, information based on ASM is applied as a thresholding technique, it can be define as (Haralick et al. 1973):

$$ASM = \sum_i \sum_j C(i, j)^2 \quad (3.7)$$

where  $C(i, j)$  is a normalized GLCM entry. ASM feature matrix across different orientations (horizontal:  $0^\circ$ , diagonal:  $45^\circ$ , vertical:  $90^\circ$ , and anti-diagonal:  $135^\circ$ ) and distances ( $d_i$ ) $_{i=1,2,3,4}$  is computed and defined as (Mokji & Bakar 2007):

$$F = (f_{i,j}), \quad 1 \leq i, j \leq 4 \quad (3.8)$$

where

$$f_{i,j} = ASM_{(d_i, \phi_j)}, \quad 1 \leq i, j \leq 4 \quad (3.9)$$

The range of F is defined as follow (Mokji & Bakar 2007):

$$R_\phi = Range(F) \quad (3.10)$$

where  $R_\phi$  is a row vector containing the range of each column of F. Based on the  $R_\phi$  value, the threshold value is calculated as follow:

$$T = MAX(R_\phi) + MEAN(R_\phi), \quad (3.11)$$

Finally,  $T$  is used with MFR to obtained the segmented image as:

$$S(x, y) = \begin{cases} 0 & \text{if } Z(x, y) \leq T, \\ 1 & \text{otherwise,} \end{cases}$$

where  $Z(x, y)$  is matched filter's response.

### 3.4.2 Scattering Transform (ST)

A scattering transform is a local descriptor introduced by Stephane Mallat in 2010. It is computed with a cascade of wavelet decompositions and complex modulus. Scattering operators provide much richer descriptors of complex structures such as corners, junctions and multi-scale texture variations. These coefficients are locally translation invariant and they linearize small deformations. They are computed with a convolution network which cascades contractive wavelet transforms and modulus operators, as shown in Figure 3.10 (Bruna & Mallat 2011).

Let  $I_i(x)$ , where  $x \in R^2$  is an input image and  $R_\gamma x$  is the rotation of  $x$  by an angle  $\gamma$  where  $\gamma \in \Gamma$  is a group of rotations. Directional wavelets  $\psi$  in angle  $\gamma$  and scale  $2^j$  are (Bruna & Mallat 2011):

$$\psi_{j,\gamma}(x) = 2^{-2j}\psi(2^{-j}R_\gamma x) \quad (3.12)$$

The coefficients vector of a directional wavelet transform of  $f$  at position  $x$  is given by (Bruna & Mallat 2011):

$$W_J f(x) = \begin{pmatrix} f \star \psi_{j,\gamma}(x) \\ f \star \phi_J(x) \end{pmatrix}_{j < J, \gamma \in \Gamma} \quad (3.13)$$

Where  $\phi_J(x)$  cover the low frequencies using a low-pass filter. Let  $\hat{f}(\omega)$  be the Fourier transform of  $f$ , if all frequencies are covered by a wavelet in a frequency domain (Bruna & Mallat 2011):

$$\int f \quad |\hat{\phi}(\omega)|^2 + \sum_{\gamma} (|\hat{\psi}_{\gamma}(\omega)|^2) = 1 \quad (3.14)$$

Then the wavelet transform can be contractive and unitary.

The wavelet is very localized at high frequency (sensitive to translation). To build a wavelet coefficients that is an invariant to translation and stable to deformations, compute the average of the partial derivative amplitudes of  $f$  in the  $K$  directions  $\gamma \in \Gamma$  with a low-pass filter  $\phi_J$  (Bruna & Mallat 2011):

$$|f \star \psi_{j,\gamma}| \star \phi_J(x) \quad (3.15)$$

Which forms the first layer coefficients of scattering transform that shown in Figure 3.10.

However, due to the averaging, this wavelet might lost some informations that is essential to discriminate textures. Scattering operators recover part of the information that lost in averaging ( $|f \star \psi_{j_1,\gamma_1}| \star \phi_J(x)$ ) by convolutions with wavelets ( $|f \star \psi_{j_1,\gamma_1}| \star$

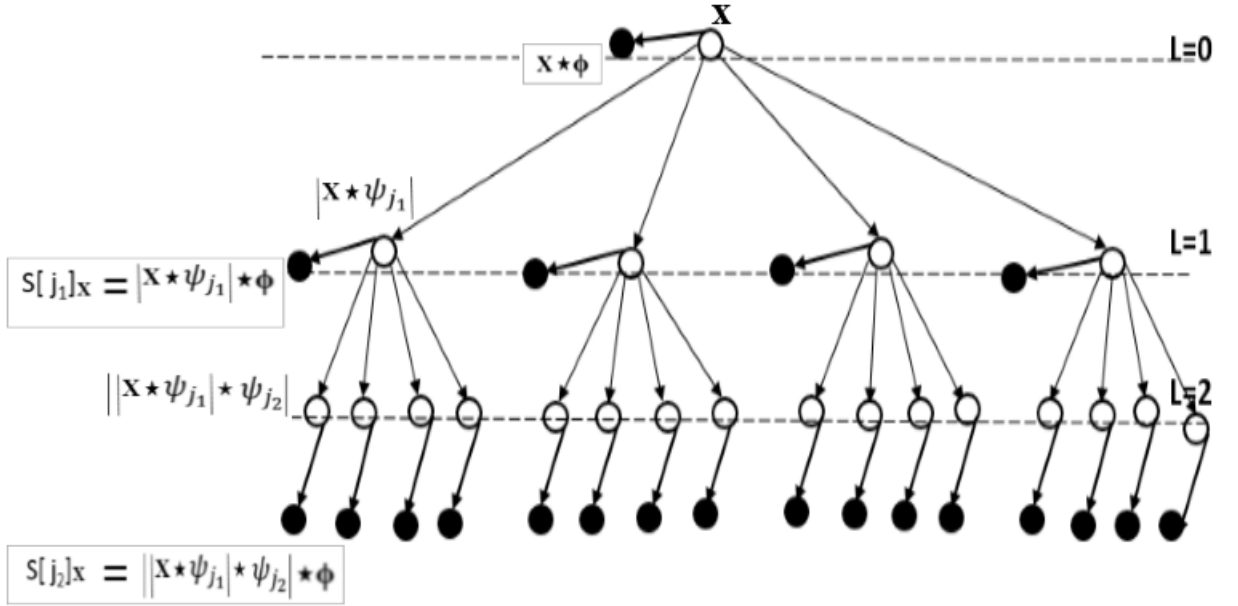


Figure 3.10: Scattering Transform Architecture.

$\psi_{j_2, \gamma_2}$ ), the complex phase is removed by a complex modulus then averaged by  $\phi_J$  (Bruna & Mallat 2011):

$$||f \star \psi_{j_1, \gamma_1}| \star \psi_{j_2, \gamma_2} \star \phi_J \quad (3.16)$$

This form output the second layer called " Scattering coefficients ", it is stable to deformations and invariance to transformations. The lost information in (3.15) can recovered again by get the modulus, convolution with wavelet then averaging. Figure 3.10 illustrate the above procedure, the output in this network at all layers (the output at each layer is demonstrated as a black node). In this thesis ST was proposed as a local features descriptor for age estimation.

### 3.5 Age Prediction

A support vector regression function called Sequential Minimal Optimization (SMO) was applied to solve age estimation problem as a regression problem. According to Guo et al. (Guo et al. 2008a) a non-linear regression function such as SMO is more suitable to model the complex aging process. It can be obtained using kernels such as polynomials and Radial Basis Function (RBF) functions. In the non-linear case, the optimization problem corresponds to finding the flattest or linear regression function in the higher dimensional feature space instead of input space (Guo et al. 2008a). SMO is very efficient in terms of both time and space, it often converges in a small



number of iterations. It does not require extra matrix storage except the amounts of memory required to store  $2 \times 2$  matrices required by SMO.

SMO is an iterative algorithm for solving the optimization problem by operating on a fixed size subset of the training set at a time. SMO breaks this problem into a series of smallest possible sub-problems, which are then solved analytically. SMO algorithm puts chunking to the extreme by iteratively selecting working sets of size two and optimizing the target function with respect to them. One advantage of using working sets of size two is that the optimization sub-problem can be solved analytically.

## 3.6 Validation

For wrinkle detection, JSI and boundary F1 measure (BF score) was used to validate the new algorithm, and two types of measurement were adopted to validate age estimation methods: Mean Absolute Error(MAE) and Cumulative Score (CS) (Choi et al. 2011, Guo, Mu, Fu & Huang 2009, El Dib & Onsi 2011, Chang & Chen 2015).

### 3.6.1 Jaccard Similarity Index (JSI)

The segmentation results can be assessed using JSI to measure the overlap between the computerized method with manual annotation. In this context, JSI is used (Ng et al. 2014a) to measure the reliability of wrinkle detection method. The Jaccard index  $J$  is calculated by the intersection of  $A$  and  $B$  divided by the union of  $A$  and  $B$ . Where  $A$  is manual annotation and  $B$  is the automatic annotation.

$$J(A, B) = \frac{|A \cap B|}{|A \cup B|} \quad (3.17)$$

### 3.6.2 BF score

Existing methods on automatic wrinkle detection can be classified into: edge-based and curvilinear-based. Due to the variation on how wrinkle is detected, there is still no benchmark metrics to measure the performance of automatic wrinkle detection methods. Ng et al. (Ng et al. 2015b) detected wrinkle as a line and used Jaccard similarity index (JSI) to evaluate their method. Batool et al. (Batool & Chellappa 2015) proposed a quantitative evaluation setup to assess their method performance where the wrinkle was detected as a curve.

Global metrics such as precision, recall and Jaccard Similarity Index (JSI) have been popularly used to evaluate segmentation algorithms, however, these metrics are

not satisfactory enough when the wrinkle is detected as a region. Furthermore, it can display divergent outcomes making it difficult to rank different segmentation solutions (Csurka et al. 2013). Therefore, a new metrics called BF (Boundary F1) measure (Csurka et al. 2013) was introduced in this work to evaluate the proposed wrinkle detection method. Its complementary to JSI and appropriate for non-uniform wrinkle properties (length, width and depth) (Csurka et al. 2013).

The BF score is defined as the harmonic mean (F1-measure) of the precision and recall values with a distance error tolerance to decide whether a point on the predicted boundary has a match on the ground truth boundary or not (Csurka et al. 2013). BF score measures can be defined as (Csurka et al. 2013):

$$BF1 = \frac{2 * P * R}{R + P} \quad (3.18)$$

where P is the “precision”, or positive predictive value (PPV), which is the relation between true positives and all elements classified as positives. R is the “Recall”, or true positive value (TPV), is the relation between true positives and all positive elements. For a given distance threshold  $\theta$ , P and R can be defined as (Csurka et al. 2013):

$$P = \frac{1}{|B_{ps}|} \sum_{x \in B_{ps}} [[d(x, B_{gt}) < \theta]] \quad (3.19)$$

and

$$R = \frac{1}{|B_{gt}|} \sum_{x \in B_{gt}} [[d(x, B_{ps}) < \theta]] \quad (3.20)$$

$[[z]] = 1$  if  $z = \text{true}$  and 0 otherwise,  $d()$  is the Euclidean distance,  $B_{gt}$  and  $B_{ps}$  is a boundary map of the ground truth and predicted map respectively.

### 3.6.3 Mean Absolute Error

MAE is the average of the absolute errors between estimated age and the ground truth (Ng et al. 2015a), MAE is commonly used in previous age estimation research to measure the accuracy of a system. The mathematical form of MAE shown in equation (3.22) (Ng et al. 2015a).

$$MAE = \frac{1}{X} \sum_{n=1}^X |a'_n - a_n| \quad (3.21)$$

where X is the number of images in testing dataset,  $a_n$  is the n-th ground truth, and  $a'_n$  is estimated age (Nguyen et al. 2014). In addition to general MAE, Guo et al (Guo et al. 2008a) used ”MAE per age” and ”MAE per decade” to show the performance

of age estimation in more details and allow to compare different approaches to show which method produce better result at each decade or age (Guo, Mu, Fu & Huang 2009, Guo et al. 2008a).

### 3.7 The Modified Hybrid Hessian Filter

This section describe the methods that used to study the effect of smoking on facial wrinkles. The original HHF (Ng et al. 2014a) algorithm detected only horizontal lines, but the facial wrinkles can appear as vertical lines in some face regions, and some of these regions can mainly be effected by smoking (Model 1985). So the HHF algorithm was modified to detect the vertical lines in addition to horizontal lines (Osman et al. 2017).

The 2D face color image is converted to gray-scale image, and denoted as  $I(x,y)$ . The directional gradient ( $Gx, Gy$ ) is computed from the gray-scale image as (Ng et al. 2014a):

$$\Delta I(x, y) = \left( \frac{\partial I}{\partial x}, \frac{\partial I}{\partial y} \right) \quad (3.22)$$

where  $\frac{\partial I}{\partial x}$  and  $\frac{\partial I}{\partial y}$  are the directional gradients.  $Gx$  is  $\frac{\partial I}{\partial x}$  and  $Gy$  is  $\frac{\partial I}{\partial y}$ . The directional gradient has greatly smoothed the image and preserved the data of interest.

The  $Gy$  has been used as the input images for HHF to calculate Hessian matrix  $H$  and extract the horizontal lines. To modify the algorithm for vertical lines detection,  $Gx$  is used as the input for our modified HHF. The Hessian matrix  $H$  then is defined as (Osman et al. 2017):

$$H(x, y, \sigma) = \begin{vmatrix} \frac{\partial^2 I(x,y)}{\partial I(y)\partial I(y)} & \frac{\partial^2 I(x,y)}{\partial I(x)\partial I(y)} \\ \frac{\partial^2 I(x,y)}{\partial I(x)\partial I(y)} & \frac{\partial^2 I(x,y)}{\partial I(x)\partial I(x)} \end{vmatrix} = \begin{vmatrix} H_a H_b \\ H_b H_c \end{vmatrix} \quad (3.23)$$

where  $H_a$ ,  $H_b$  and  $H_c$  are the outputs of second derivative. The remaining steps to detect the wrinkles are as described in (Ng et al. 2014a).

#### 3.7.1 Wrinkles Detection and Quantification

To detect wrinkles, face template or mask (as shown in Figure 3.11) has been used with ten predefined wrinkles regions and fixed coordinates for mouth and eyes (Ng et al. 2015a). The mask was divided to 10 regions which represents as: forehead, glabella, upper eyelids, crow's feet (or eye corners), lower eyelids (or eyebag), cheeks, nasolabial grooves (or nasolabial folds), upper lips, marionette and lower lips, all these

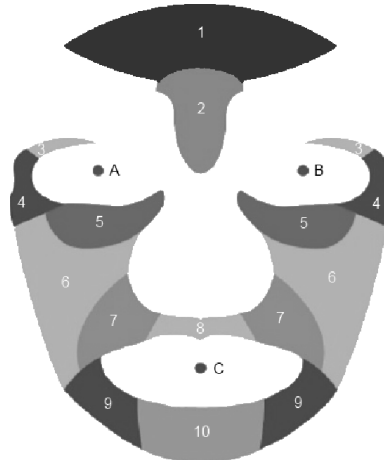


Figure 3.11: Face mask with ten predefined wrinkle regions by (Ng et al. 2015a).

regions have been used to construct aging patterns. Based on the three points (eye, mouth, and nose), each face image was normalized to the mask by using piecewise affine warping (Cootes et al. 2001). Finally, the wrinkles pattern for ten regions was constructed using proposed modified HHF (Ng et al. 2014a).

### 3.8 Conclusion

The techniques, measurements and datasets described in this chapter provide the base knowledges for contributions that discussed in the next chapter.

# Chapter 4

## Results and Discussion

### 4.1 Introduction

This chapter describes several experimentation results for the proposed methods described in chapter 3. First experiment was applied to detect wrinkle regions using the proposed method. Second experiment was applied to estimate the age using the proposed WLD method for features representation. last experiment applied to study the effect of smoking on face wrinkles. Next sections describe details of these experiment.

### 4.2 Experimental Results for Wrinkle Detection

The experiments were executed on Matlab R2017b. The proposed method was evaluated using three sets of images with a different resolution: 45 images were selected from FERET (Phillips et al. 1996), 52 from social habits dataset (Alarifi et al. 2017) and 41 from in-house Sudanese dataset, where the resolution is  $282 \times 407$ ,  $642 \times 947$  and  $846 \times 1300$  for three datasets respectively. As clear in Figure 4.1 social Habits dataset was collected in a control environment, where Sudanese and FERET were collected in uncontrolled environment with more variations that have a direct effect on automatic wrinkle detection.

As mentioned before, detecting wrinkle as pixel line is inefficient due to the variations and non-wrinkle skin features that caused intensity gradients similar to that caused by wrinkle, as shown in Figure 4.2 (a) the forehead images include three wrinkle regions. However, in Figure 4.2 (b) when wrinkle is detected as a line using HLT (Ng et al. 2015b) each changes in intensity gradients was detected as wrinkle. Its clear that in Figure 4.2 (c) the three wrinkle regions was detected correctly using our proposed method.



Figure 4.1: Dataset Samples. First row shows samples from Social habits dataset, where sccond raw for Sudanese dataset, and last row shows FERET samples.

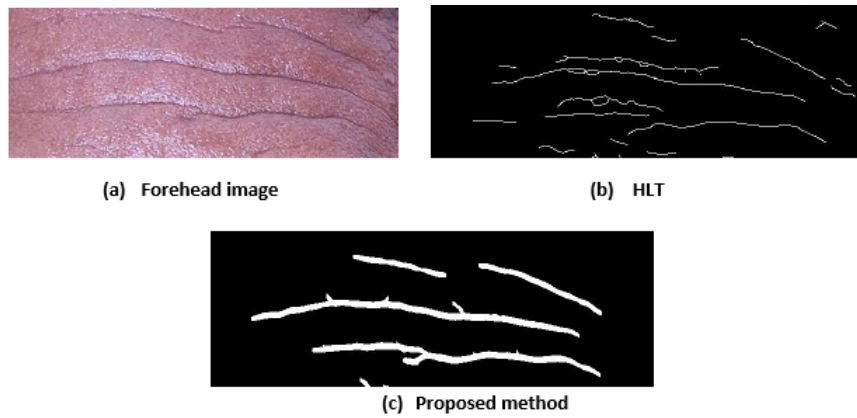


Figure 4.2: Detection of wrinkle as region vs detection as line: (a) cropped forehead image, redrawn from Sudanese dataset; (b) wrinkle detection as a line using HLT (Ng et al. 2015b); and (c) detection of wrinkle region using our proposed method.

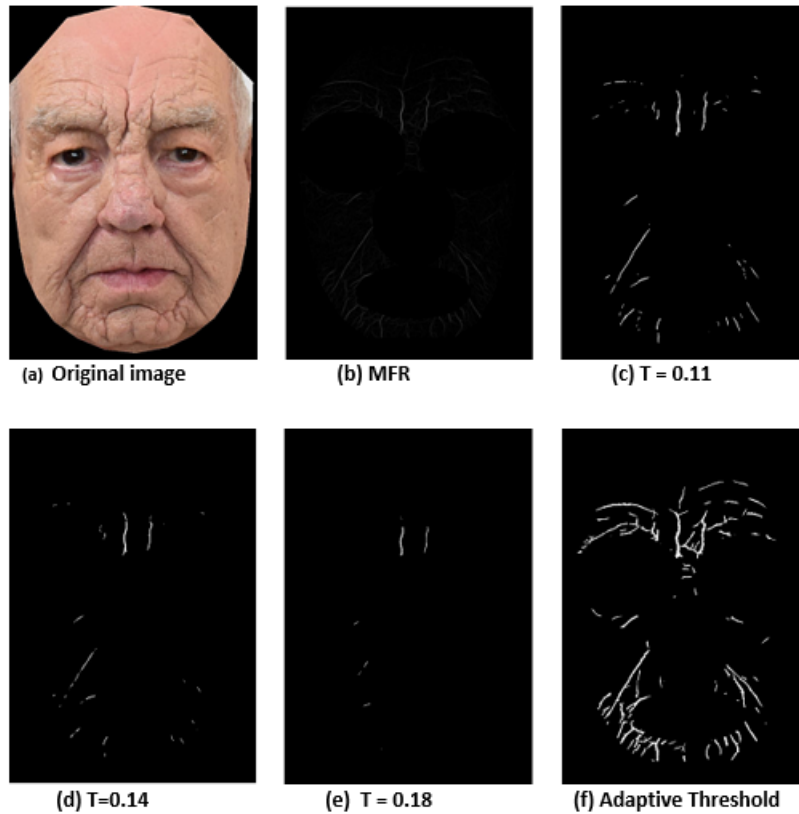


Figure 4.3: A global thresholding of matched filter response. Original image is redrawn from Social Habits dataset.  $T$  is a threshold value

However, applying global threshold with MFR is unable to segment wrinkles well. Figure 4.3 shows the matched filter response and output of different threshold values compared with adaptive thresholding, Figure 4.3 (b) clearly shows that wrinkle was localized well using matched filter. However, the results using global thresholding with a different values (Figure 4.3 (c),(d) and(e)) were not segmented the wrinkles well. It's clear that in Figure 4.3 (f) the wrinkle regions were segmented well using adaptive thresholding. In addition adaptive thresholding reduce non-wrinkle parts (e.g. hair) that detected as wrinkle (see Figure 4.5). Although adaptive threshold was applied in HLT (Ng et al. 2015b), the thresh value did not calculated from the local image features, where the value is set to 15 if the largest area of connected pixels in the initial wrinkle map is higher than 10% of the image size, otherwise its set to 3. The input image was enhanced firstly using average and Gaussian filters, then annotated automatically using automatic annotator (Yap et al. 2018), the annotated images were used as a ground truth to calculate BF score. BF score captures complementary information with the JSI, it count the number of pixels misclassified in the region surrounding the actual object boundary and not over the entire image. Different

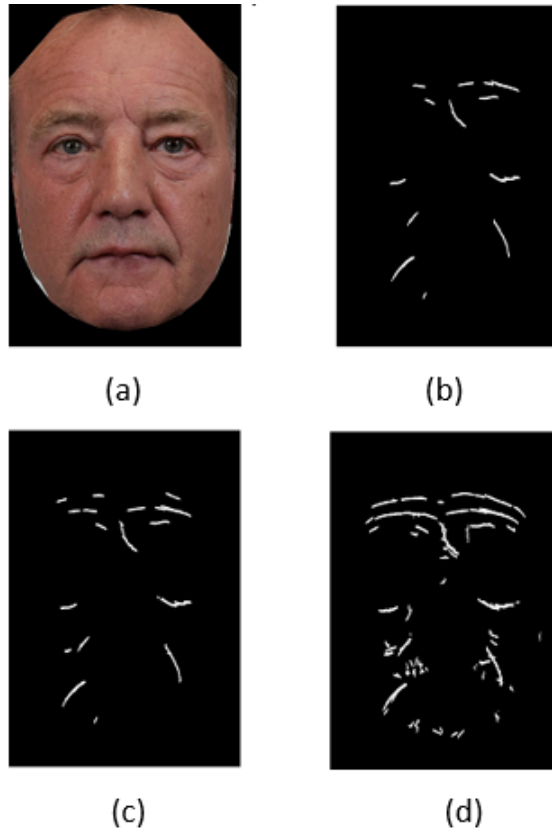


Figure 4.4: The effect of image enhancement step: (a) original images; (b) without CLAHE; (c) without filters; and (d) with filters

parameters setup were used in the experiment due to the variations in dataset, these parameters were illustrated in Table 4.1.

The effect of image enhancement techniques on the final result was shown in Figure 4.4, it's clear that in Figure 4.4 (d) the result is more accurate than others. In Figure 4.4 (b) average and Gaussian filters were applied without CLAHE, where Figure 4.4 (c) shows the result without enhancement techniques.

To compare the proposed method with HLT (Ng et al. 2015b) and Batool and Chellappa method (Batool & Chellappa 2015) we ran their Matlab codes using the same datasets and skeletonization process was applied to proposed method. Table 4.2 shows the comparison results. The proposed method achieved the best result on FERET wrinkle line detection in terms of JSI and BF Score, with 0.33 and 0.48, respectively. On the other two datasets, it achieved comparable results with HLT. Although HLT performed good results, it is not designed to segment the wrinkle regions. However, when manual annotation is used it is better to have intra- and inter reliability measurements from different coder, where in this work the annotation was





Figure 4.5: (a) Original image redrawn from FERET; (b) HLT (Ng et al. 2015b); (c) Method in (Batool & Chellappa 2015); and (d) Proposed method

Table 4.1: Parameter values for experiments in the three datasets.

Parameter	FERET	Social Habits	Sudanese
$\sigma$ (equation 3.2)	0.8	0.9	2
L (equation 3.2)	13	15	16
Median filter window size	3*3	4*4	7*7
Average filter size	3*3	3*3	60*60
Number of CLAHE tiles	70	200	160
Clip limits in CLAHE	0.09	0.17	0.05

done by single coder.

### 4.3 Experimental Results for Age estimation

As mentioned in section 1.2, aging is a complicated process, different subjects at same age may have a different features. To represent a facial image as a feature vector that is insensitive to translation and small displacement but reactive to large deformation, scattering transform(ST) (Bruna & Mallat 2011, 2013) was used.

The scattering transform of an input signal  $x$  is defined as the set of all paths that  $x$  might take from layer to layer. In this sense, the architecture of a scattering network closely resembles a convolutional deep network as shown in Figure 3.10. Scattering coefficients provide new local descriptors, carrying co-occurrence information at different scales and orientations(based on the experiments 4 scales and 8 orientations achieved better results). Despite the remarkable successes of deep convolution

Table 4.2: Comparison of BF score results for proposed method and other state-of-the-art methods using manual annotation as a ground truth.

Method	social habits	FERET	Sudanese
HLT (Ng et al. 2015 <sub>b</sub> )	0.38	0.45	0.27
Batool’s method (Batool & Chellappa 2015)	0.31	0.40	0.14
Proposed method	0.36	0.48	0.25

networks, the properties and optimal configurations of these networks are complex. Where ST network architecture is optimized to retain important information while avoiding useless computations (Bruna & Mallat 2013). Table 4.3 shows that ST outperform the state-of-the-arts methods on FERET and PAL with a smaller MAE 2.09 and 2.15 years respectively.

The wrinkle statistic was combined with ST to investigate the discriminative power of using only local feature for age estimation. Where the wrinkle was detected firstly using the proposed wrinkle detection method. The wrinkle was extracted from six regions: forehead, glabella, lower eyelids and crow’s feet, nasolabial grooves, marionette and lower lips. Each face image is normalised to the mask (as shown in Figure 4.6 (b)) using a piecewise affine warping. With consistent area size for the six face regions, all regions are used to construct the wrinkle patterns, which produce a standard feature vector subsequently used for training and testing (Ng, Yap, Cheng & Hsu 2017). From the wrinkle map  $\mathcal{X}$  and region of interest  $\mathcal{Z}_\gamma$ , the wrinkle image  $\mathcal{Y}_\gamma$  is defined as (Ng, Yap, Cheng & Hsu 2017):

$$\mathcal{Y}_\gamma(x, y) = \begin{cases} I(x, y) & \text{if } \mathcal{X}(x, y) \cap \mathcal{Z}_\gamma(x, y) = 1 \\ 0 & \text{otherwise} \end{cases} \quad (4.1)$$

The wrinkle pattern was constructed as follow: let  $P = \{f_1, f_2, \dots, f_n, g_1, g_2, \dots, g_n\}$ , where  $n$  is number of regions  $n = 6$ . The wrinkle intensity  $f_i$  of one particular region is defined as (Ng, Yap, Cheng & Hsu 2017):

$$f_i = \log \sum_{x=1}^{wt} \sum_{y=1}^{ht} \mathcal{Y}_\gamma(x, y) \quad (4.2)$$

where  $wt$  and  $ht$  are the width and height of  $\mathcal{Y}$ . The wrinkle density  $g_i$  of one particular region is defined as (Ng, Yap, Cheng & Hsu 2017)

$$g_i = \frac{area_1(i)}{area_2(i)} \quad (4.3)$$

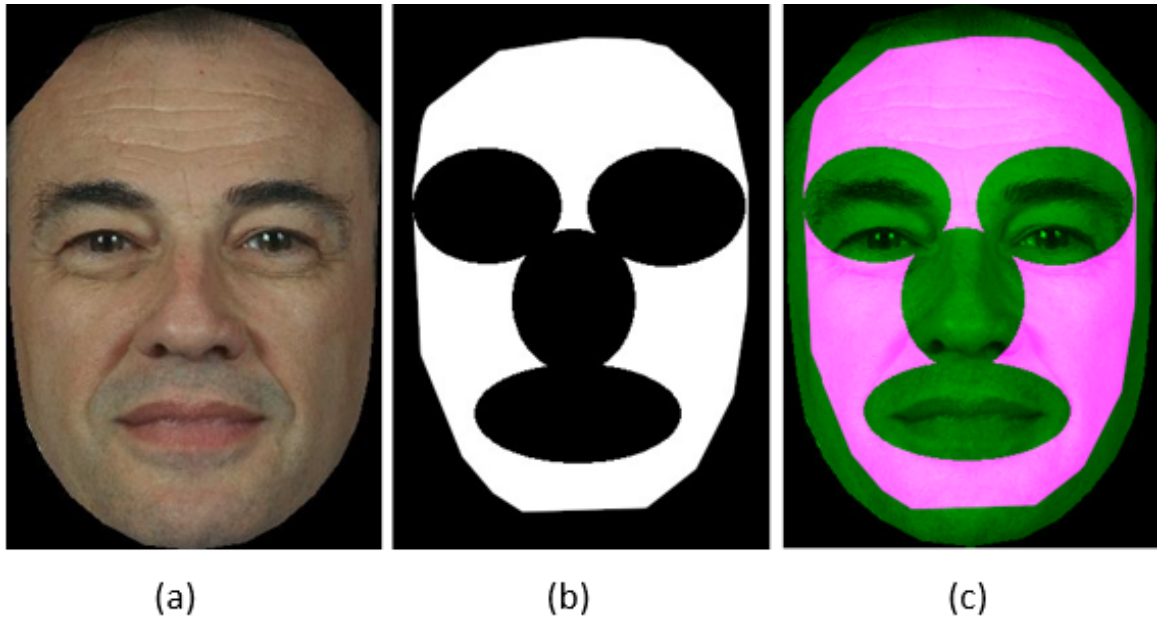


Figure 4.6: Wrinkle template. (a) Original images; (b) wrinkle template for wrinkles regions; and (c) Overlay the template on face image.

where  $area_1$  is the wrinkle area found in a particular region  $i$  and  $area_2$  is the area of region  $i$ . The results show that wrinkle-based features (location, intensity, length and density) can be used as discriminative features for age estimation. Table 4.3 shows the MAE for wrinkle pattern on FERET, also shows the result of combination of wrinkle pattern and ST on FERET. However, FG-NET was not used in this experiment, due to the low resolution images that collected from scanning process. It is difficult to detect wrinkle from low resolution images such as FG-NET, therefore it was used just with ST as in table 4.3.

#### 4.4 Experimental Results for Smoking and Wrinkles

This study investigates the effect of smoking on facial wrinkling using computerized algorithm. Most of the previous study were conducted using clinical assessment for wrinkles and other face features as in (Aizen & Gilhar 2001, Ippen & Ippen 1965, Model 1985, Bulpitt et al. 2001). The computerized studies either used wrinkles in addition to other face features (Raitio et al. 2004) or on skin replica rather than face images (Yin et al. 2001).

For this experiment, the wrinkles density was assessed in 83 images, with 42 smokers and 41 non-smokers in 18 to 88 age range. After constructing the wrinkles

Table 4.3: Comparison of MAE results between proposed method and state-of-the-arts methods on different datasets.

Method	FERET	PAL	FG-NET	Sudanese
(Choi et al. 2011) (Hybrid)	-	4.32	4.65	-
(Günay & Nabiyev 2013) (Local)	6.89	-	6.18	-
FAM+MWP (Ng, Yap, Cheng & Hsu 2017)(Hybrid)	3.02	6.50	5.66	-
Proposed method				
ST	2.12	2.22	7.31	4.04
wrinkle pattern	2.81	3.34	-	7.86
ST + wrinkle pattern	2.09	2.15	-	4.72

Table 4.4: The average wrinkles density for smokers and non-smokers.

Age group	Overall Average Density	Smoker Average Density	Non-Smoker Average Density
18 - 27	1121.61	1232.75	1032.70
28 - 37	1249.83	1227.40	1265.86
38 - 47	1307.67	1641.40	1069.29
48 - 57	2676.13	2588.39	2938.00
58 - 67	2347.71	2886.67	1943.50
68 - 77	2340.44	3172.22	3308.67
$\geq 78$	5311.00	6006.00	3226.00

Table 4.5: The average wrinkles density for smokers and non-smokers at each face region.

Regions	Average density of wrinkles for non-smoker	Average density of wrinkles for smoker	p-value
Region 1	56.9268	27.5714	0.051
Region 2	26.2927	45.8810	0.186
Region 3	76.5366	89.8333	0.946
Region 4	49.8293	59.6905	0.432
Region 5	161.0488	206.7857	0.936
Region 6	1295.7561	1875.9524	0.297
Region 7	70.9512	167.2381	0.000
Region 8	26.6585	54.4524	0.015
Region 9	63.0488	107.5952	0.064
Region 10	40.0976	55.11905	0.426

pattern using the a modified HHF (Osman et al. 2017), the wrinkles on a defined face region was extracted from the wrinkles pattern using threshold segmentation. The wrinkles density was calculated for each image, which is the area of wrinkle region (depth) divided by the area of the face mask. To analyze the correlation of age and the wrinkles density for smokers, non-smokers and both, the data was divided into 7 groups with 10 intervals (to ensured that each group consisted of a balanced number of smokers and non-smokers). The average of wrinkles density for the grouped data was calculated for smokers, non-smokers and both as shown in Table 4.4.

The result showed that the correlation is 0.8354, 0.8996 and 0.8604 between age and average density, age and smoker average density, age and non-smoker average density, respectively. This result showed that the wrinkles density for smoker is higher than non-smoker through age progression, this result is illustrated in Figure 4.7. The average density of wrinkles at each region was calculated for smoker and non-smoker as shown in Table 4.5, and the graph in Figure 4.8 illustrates the comparison between the average density of wrinkles for smokers and non-smokers at each region.

The data was analyzed statistically using SPSS, for each region, the wrinkles density was compared between smoker and non-smoker. The result showed that the density of wrinkles for smokers in region 7 and 8 (around the mouth) was significantly higher than the density of wrinkles for non-smokers in the same regions, with the p-value of 0.000 and 0.015 for region 7 and region 8, respectively. This result can be shown clearly in the visual comparison of the wrinkles in Figure 4.9, where

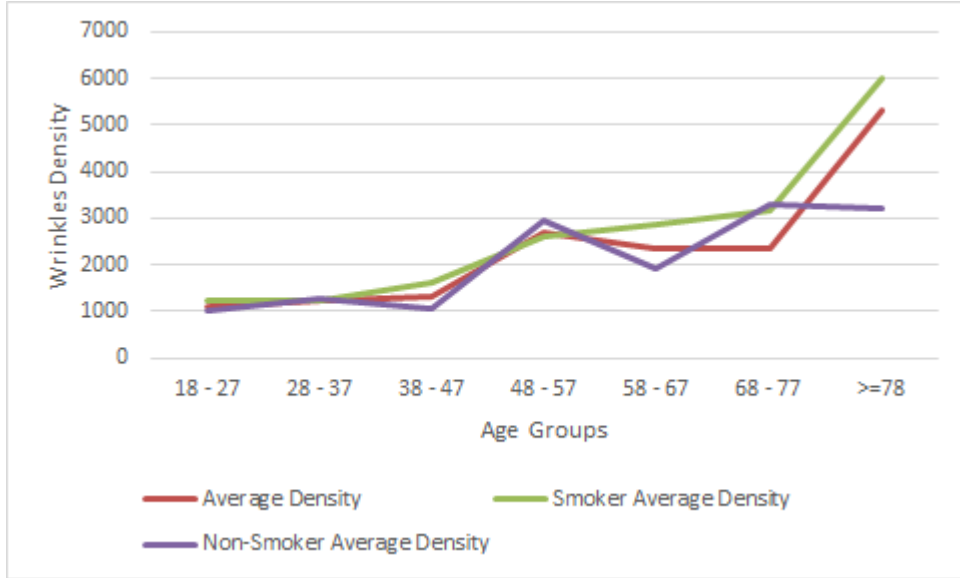


Figure 4.7: A graph illustrates the average wrinkles density versus the age groups.

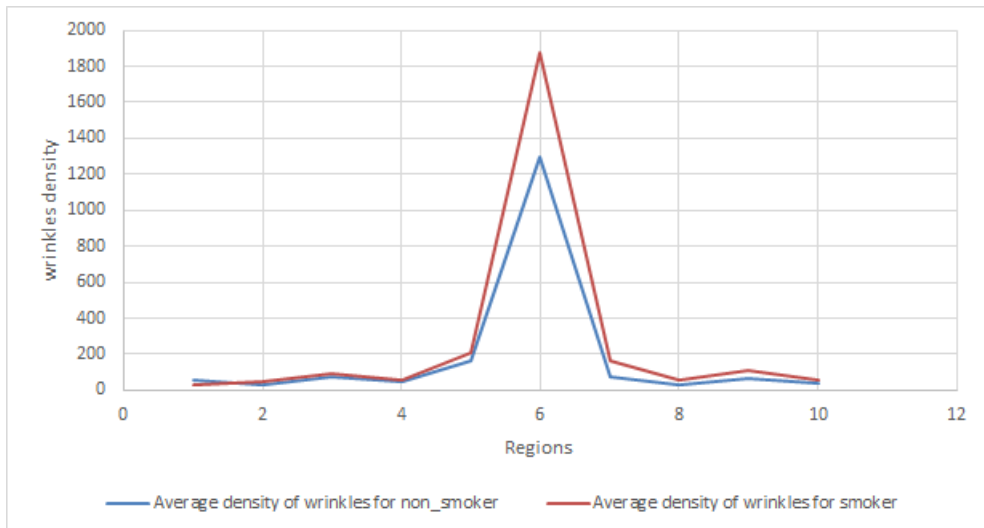


Figure 4.8: A graph illustrates the average wrinkles density at each region.

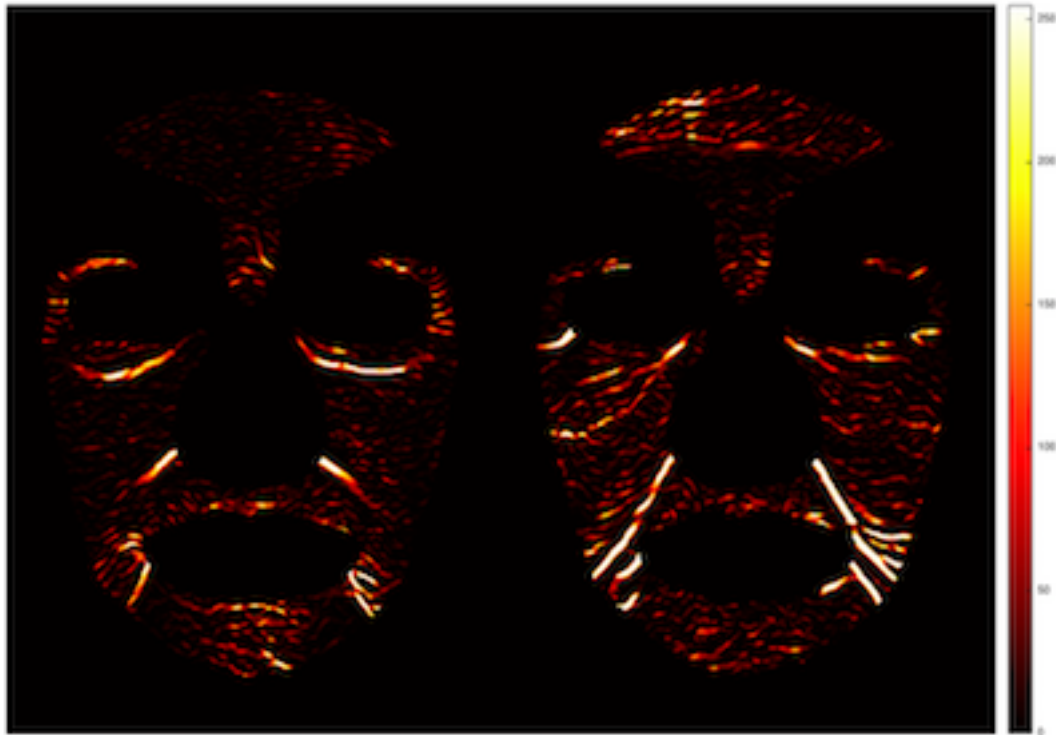


Figure 4.9: Visual comparison of the wrinkles extracted from two participants. Left image: Wrinkles extracted from non-smoker at age 80. Right image: Wrinkles extracted from smoker at age 78 shows more prominent wrinkles in terms of depth and density.

the wrinkles density is higher in the regions around the mouth and eyes for smoker participant. However, due to the lack of large-scale images in this experiment, some of the results are inconclusive.

## 4.5 Summary

This chapter present the experimental results for the proposed methods described in chapter 3. The results showed the evidence that ST and wrinkle features able to predict the face age on high resolution images. The third experimental result showed that there was a significant association between smoking and increasing the density of wrinkles with age progression. The visual comparison of wrinkles also showed the differences between smoker face and non-smoker, where the number and depth of wrinkles is clearest in smoker face.

# Chapter 5

## Conclusion and Future Works

### 5.1 Conclusion

Age estimation from input face image is one of the popular research topic. It is an important technique that used in many real-world applications, such as: security control and monitoring, soft biometrics, Electronic Customer Relationship Management (ECRM), forensic art, social psychology, and entertainment. The goal of automatic face age estimation is to estimate age that is close to real or appearance age as possible, by extracting important features from faces of known ages, the age can be estimated for an individual face by solving the inverse problem using the same feature extraction technique.

This thesis firstly proposed a new wrinkle detection algorithm to detect wrinkle regions (not line) and investigated the efficiency of the adaptive thresholding technique for wrinkle detection algorithms. The majority of work on wrinkle detection was focused on how to localize wrinkles efficiently. However, the experimental results shows that, the next step on how to segment the localised wrinkle has a direct effect on the performance of automated wrinkle detection algorithms. The proposed algorithm achieved good results when tested on a new type of facial skin using our in-house Sudanese dataset as well as other datasets. Secondly, Scattering Transform (ST) which is a recently new frontier along the feature representation direction was introduced as local features descriptor for face age estimation. Thirdly, a combination of ST and wrinkle pattern was used to investigate the efficiency of using only local features for age estimation. However, the experimental results shows that local features can estimate the age accurately using high and mid resolution images only. Where ST achieved better for FERET and PAL with MAE 2.12 and 2.22 year respectively, and a good result for collected Sudanese dataset with MAE 4.04 year (using only 638 images), and the combination of ST and wrinkle pattern yielded a superior



result on FERET with MAE 2.09 years. Finally The effect of smoking on wrinkle was investigated using computer vision algorithms. The result showed that the density of wrinkles for smokers in two regions around the mouth was significantly higher than the non-smokers, at p-value of 0.05. However, due to the limitations in Sudanese dataset dose not included in the smoking experiment. Despite the limitations of this experiment, it gave new insights to the potential use of computerised algorithms, with has high correlation between the age and the wrinkles density, and aligned with the state-of-the-art research.

## 5.2 Future Works

Based on the experiments that conducted in this thesis, here are some suggestions for future works for wrinkle detection and face age estimation:

1. Tracing of the wrinkle segment is one of the key step for efficient wrinkle detection algorithms.
2. An algorithm that differentiate between hair and wrinkle is needed as a part of automatic wrinkle detection algorithm.
3. Enhance the automatic annotator (Yap et al. 2018) by using different enhancement filters for input images and applying adaptive threshold technique to excluding non-wrinkle region.
4. Web collected images are an efficient way to collect a huge amount of images to establish face aging database, with balance in distribution of age, gender, ethnicity, expression, and pose. Developed web applications to collect images from internet (Escalera et al. 2015) can facilitate the collection process. Large-scale database will have a positive impact on the performance of automatic age estimation system.
5. Implementation of general framework that considers most of the factors affecting the performance of age estimation.
6. In feature combination, finding a fusion strategy such as feature pooling (Huerta et al. 2015) can produce more accurate results than just concatenating the features in hybrid approach.

7. Combination or fusion of methods produces better result for low and high resolution images, e.g., combining wrinkle features with other local and global features (Ng et al. 2015a, Ng, Yap, Cheng & Hsu 2017). A similar strategy can be applied for scattering transform (Chang & Chen 2015). Combining deep learning, ordinal ranking and CBIF. By combining these new techniques, the machine may outperforms the ability of human in face age estimation.
8. Extended the the experiment that study the effect of smoking on wrinkle by using additional number of images, including more frontal face images and the profile face images to analysis the regions around eyes, particularly the crow feet.

# Appendix A

## Dataset Questioner


## دراسة تأثير التدخين على مظهر الوجه وعلى العمر باستخدام خوارزميات الحاسوب

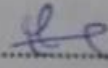
### نموذج الموافقة

هذه الدراسة تتطلب التوقيع على نموذج الموافقة قبل البدء في التقاط الصور للمشارك. تخضع هذه الدراسة لقواعد ولوائح جامعة السودان للعلوم والتكنولوجيا بغرض التطوير والمساهمة في البحث العلمي.

1. لقد فهمت الغرض من الدراسة، وتمت الإجابة على جميع أسئلتى بوضوح.
2. مشاركتي في هذه الدراسة تطوعية، واستطيع الانسحاب منها متى ماثلت دون إعطاء أي أسباب حتى انتهاء الدراسة في ديسمبر 2018.
3. أعلم تماماً أن البيانات التي جمعت خلال هذه الدراسة سوف تستخدم بغرض البحث العلمي حتى 10 أعوام قادمة وبالتالي فقد تستخدم في بحوث علمية أخرى، و في المؤتمرات العلمية.
4. أوافق أن جامعة السودان للعلوم والتكنولوجيا قد تستخدم جزء من هذه البيانات في المجلات والمؤتمرات العلمية.
5. البيانات الخاصة بي ستكون بيانات مجهولة المصدر طوال فترة الدراسة (عدم ذكر الاسم أو التفاصيل الشخصية).
6. أعلم تماماً أن البيانات ستكون مخزنة رقمياً ومحمية بكلمات مرور، وسوف تكون هوية المشاركين في الاستبيان معرفة فقط من خلال رقم مميز لكل مشارك.
7. أعلم تماماً أنه سيتم التعامل مع بياناتي من خلال الرقم المميز فقط و الذي سيتم تخزينه رقمياً.

قرأت الاتفاق المبين اعلاه، و انا أوافق على المشاركة في هذه الدراسة.

الاسم: ..... 

التوقيع: ..... 

التاريخ: ..... 17/11/14

دراسة تأثير التدخين على مظهر الوجه وعلى العمر باستخدام خوارزميات الحاسوب  
الإستبيان

الجزء الاول: معلومات اساسية

1. ماهو عمرك؟ ..... 33 .....
2. ذكر  أنثى
3. ماهي ديانتك؟ ..... مسلم .....

الجزء الثاني: معلومات عن العادات الاجتماعية الضاره (التدخين)

1. هل دخلت سيجاره من قبل؟  نعم:  لا:
2. هل أنت الآن مدخن؟  نعم:  لا:

3. إذا كانت الإجابة بنعم، فكم سيجارة تدخن؟

- a. على الأقل واحده كل يوم.  
b. على الأقل واحده كل إسبوع.  
c. على الأقل واحده كل شهر.  
d. في كثير من الأحيان أقل من واحده في الشهر.

4. إذا كانت الإجابة بلا، كيف كنت تدخن حتى اقلعت؟

- a. أقل من 24 ساعه.

جامعة السودان للعلوم والتكنولوجيا - كلية علوم الحاسوب وتقانة المعلومات

- b. من يوم إلى اسبوع.  
c. من اسبوع إلى ٤ أسابيع.  
d. من ٤ أسابيع إلى ١٢ اسبوع.  
e. من ١٢ اسبوع إلى ٦ أشهر.  
f. أكثر من ٦ أشهر.

.....

٦. كم سيجاره تخن في اليوم؟

- a. ٣ - ١  
b. ٦ - ٤  
c. ١٠ - ٧  
d. ١٥ - ١٠  
e. ٢٠ - ١٦  
f. ٢٥ - ٢١  
g. ٢٦+

٧. خلال ٧ ايام فائته، كم شخص دخن بقرتك؟

- a. ٠  
b. ٢ - ١  
c. ٤ - ٣  
d. ٦ - ٥  
e. ٧+ ✓

هذا الجزء خاص بالباحث

رقم المشارك (Participant ID) ..... 4

أحمد محمد  
مستشار  
التقانة  
المعلوماتية



## دراسة تأثير المتكلمين على مظهر الوجه وعلى العمر باستخدام خوارزميات الحاسوب

### نموذج الموافقة

هذه الدراسة تتطلب التوقيع على نموذج الموافقة قبل البدء في النقاط الصور للمشاركة. تخضع هذه الدراسة لقواعد ولوائح جامعة السودان للعلوم والتكنولوجيا بغرض التطوير والمساهمة في البحث العلمي.

1. لقد فهمت الغرض من الدراسة وتمت الإجابة على جميع أسئلتى بوضوح.
2. مشاركتي في هذه الدراسة تطوعية، واستطعت الانسحاب منها متى ماثلت دون إعطاء أي أسباب حتى انتهاء الدراسة في ديسمبر 2018.
3. أعلم تماماً أن البيانات التي جمعت خلال هذه الدراسة سوف تستخدم بغرض البحث العلمي حتى 10 أعوام قادمة وبالتالي فقد تستخدم في بحوث علمية أخرى، و في المؤتمرات العلمية.
4. أوافق أن جامعة السودان للعلوم والتكنولوجيا قد تستخدم جزء من هذه البيانات في المجلات والمؤتمرات العلمية.
5. البيانات الخاصة بي ستكون بيانات مجهولة المصدر طوال فترة الدراسة (عدم ذكر الاسم أو التفاصيل الشخصية).
6. أعلم تماماً أن البيانات ستكون مخزنة رقمياً ومحمية بكلمات مرور، وسوف تكون هوية المشاركين في الاستبيان معرفة فقط من خلال رقم مميز لكل مشارك.
7. أعلم تماماً أنه سيتم التعامل مع بياناتي من خلال الرقم المميز فقط و الذي سيتم تخزينه رقمياً.

قرأت الاتفاق المبين اعلاه، و انا اوافق على المشاركة في هذه الدراسة.

الاسم: .....  
.....

التوقيع: .....  
.....

التاريخ: .....  
.....

دراسة تأثير التدخين على مظهر الوجه وعلى العمر باستخدام خوارزميات الحاسوب

الإستبيان

الجزء الأول: معلومات أساسية

1. ماهو عمرك؟ ..... ٥٧ .....
2. ذكر  أنثى
3. ماهي ديانتك؟ ..... مسلم .....

الجزء الثاني: معلومات عن العادات الاجتماعية الضاره (التدخين)

1. هل تدخن سيجاره من قبل؟ نعم:  لا:
2. هل أنت الآن مدخن؟ نعم:  لا:

3. إذا كانت الإجابة بنعم، فكم سيجارة تدخن؟

- a. على الأقل واحد كل يوم.
- b. على الأقل واحد كل إسبوع.
- c. على الأقل واحد كل شهر.
- d. في كثير من الأحيان أقل من واحد في الشهر.

4. إذا كانت الإجابة بلا، كيف كنت تدخن حتى اقلعت؟

- a. أقل من 24 ساعة.





# Bibliography

- Aizen, E. & Gilhar, A. (2001), ‘Smoking effect on skin wrinkling in the aged population’, *International journal of dermatology* **40**(7), 431–433.
- Alarifi, J., Goyal, M., Davison, A., Dancey, D., Khan, R. & Yap, M. H. (2017), Facial skin classification using convolutional neural networks, *in* ‘Image Analysis and Recognition: 14th International Conference, ICIAR 2017, Montreal, QC, Canada, July 5–7, 2017, Proceedings’, Vol. 10317, Springer, p. 479.
- Albert, A. M., Ricanek, K. & Patterson, E. (2007), ‘A review of the literature on the aging adult skull and face: Implications for forensic science research and applications’, *Forensic Science International* **172**(1), 1–9.
- Angulu, R., Tapamo, J. R. & Adewumi, A. O. (2017), Human age estimation using multi-frequency biologically inspired features (mf-bif), *in* ‘AFRICON, 2017 IEEE’, IEEE, pp. 26–31.
- Aznar-Casanova, J., Torro-Alves, N. & Fukusima, S. (2010), ‘How much older do you get when a wrinkle appears on your face? modifying age estimates by number of wrinkles’, *Aging, Neuropsychology, and Cognition* **17**(4), 406–421.
- Bando, Y., Kuratate, T. & Nishita, T. (2002), A simple method for modeling wrinkles on human skin, *in* ‘10th Pacific Conference on Computer Graphics and Applications, 2002. Proceedings.’, IEEE, pp. 166–175.
- Bastanfard, A., Nik, M. A. & Dehshibi, M. M. (2007), Iranian face database with age, pose and expression, *in* ‘Machine Vision, 2007. ICMV 2007. International Conference on’, IEEE, pp. 50–55.
- Batool, N. & Chellappa, R. (2012), Modeling and detection of wrinkles in aging human faces using marked point processes, *in* ‘European Conference on Computer Vision’, Springer, pp. 178–188.

- Batool, N. & Chellappa, R. (2014), ‘Detection and inpainting of facial wrinkles using texture orientation fields and markov random field modeling’, *IEEE transactions on image processing* **23**(9), 3773–3788.
- Batool, N. & Chellappa, R. (2015), ‘Fast detection of facial wrinkles based on gabor features using image morphology and geometric constraints’, *Pattern Recognition* **48**(3), 642–658.
- Batool, N., Taheri, S. & Chellappa, R. (2013), Assessment of facial wrinkles as a soft biometrics, in ‘2013 10th IEEE International Conference and Workshops on Automatic Face and Gesture Recognition (FG)’, IEEE, pp. 1–7.
- Bekhouche, S. E., Ouafi, A., Taleb-Ahmed, A., Hadid, A. & Benlamoudi, A. (2016), ‘Facial age estimation using bsif and lbp’, *arXiv preprint arXiv:1601.01876* .
- Bouchrika, I., Ladjailia, A., Harrati, N. & Khedairia, S. (2015), Automated clustering and estimation of age groups from face images using the local binary pattern operator, in ‘Electrical Engineering (ICEE), 2015 4th International Conference on’, IEEE, pp. 1–4.
- Bruna, J. & Mallat, S. (2011), Classification with scattering operators, in ‘Computer Vision and Pattern Recognition (CVPR), 2011 IEEE Conference on’, IEEE, pp. 1561–1566.
- Bruna, J. & Mallat, S. (2013), ‘Invariant scattering convolution networks’, *IEEE transactions on pattern analysis and machine intelligence* **35**(8), 1872–1886.
- Bukar, A. M., Ugail, H. & Connah, D. (2016), ‘Automatic age and gender classification using supervised appearance model’, *Journal of Electronic Imaging* **25**(6), 061605–061605.
- Bulpitt, C., Markowe, H. & Shipley, M. (2001), ‘Why do some people look older than they should?’, *Postgraduate medical journal* **77**(911), 578–581.
- Campanile, G., Hautmann, G. & Lotti, T. (1998), ‘Cigarette smoking, wound healing, and face-lift’, *Clinics in dermatology* **16**(5), 575–578.
- Chang, K.-Y. & Chen, C.-S. (2015), ‘A learning framework for age rank estimation based on face images with scattering transform’, *IEEE Transactions on Image Processing* **24**(3), 785–798.

- Chang, K.-Y., Chen, C.-S. & Hung, Y.-P. (2010), A ranking approach for human ages estimation based on face images, *in* 'Pattern Recognition (ICPR), 2010 20th International Conference on', IEEE, pp. 3396–3399.
- Chang, K.-Y., Chen, C.-S. & Hung, Y.-P. (2011), Ordinal hyperplanes ranker with cost sensitivities for age estimation, *in* 'Computer vision and pattern recognition (cvpr), 2011 IEEE Conference on', IEEE, pp. 585–592.
- Chao, W.-L., Liu, J.-Z. & Ding, J.-J. (2013), 'Facial age estimation based on label-sensitive learning and age-oriented regression', *Pattern Recognition* **46**(3), 628–641.
- Chaudhuri, S., Chatterjee, S., Katz, N., Nelson, M. & Goldbaum, M. (1989), 'Detection of blood vessels in retinal images using two-dimensional matched filters', *IEEE Transactions on medical imaging* **8**(3), 263–269.
- Chen, B.-C., Chen, C.-S. & Hsu, W. H. (2014), Cross-age reference coding for age-invariant face recognition and retrieval, *in* 'European Conference on Computer Vision', Springer, pp. 768–783.
- Chen, C., Dantcheva, A. & Ross, A. (2013), Automatic facial makeup detection with application in face recognition, *in* 'Biometrics (ICB), 2013 International Conference on', IEEE, pp. 1–8.
- Chen, C., Dantcheva, A. & Ross, A. (2014), Impact of facial cosmetics on automatic gender and age estimation algorithms, *in* 'Computer Vision Theory and Applications (VISAPP), 2014 International Conference on', Vol. 2, IEEE, pp. 182–190.
- Chen, S., Zhang, C., Dong, M., Le, J. & Rao, M. (2017), Using ranking-cnn for age estimation, *in* 'Proceedings of the IEEE Conference on Computer Vision and Pattern Recognition', pp. 5183–5192.
- Choi, S. E., Lee, Y. J., Lee, S. J., Park, K. R. & Kim, J. (2010), A comparative study of local feature extraction for age estimation, *in* '2010 11th International Conference on Control Automation Robotics & Vision', IEEE, pp. 1280–1284.
- Choi, S. E., Lee, Y. J., Lee, S. J., Park, K. R. & Kim, J. (2011), 'Age estimation using a hierarchical classifier based on global and local facial features', *Pattern Recognition* **44**(6), 1262–1281.

- CLATICI, V. G., RACOCEANU, D., DALLE, C., VOICU, C., TOMAS-ARAGONES, L., MARRON, S. E., WOLLINA, U. & FICA, S. (2017), 'Perceived age and life style. the specific contributions of seven factors involved in health and beauty.', *Maedica-a Journal of Clinical Medicine* **12**(3).
- Cootes, T. F., Edwards, G. J. & Taylor, C. J. (2001), 'Active appearance models', *IEEE Transactions on Pattern Analysis & Machine Intelligence* (6), 681–685.
- Cope, G. (2013), 'Smoking and skin ageing: how aesthetic nurses can identify and prevent damage', *Journal of Aesthetic Nursing* **2**(7), 328–332.
- Csurka, G., Larlus, D., Perronnin, F. & Meylan, F. (2013), What is a good evaluation measure for semantic segmentation?., in 'BMVC', Vol. 27, Citeseer, p. 2013.
- Cula, G. O., Bargo, P. R., Nkengne, A. & Kollias, N. (2013), 'Assessing facial wrinkles: automatic detection and quantification', *Skin Research and Technology* **19**(1), e243–e251.
- DANIELL, H. W. (1971), 'Smoker's wrinkles: A study in the epidemiology of crow's feet', *Annals of internal medicine* **75**(6), 873–880.
- Dantcheva, A., Elia, P. & Ross, A. (2016), 'What else does your biometric data reveal? a survey on soft biometrics', *IEEE Transactions on Information Forensics and Security* **11**(3), 441–467.
- Dibeklioglu, H., Alnajar, F., Salah, A. A. & Gevers, T. (2015), 'Combining facial dynamics with appearance for age estimation', *IEEE Transactions on Image Processing* **24**(6), 1928–1943.
- Doll, R., Peto, R., Boreham, J. & Sutherland, I. (2004), 'Mortality in relation to smoking: 50 years' observations on male british doctors', *Bmj* **328**(7455), 1519.
- Dong, Y., Liu, Y. & Lian, S. (2016), 'Automatic age estimation based on deep learning algorithm', *Neurocomputing* **187**, 4–10.
- Ekman, P. & Keltner, D. (1997), 'Universal facial expressions of emotion', *Segerstrale U, P. Molnar P, eds. Nonverbal communication: Where nature meets culture* pp. 27–46.
- El Dib, M. Y. M. H. (2011), Automatic facial age estimation, PhD thesis, Cairo University.

- El Dib, M. Y. & Onsi, H. M. (2011), ‘Human age estimation framework using different facial parts’, *Egyptian Informatics Journal* **12**(1), 53–59.
- Escalera, S., Gonzalez, J., Baró, X., Pardo, P., Fabian, J., Olliu, M., Escalante, H. J., Huerta, I. & Guyon, I. (2015), Chalearn looking at people 2015 new competitions: Age estimation and cultural event recognition, *in* ‘Neural Networks (IJCNN), 2015 International Joint Conference on’, IEEE, pp. 1–8.
- Farage, M., Miller, K., Elsner, P. & Maibach, H. (2008), ‘Intrinsic and extrinsic factors in skin ageing: a review’, *International Journal of Cosmetic Science* **30**(2), 87–95.
- Farkas, L. G. (1994), *Anthropometry of the Head and Face*, Raven Pr.
- FERET Database* (n.d.), <https://www.nist.gov/programs-projects/face-recognition-technology-feret>. Accessed: 2016-06-9.
- Friedman, O. (2005), ‘Changes associated with the aging face’, *Facial Plastic Surgery Clinics* **13**(3), 371–380.
- Fu, Y., Guo, G. & Huang, T. S. (2010), ‘Age synthesis and estimation via faces: A survey’, *Pattern Analysis and Machine Intelligence, IEEE Transactions on* **32**(11), 1955–1976.
- Fu, Y., Xu, Y. & Huang, T. S. (2007), Estimating human age by manifold analysis of face pictures and regression on aging features, *in* ‘Multimedia and Expo, 2007 IEEE International Conference on’, IEEE, pp. 1383–1386.
- Fu, Y. & Zheng, N. (2006), ‘M-face: An appearance-based photorealistic model for multiple facial attributes rendering’, *Circuits and Systems for Video Technology, IEEE Transactions on* **16**(7), 830–842.
- Fukai, H., Takimoto, H., Fukumi, M. & Mitsukura, Y. (2011), *Apparent age estimation system based on age perception*, INTECH Open Access Publisher.
- Gao, F. & Ai, H. (2009), Face age classification on consumer images with gabor feature and fuzzy lda method, *in* ‘Advances in biometrics’, Springer, pp. 132–141.
- Geng, X., Fu, Y. & Smith-Miles, K. (2010), Automatic facial age estimation, *in* ‘11th Pacific Rim International Conference on Artificial Intelligence’, pp. 1–130.

- Geng, X. & Smith-Miles, K. (2009), Facial age estimation by multilinear subspace analysis, *in* ‘Acoustics, Speech and Signal Processing, 2009. ICASSP 2009. IEEE International Conference on’, IEEE, pp. 865–868.
- Geng, X., Zhou, Z.-H. & Smith-Miles, K. (2007), ‘Automatic age estimation based on facial aging patterns’, *Pattern Analysis and Machine Intelligence, IEEE Transactions on* **29**(12), 2234–2240.
- Gill, J. F., Siegrid, S. Y. & Neuhaus, I. M. (2013), ‘Tobacco smoking and dermatologic surgery’, *Journal of the American Academy of Dermatology* **68**(1), 167–172.
- Goodall, C. (1991), ‘Procrustes methods in the statistical analysis of shape’, *Journal of the Royal Statistical Society: Series B (Methodological)* **53**(2), 285–321.
- Grogan, S., Flett, K., Clark-Carter, D., Gough, B., Davey, R., Richardson, D. & Rajaratnam, G. (2011), ‘Women smokers’ experiences of an age-appearance anti-smoking intervention: A qualitative study’, *British Journal of Health Psychology* **16**(4), 675–689.
- Grove, G. L., Grove, M. J. & Leyden, J. J. (1989), ‘Optical profilometry: an objective method for quantification of facial wrinkles’, *Journal of the American Academy of Dermatology* **21**(3), 631–637.
- Günay, A. & Nabiyeve, V. V. (2008), Automatic age classification with lbp, *in* ‘Computer and Information Sciences, 2008. ISCIS’08. 23rd International Symposium on’, IEEE, pp. 1–4.
- Günay, A. & Nabiyeve, V. V. (2013), Age estimation based on local radon features of facial images, *in* ‘Computer and Information Sciences III’, Springer, pp. 183–190.
- Günay, A. & Nabiyeve, V. V. (2015), ‘Age estimation based on aam and 2d-dct features of facial images’, *International Journal of Computer Science and Applications* **6**(2).
- Günay, A. & Nabiyeve, V. V. (2016), Age estimation based on hybrid features of facial images, *in* ‘Information Sciences and Systems 2015’, Springer, pp. 295–304.
- Guo, G. (2012), Human age estimation and sex classification, *in* ‘Video Analytics for Business Intelligence’, Springer, pp. 101–131.
- Guo, G., Fu, Y., Dyer, C. R. & Huang, T. S. (2008a), ‘Image-based human age estimation by manifold learning and locally adjusted robust regression’, *IEEE Transactions on Image Processing* **17**(7), 1178–1188.

- Guo, G., Fu, Y., Dyer, C. R. & Huang, T. S. (2008*b*), A probabilistic fusion approach to human age prediction, *in* 'Computer Vision and Pattern Recognition Workshops, 2008. CVPRW'08. IEEE Computer Society Conference on', IEEE, pp. 1–6.
- Guo, G. & Mu, G. (2010), Human age estimation: What is the influence across race and gender?, *in* 'Computer Vision and Pattern Recognition Workshops (CVPRW), 2010 IEEE Computer Society Conference on', IEEE, pp. 71–78.
- Guo, G. & Mu, G. (2011), Simultaneous dimensionality reduction and human age estimation via kernel partial least squares regression, *in* 'Computer vision and pattern recognition (cvpr), 2011 IEEE conference on', IEEE, pp. 657–664.
- Guo, G., Mu, G., Fu, Y., Dyer, C. R. & Huang, T. S. (2009), A study on automatic age estimation using a large database, *in* 'ICCV', pp. 1986–1991.
- Guo, G., Mu, G., Fu, Y. & Huang, T. S. (2009), Human age estimation using bio-inspired features, *in* 'Computer Vision and Pattern Recognition, 2009. CVPR 2009. IEEE Conference on', IEEE, pp. 112–119.
- Guo, J.-M., Liou, Y.-M. & Nguyen, H.-S. (2011), Human face age estimation with adaptive hybrid features, *in* 'System Science and Engineering (ICSSE), 2011 International Conference on', IEEE, pp. 55–58.
- Gurpinar, F., Kaya, H., Dibeklioglu, H. & Salah, A. (2016), Kernel elm and cnn based facial age estimation, *in* 'Proceedings of the IEEE Conference on Computer Vision and Pattern Recognition Workshops', pp. 80–86.
- Guyuron, B., Rowe, D. J., Weinfeld, A. B., Eshraghi, Y., Fathi, A. & Iamphongsai, S. (2009), 'Factors contributing to the facial aging of identical twins', *Plastic and reconstructive surgery* **123**(4), 1321–1331.
- Hadchum, P. & Wongthanavas, S. (2015), Facial age estimation using a hybrid of svm and fuzzy logic, *in* 'Electrical Engineering/Electronics, Computer, Telecommunications and Information Technology (ECTI-CON), 2015 12th International Conference on', IEEE, pp. 1–6.
- Han, H., Otto, C. & Jain, A. K. (2013), Age estimation from face images: Human vs. machine performance, *in* 'Biometrics (ICB), 2013 International Conference on', IEEE, pp. 1–8.



- Han, H., Otto, C., Liu, X. & Jain, A. K. (2015), ‘Demographic estimation from face images: Human vs. machine performance’, *IEEE transactions on pattern analysis and machine intelligence* **37**(6), 1148–1161.
- Han, X., Yap, M. H. & Palmer, I. (2012), ‘Face recognition in the presence of expressions’, *Journal of Software Engineering and Applications* **5**(05), 321.
- Haralick, R. M., Shanmugam, K. & Dinstein, I. H. (1973), ‘Textural features for image classification’, *IEEE Transactions on systems, man, and cybernetics* (6), 610–621.
- Hayashi, J.-i., Yasumoto, M., Ito, H. & Koshimizu, H. (2002), Age and gender estimation based on wrinkle texture and color of facial images, *in* ‘Object recognition supported by user interaction for service robots’, Vol. 1, IEEE, pp. 405–408.
- Horng, W.-B., Lee, C.-P. & Chen, C.-W. (2001), ‘Classification of age groups based on facial features’, *Tamkang Journal of Science and Engineering* **4**(3), 183–192.
- Huerta, I., Fernández, C., Segura, C., Hernando, J. & Prati, A. (2015), ‘A deep analysis on age estimation’, *Pattern Recognition Letters* **68**, 239–249.
- Ippen, M. & Ippen, H. (1965), ‘Approaches to a prophylaxis of skin aging’, *J Soc Cosmetic Chemists* **16**, 305–8.
- Iqbal, M. T. B., Shoyaib, M., Ryu, B., Abdullah-Al-Wadud, M. & Chae, O. (2017), ‘Directional age-primitive pattern (dapp) for human age group recognition and age estimation’, *IEEE Transactions on Information Forensics and Security* .
- Jadid, M. A. & Sheijani, O. S. (2016), Facial age estimation under the terms of local latency using weighted local binary pattern and multi-layer perceptron, *in* ‘Control, Instrumentation, and Automation (ICCIA), 2016 4th International Conference on’, IEEE, pp. 184–189.
- Japanese smokers to face age test* (n.d.), <http://news.bbc.co.uk/2/hi/asia-pacific/7395910.stm>. Accessed: 2016-07-3.
- Jison Hsu, G.-S., Cheng, Y.-T., Ching Ng, C. & Hoon Yap, M. (2017), Component biologically inspired features with moving segmentation for age estimation, *in* ‘Proceedings of the IEEE Conference on Computer Vision and Pattern Recognition Workshops’, pp. 38–45.

- Just, M., Ribera, M., Monso, E., Lorenzo, J. & Ferrandiz, C. (2007), ‘Effect of smoking on skin elastic fibres: morphometric and immunohistochemical analysis’, *British Journal of Dermatology* **156**(1), 85–91.
- Khan, S., Khan, S., Khan, T., Hussain, A., Siddique, A. & Ahmad, N. (2015), Wrinkles energy based age estimation using discrete cosine transform, *in* ‘Emerging Technologies (ICET), 2015 International Conference on’, IEEE, pp. 1–4.
- KLOEPPPEL, J. E. (2010), ‘People who hope to keep their age a secret won’t want to go near a computer running this software’.  
**URL:** <https://news.illinois.edu/blog/view/6367/206178>
- Kwon, Y. H. & da Vitoria Lobo, N. (1999), ‘Age classification from facial images’, *Computer Vision and Image Understanding* **74**(1), 1–21.
- Kwon, Y. H. & Lobo, N. D. V. (1994), Age classification from facial images, *in* ‘Computer Vision and Pattern Recognition, 1994. Proceedings CVPR’94., 1994 IEEE Computer Society Conference on’, IEEE, pp. 762–767.
- Lanitis, A., Draganova, C. & Christodoulou, C. (2004), ‘Comparing different classifiers for automatic age estimation’, *Systems, Man, and Cybernetics, Part B: Cybernetics, IEEE Transactions on* **34**(1), 621–628.
- Lanitis, A., Taylor, C. J. & Cootes, T. F. (2002), ‘Toward automatic simulation of aging effects on face images’, *Pattern Analysis and Machine Intelligence, IEEE Transactions on* **24**(4), 442–455.
- Li, W., Wang, Y. & Zhang, Z. (2012), A hierarchical framework for image-based human age estimation by weighted and ohranked sparse representation-based classification, *in* ‘Biometrics (ICB), 2012 5th IAPR International Conference on’, IEEE, pp. 19–25.
- Lian, H.-C. & Lu, B.-L. (2005), Age estimation using a min-max modular support vector machine, *in* ‘Twelfth International Conference on Neural Information Processing’, pp. 83–88.
- Lin, C.-T., Li, D.-L., Lai, J.-H., Han, M.-F. & Chang, J.-Y. (2012), ‘Automatic age estimation system for face images’, *International Journal of Advanced Robotic Systems* **29**.

- Liu, H., Lu, J., Feng, J. & Zhou, J. (2017), Ordinal deep feature learning for facial age estimation, *in* ‘Automatic Face & Gesture Recognition (FG 2017), 2017 12th IEEE International Conference on’, IEEE, pp. 157–164.
- Liu, H. & Sun, X. (2016), A partial least squares based ranker for fast and accurate age estimation, *in* ‘Acoustics, Speech and Signal Processing (ICASSP), 2016 IEEE International Conference on’, IEEE, pp. 2792–2796.
- Liu, L., Liu, J. & Cheng, J. (2012), Age-group classification of facial images, *in* ‘Machine Learning and Applications (ICMLA), 2012 11th International Conference on’, Vol. 1, IEEE, pp. 693–696.
- Liu, T.-J., Liu, K.-H., Liu, H.-H. & Pei, S.-C. (2016), Age estimation via fusion of multiple binary age grouping systems, *in* ‘Image Processing (ICIP), 2016 IEEE International Conference on’, IEEE, pp. 609–613.
- Lu, J. & Tan, Y.-P. (2010), Cost-sensitive subspace learning for face recognition, *in* ‘Computer Vision and Pattern Recognition (CVPR), 2010 IEEE Conference on’, IEEE, pp. 2661–2666.
- Luu, K., Bui, T. D., Suen, C. Y. & Ricanek Jr, K. (2010), Combined local and holistic facial features for age-determination, *in* ‘Control Automation Robotics & Vision (ICARCV), 2010 11th International Conference on’, IEEE, pp. 900–904.
- Luu, K., Ricanek Jr, K., Bui, T. D. & Suen, C. Y. (2009), Age estimation using active appearance models and support vector machine regression, *in* ‘Biometrics: Theory, Applications, and Systems, 2009. BTAS’09. IEEE 3rd International Conference on’, IEEE, pp. 1–5.
- Malli, R. C., Aygun, M. & Ekenel, H. K. (2016), ‘Apparent age estimation using ensemble of deep learning models’, *arXiv preprint arXiv:1606.02909* .
- Mapayi, T., Viriri, S. & Tapamo, J.-R. (2015), ‘Adaptive thresholding technique for retinal vessel segmentation based on glcm-energy information’, *Computational and mathematical methods in medicine* **2015**.
- Meyers, E. & Wolf, L. (2008), ‘Using biologically inspired features for face processing’, *International Journal of Computer Vision* **76**(1), 93–104.

- mi Im, S., yeon Cho, H. & Kim, T. (2016), ‘Age estimation based on facial wrinkles by using the gabor filter and svm’, *TECHART: Journal of Arts and Imaging Science* **3**(4), 24–26.
- Minear, M. & Park, D. C. (2004), ‘A lifespan database of adult facial stimuli’, *Behavior Research Methods, Instruments, & Computers* **36**(4), 630–633.
- Mirzaei, F. & Toygar, Ö. (2011), ‘Facial age classification using subpattern-based approaches’, *studies* **2**(5), 15.
- Model, D. (1985), ‘Smoker’s face: an underrated clinical sign?’, *Br Med J (Clin Res Ed)* **291**(6511), 1760–1762.
- Mohan, M. C., Vijaya Kumar, V. & Venkata Krishna, V. (2010), ‘Novel method of adult age classification using linear wavelet transforms’, *IJCSNS* **10**(3), 61.
- Mokji, M. M. & Bakar, S. A. (2007), Adaptive thresholding based on co-occurrence matrix edge information, *in* ‘First Asia International Conference on Modelling & Simulation (AMS’07)’, IEEE, pp. 444–450.
- Morita, A. (2007), ‘Tobacco smoke causes premature skin aging’, *Journal of dermatological science* **48**(3), 169–175.
- MORPH Database* (n.d.), <http://www.faceaginggroup.com/morph/>. Accessed: 2010-09-30.
- Ng, C.-C., Cheng, Y.-T., Hsu, G.-S. & Yap, M. H. (2017), Multi-layer age regression for face age estimation, *in* ‘Machine Vision Applications (MVA), 2017 Fifteenth IAPR International Conference on’, IEEE, pp. 294–297.
- Ng, C.-C., Yap, M. H., Cheng, Y.-T. & Hsu, G.-S. (2017), ‘Hybrid ageing patterns for face age estimation’, *Image and Vision Computing*.
- Ng, C.-C., Yap, M. H., Costen, N. & Li, B. (2014a), Automatic wrinkle detection using hybrid hessian filter, *in* ‘Asian Conference on Computer Vision’, Springer, pp. 609–622.
- Ng, C.-C., Yap, M. H., Costen, N. & Li, B. (2014b), An investigation on local wrinkle-based extractor of age estimation, *in* ‘Computer Vision Theory and Applications (VISAPP), 2014 International Conference on’, Vol. 1, IEEE, pp. 675–681.

- Ng, C.-C., Yap, M. H., Costen, N. & Li, B. (2015*a*), Will wrinkle estimate the face age?, *in* ‘Systems, Man, and Cybernetics (SMC), 2015 IEEE International Conference on’, IEEE, pp. 2418–2423.
- Ng, C.-C., Yap, M. H., Costen, N. & Li, B. (2015*b*), ‘Wrinkle detection using hessian line tracking’, *IEEE Access* **3**, 1079–1088.
- Ngan, M. L. & Grother, P. J. (2014), Face recognition vendor test (frvt)-performance of automated age estimation algorithms, Technical report.
- Nguyen, D. T., Cho, S. R., Shin, K. Y., Bang, J. W. & Park, K. R. (2014), ‘Comparative study of human age estimation with or without preclassification of gender and facial expression’, *The Scientific World Journal* **2014**.
- Ni, B., Song, Z. & Yan, S. (2009), Web image mining towards universal age estimator, *in* ‘Proceedings of the 17th ACM international conference on Multimedia’, ACM, pp. 85–94.
- Niu, Z., Zhou, M., Wang, L., Gao, X. & Hua, G. (2016), Ordinal regression with multiple output cnn for age estimation, *in* ‘Proceedings of the IEEE Conference on Computer Vision and Pattern Recognition’, pp. 4920–4928.
- Novel Aspects of Intrinsic and Extrinsic Aging of Human Skin: Beneficial Effects of Soy Extract* ¶ (n.d.).
- O’Gorman, L. & Nickerson, J. V. (1988), Matched filter design for fingerprint image enhancement, *in* ‘ICASSP-88., International Conference on Acoustics, Speech, and Signal Processing’, IEEE, pp. 916–919.
- Osman, O. F., Elbashir, R. M. I., Abbass, I. E., Kendrick, C., Goyal, M. & Yap, M. H. (2017), Automated assessment of facial wrinkling: A case study on the effect of smoking, *in* ‘2017 IEEE International Conference on Systems, Man, and Cybernetics (SMC)’, IEEE, pp. 1081–1086.
- Osman, O. F. & Yap, M. H. (2018), ‘Computational intelligence in automatic face age estimation: A survey’, *IEEE Transactions on Emerging Topics in Computational Intelligence* (99), 1–15.
- Panis, G., Lanitis, A., Tsapatsoulis, N. & Cootes, T. F. (2015), ‘Overview of research on facial ageing using the fg-net ageing database’, *IET Biometrics* .

- Phillips, P. J., Rauss, P. J., Der, S. Z. et al. (1996), *FERET (face recognition technology) recognition algorithm development and test results*, Army Research Laboratory Adelphi, MD.
- Qin, T., Zhang, X.-D., Wang, D.-S., Liu, T.-Y., Lai, W. & Li, H. (2007), Ranking with multiple hyperplanes, *in* ‘Proceedings of the 30th annual international ACM SIGIR conference on Research and development in information retrieval’, ACM, pp. 279–286.
- Qiu, J. et al. (2016), ‘Convolutional neural network based age estimation from facial image and depth prediction from single image’.
- Raitio, A., Kontinen, J., Rasi, M., Bloigu, R., Roning, J. & Oikarinen, A. (2004), ‘Comparison of clinical and computerized image analyses in the assessment of skin ageing in smokers and non-smokers’, *Acta dermato-venereologica* **84**(6), 422–427.
- Ramanathan, N. & Chellappa, R. (2006), Modeling age progression in young faces, *in* ‘Computer Vision and Pattern Recognition, 2006 IEEE Computer Society Conference on’, Vol. 1, IEEE, pp. 387–394.
- Ramanathan, N., Chellappa, R., Biswas, S. et al. (2009), ‘Age progression in human faces: A survey’, *Journal of Visual Languages and Computing* **15**, 3349–3361.
- Ren, H. & Li, Z.-N. (2014), Age estimation based on complexity-aware features, *in* ‘Asian Conference on Computer Vision’, Springer, pp. 115–128.
- Ricanek Jr, K. & Tesafaye, T. (2006), Morph: A longitudinal image database of normal adult age-progression, *in* ‘Automatic Face and Gesture Recognition, 2006. FGR 2006. 7th International Conference on’, IEEE, pp. 341–345.
- Riesenhuber, M. & Poggio, T. (1999), ‘Hierarchical models of object recognition in cortex’, *Nature neuroscience* **2**(11), 1019–1025.
- Rothe, R., Timofte, R. & Van Gool, L. (2016), ‘Deep expectation of real and apparent age from a single image without facial landmarks’, *International Journal of Computer Vision* pp. 1–14.
- Rothe, R., Timofte, R. & Van Gool, L. (2018), ‘Deep expectation of real and apparent age from a single image without facial landmarks’, *International Journal of Computer Vision* **126**(2-4), 144–157.

- Russakovsky, O., Deng, J., Su, H., Krause, J., Satheesh, S., Ma, S., Huang, Z., Karpathy, A., Khosla, A., Bernstein, M. et al. (2015), ‘Imagenet large scale visual recognition challenge’, *International Journal of Computer Vision* **115**(3), 211–252.
- Sarode, N. & Bhatia, S. (2010), ‘Facial expression recognition’, *International Journal on computer science and Engineering* **2**(5), 1552–1557.
- Scherbaum, K., Sunkel, M., Seidel, H.-P. & Blanz, V. (2007), Prediction of individual non-linear aging trajectories of faces, *in* ‘Computer Graphics Forum’, Vol. 26, Wiley Online Library, pp. 285–294.
- Serre, T., Wolf, L., Bileschi, S., Riesenhuber, M. & Poggio, T. (2007), ‘Robust object recognition with cortex-like mechanisms’, *Pattern Analysis and Machine Intelligence, IEEE Transactions on* **29**(3), 411–426.
- Simonyan, K. & Zisserman, A. (2014), ‘Very deep convolutional networks for large-scale image recognition’, *arXiv preprint arXiv:1409.1556* .
- Stone, A. (n.d.), ‘The aging process of the face & techniques of rejuvenation’, <https://aaronstonemd.com/plastic-surgery-links/facial-aging-and-rejuvenation/>. Accessed: 2019-01-01.
- Strack, R. W. & Wyrick, D. L. (2012), ‘Cigarette smoking and facial wrinkles: A review of the literature’.
- Su, Y., Shan, S., Chen, X. & Gao, W. (2009), ‘Hierarchical ensemble of global and local classifiers for face recognition’, *Image Processing, IEEE Transactions on* **18**(8), 1885–1896.
- Sun, Y., Wang, X. & Tang, X. (2013), Deep convolutional network cascade for facial point detection, *in* ‘Proceedings of the IEEE conference on computer vision and pattern recognition’, pp. 3476–3483.
- Suo, J., Min, F., Zhu, S., Shan, S. & Chen, X. (2007), A multi-resolution dynamic model for face aging simulation, *in* ‘Computer Vision and Pattern Recognition, 2007. CVPR’07. IEEE Conference on’, IEEE, pp. 1–8.
- Suo, J., Wu, T., Zhu, S., Shan, S., Chen, X. & Gao, X. (2008), Design sparse features for age estimation using hierarchical face model, *in* ‘Automatic Face & Gesture Recognition, 2008. FG’08. 8th IEEE International Conference on’, IEEE, pp. 1–6.

- Sveikata, K., Balciuniene, I. & Tutkuvienė, J. (2011), ‘Factors influencing face aging. literature review’, *Stomatologija* **13**(4), 113–6.
- Taigman, Y., Yang, M., Ranzato, M. & Wolf, L. (2014), Closing the gap to human-level performance in face verification. deepface, *in* ‘IEEE Computer Vision and Pattern Recognition (CVPR)’.
- Tharwat, A., Ghanem, A. M. & Hassanien, A. E. (2013), Three different classifiers for facial age estimation based on k-nearest neighbor, *in* ‘Computer Engineering Conference (ICENCO), 2013 9th International’, IEEE, pp. 55–60.
- Ueki, K., Hayashida, T. & Kobayashi, T. (2006), Subspace-based age-group classification using facial images under various lighting conditions, *in* ‘Automatic Face and Gesture Recognition, 2006. FGR 2006. 7th International Conference on’, IEEE, pp. 6–pp.
- Wang, J.-G., Yau, W.-Y. & Wang, H. L. (2009), Age categorization via ecoc with fused gabor and lbp features, *in* ‘Applications of Computer Vision (WACV), 2009 Workshop on’, IEEE, pp. 1–6.
- Wang, S., Xia, X., Le, J., Yang, S. & Liao, X. (2010), Classifying children’s and adults’ faces by bio-inspired features, *in* ‘Intelligent Computing and Intelligent Systems (ICIS), 2010 IEEE International Conference on’, Vol. 3, IEEE, pp. 673–677.
- Wang, X., Guo, R. & Kambhamettu, C. (2015), Deeply-learned feature for age estimation, *in* ‘2015 IEEE Winter Conference on Applications of Computer Vision’, IEEE, pp. 534–541.
- Wang, X., Ly, V., Lu, G. & Kambhamettu, C. (2013), Can we minimize the influence due to gender and race in age estimation?, *in* ‘Machine Learning and Applications (ICMLA), 2013 12th International Conference on’, Vol. 2, IEEE, pp. 309–314.
- Wang, Y., Ricanek, K., Chen, C. & Chang, Y. (2010), Gender classification from infants to seniors, *in* ‘Biometrics: theory applications and systems (BTAS), 2010 Fourth IEEE international conference on’, IEEE, pp. 1–6.
- Weng, R., Lu, J., Yang, G. & Tan, Y.-P. (2013), Multi-feature ordinal ranking for facial age estimation, *in* ‘Automatic face and gesture recognition (FG), 2013 10th IEEE international conference and workshops on’, IEEE, pp. 1–6.



- Xie, W., Shen, L. & Jiang, J. (2016), ‘A novel transient wrinkle detection algorithm and its application for expression synthesis’, *IEEE Transactions on Multimedia* **19**(2), 279–292.
- Yan, S., Liu, M. & Huang, T. S. (2008), Extracting age information from local spatially flexible patches, *in* ‘Acoustics, Speech and Signal Processing, 2008. ICASSP 2008. IEEE International Conference on’, IEEE, pp. 737–740.
- Yan, S., Wang, H., Huang, T. S., Yang, Q. & Tang, X. (2007), Ranking with uncertain labels, *in* ‘Multimedia and Expo, 2007 IEEE International Conference on’, IEEE, pp. 96–99.
- Yang, M., Zhu, S., Lv, F. & Yu, K. (2011), Correspondence driven adaptation for human profile recognition, *in* ‘Computer Vision and Pattern Recognition (CVPR), 2011 IEEE Conference on’, IEEE, pp. 505–512.
- Yang, P., Zhong, L. & Metaxas, D. (2010), Ranking model for facial age estimation, *in* ‘Pattern Recognition (ICPR), 2010 20th International Conference on’, IEEE, pp. 3404–3407.
- Yap, M. H., Alarifi, J., Ng, C.-C., Batool, N. & Walker, K. (2018), Automated facial wrinkles annotator, *in* ‘European Conference on Computer Vision’, Springer, pp. 676–680.
- Yin, L., Morita, A. & Tsuji, T. (2001), ‘Skin premature aging induced by tobacco smoking: the objective evidence of skin replica analysis’, *Journal of Dermatological Science* **27**, 26–31.
- Ylioinas, J., Hadid, A., Hong, X. & Pietikäinen, M. (2013), Age estimation using local binary pattern kernel density estimate, *in* ‘International Conference on Image Analysis and Processing’, Springer, pp. 141–150.
- Zhang, Y. & Yeung, D.-Y. (2010), Multi-task warped gaussian process for personalized age estimation, *in* ‘Computer Vision and Pattern Recognition (CVPR), 2010 IEEE Conference on’, IEEE, pp. 2622–2629.
- Zhang, Z., Luo, P., Loy, C. C. & Tang, X. (2016), ‘Learning deep representation for face alignment with auxiliary attributes’, *IEEE transactions on pattern analysis and machine intelligence* **38**(5), 918–930.

- Zheng, D., Du, J., Fan, W., Wang, J. & Zhai, C. (2016), Deep learning with pcanet for human age estimation, *in* ‘International Conference on Intelligent Computing’, Springer, pp. 300–310.
- Zheng, Y., Yao, H., Zhang, Y. & Xu, P. (2013), Age classification based on back-propagation network, *in* ‘Proceedings of the Fifth International Conference on Internet Multimedia Computing and Service’, ACM, pp. 319–322.
- Zhou, E., Fan, H., Cao, Z., Jiang, Y. & Yin, Q. (2013), Extensive facial landmark localization with coarse-to-fine convolutional network cascade, *in* ‘Proceedings of the IEEE International Conference on Computer Vision Workshops’, pp. 386–391.
- Zhou, H., Miller, P. C. & Zhang, J. (2011), Age classification using radon transform and entropy based scaling svm., *in* ‘BMVC’, pp. 1–12.
- Zhu, Y., Li, Y., Mu, G. & Guo, G. (2015), A study on apparent age estimation, *in* ‘Proceedings of the IEEE International Conference on Computer Vision Workshops’, pp. 25–31.
- Zuiderveld, K. (1994), Contrast limited adaptive histogram equalization, *in* ‘Graphics gems IV’, Academic Press Professional, Inc., pp. 474–485.